PRELIMINARY RESULTS FROM AN IN-SITU COAL GASIFICATION EXPERIMENT USING EXPLOSIVE FRACTURING*

Charles B. Thorsness, Richard W. Hill, and Douglas R. Stephens

Lawrence Livermore Laboratory, University of California
Livermore, California 94550

INTRODUCTION

After almost two decades of inactivity the field of in-situ coal gasification has experienced a recent renaissance. There is at least one current industrial project, that of Texas Utilities Generating Co. in Texas lignite. They are using the very extensive Soviet technology to develop in-situ coal gasification to produce low Btu gas for electrical power generation. Three ERDA-sponsored projects are in the field, testing different modes of developing permeable paths in coal beds. The Laramie Energy Research Center is developing reverse combustion techniques to link vertical wellbores; the Lawrence Livermore Laboratory is developing explosive fracturing to create an underground packed bed; and the Morgantown Energy Research Center is developing directional drilling techniques to establish linking.

Sandia Laboratories are developing advanced instrumentation techniques for monitoring in-situ coal gasification and are cooperating with the Laramie Energy Research Center in their underground coal gasification experiments near Hanna, Wyoming. The Alberta Research Council is fielding a project near Edmonton, Alberta. Texas A & M University is fielding an experiment near College Station. The University of Texas is performing extensive systems studies on coal gasification in Texas lignite, while other in-situ coal projects are underway at the Universities of Wyoming, New Mexico, Alabama, Kentucky, West Virginia and the Pennsylvania State University. In addition, coal pyrolysis and kinetics studies are being conducted at the ERDA National Laboratories at Oak Ridge and Argonne.

The reasons for the extensive in-situ coal gasification programs are many-fold. Among them are: (1) the promise of relatively low-cost energy from in-situ coal gasification, at least as compared to other alternate fuels. (2) The promise of relatively low environmental impact from these in-situ processes. (3) The opening up of new coal reserves for development which may be uneconomic by other techniques. (4) The rather recent discovery that the Russians developed very successfully in-situ coal gasification techniques in the late 1950's, and applied them at the demonstration or pilot plant level (up to 500 tons of coal consumed per day) for up to 20 years.

In this report we summarize a recent field experiment in the ERDA-sponsored underground coal gasification program at the Lawrence Livermore Laboratory. Our project objective is to develop a commercial underground coal gasification process by using explosives to fracture the coal in place to create selectively enhanced permeability. (1) The resultant permeable coal would be gasified with steam and oxygen and the gases would be upgraded to pipeline quality in surface facilities.

Our first field gasification experiment, called Hoe Creek #1, was conducted in two phases: phase #1 included site characterization, fracturing and preliminary permeability measurements and has been reported. (1a) It is briefly described in this report, but the primary purpose of this paper is to describe phase #2 of the experiment, which included detailed fracturing and permeability measurements followed by in-situ gasification.

*This work was performed under the auspices of the U.S. Energy Research and Development Agency.

Phase #1: Site Characterization and Fracturing

One and two-dimensional computer codes, using compressive shear failure as a criterion, were used to design a multiple explosive field fracturing test, Hoe Creek #1. Extensive coal mechanical properties were input to the codes, which were normalized with laboratory fracture experiments and an earlier field test at a coal outcrop using 130# of explosives. (2)

The experimental Hoe Creek site is in the Powder River Basin, 25 miles SW of Gillette, Wyoming, in the 25' thick subbituminous Felix #2 coal at a depth of 125'. The stratigraphy of the site was derived from cores, drill-cutting samples, and downhole geophysical logs and is shown in Fig. 1. Table 1 gives the chemical analysis of the Felix #2 coal. (3) Experiment #1 was a simple two-spot fracturing experiment which was carried out at Hoe Creek on November 5, 1975.

Table 1. Analysis of coal from the Felix No. 2 seam.

	Proximate analysis (%)			Ultimate analysis (%)	
	As received	Dry basis		As received	Dry basis
Moisture	29.2	—	Moisture	29.2	—
Ash	6.37	9.00	Carbon	47.41	66.96
Volatile	31.90	45.06	Hydrogen	3.53	4.99
Fixed carbon	32.53	45.94	Nitrogen	0.91	1.28
	100.00	100.00	Chlorine	0.01	0.02
			Sulfur	0.62	0.88
Btu	8156	11522	Ash	6.37	9.00
Sulfur	0.62	0.88	Oxygen (diff)	11.95	16.87
				100.00	100.00

The purpose of the experiment was to do a small scale study of explosive fracture and gasification. It was designed to provide information on well survival, drilling techniques in fractured coal, the permeability enhancement created by two HE shots, gas flow rates, liquid plugging, burn over-ride, etc. It consisted of two 750# explosive charges fired simultaneously at the bottom of the coal seam at a depth of 150'. The explosives were placed at the bottom of the seam to enhance the permeability there for better liquid drainage and gas flow. Prior to fracturing, the site geology, hydrology and permeability were carefully characterized. (4) Post fracture characterization of the site, in late 1975, using hydrology showed that the coal permeability was stimulated from .3 darcy preshot to about 2-4 darcies postshot. (5)

During 1976 we returned to the experiment to redetermine the fracturing, take cores, remeasure the permeability distributions, dewater the coal, measure air flows, and, finally, gasify the coal.

Phase #2: Site Plan and Instrumentation

The final, as-built, well pattern for phase #2 is shown in Fig. 2. Well I-O was steel cased to the top of the Felix No. 2 seam and communicates directly with

the rubble-filled HE cavity below it. Well P-1 was steel cased and cemented within the bottom 5' of the coal bed. The HE well was cemented to the surface after the shot. All of the wells I-1 through I-8 were uncased instrument wells. They contained thermocouples and tubes for water level measurements and gas sampling.

The dewatering wells DW-1 thru DW-6 were steel cased to the top of the coal, screened thru the coal and had a steel pump section below the coal. These wells each contained a 25 gpm capacity water pump in the sump section. The preliminary hydrology tests indicated that calculating the well distribution required to dewater this very non-homogeneous zone would be very difficult. Therefore, we decided to surround the anticipated burn zone with dewatering pumps. The positions of DW-1 and DW-6 were chosen to give two different radial distances from a shot center for permeability measurements.

Installing the instrument packages in uncased holes close to the shot points was accomplished successfully but not without some difficulty. Once the drill reached the bottom third of the Felix No. 2 seam, wall collapse became a serious problem. All drilling was done with air and foam to prevent clogging of the fractured coal but this provided no stabilization for the hole walls in the highly fractured coal. Most of the instrument emplacements were done by flowing water into the hole as the instrument package was being lowered.

No unusual problems were encountered during the construction of the dewatering wells, although the driller did notice that the major zone of water production within the Felix No. 2 seam was in the top few feet for all the wells drilled.

This program is described in more detail in reference 6.

In the design of the instrumentation for this experiment, we decided to concentrate on three major measurement requirements. They were; air and gas flow rates, product gas composition and gasification zone temperature distribution.

The air and gas flow rates were measured with standard orifice plates using remote readout pressure transducers and thermocouples for the P, ΔP, and T measurements. These data, as were all others, were recorded on strip charts in parallel with a data logger that recorded digitally on magnetic tape.

The orifice flow meters were rugged and survived flooding with water, tars, and coal fines. Maintenance was inconvenient and messy but it was possible.

The product gas composition was measured with two on-line gas chromatographs that sampled automatically at hourly or shorter intervals throughout the experiment. The operation was quite successful with no major problems.

Two of the instrumentation wells, I-1 and I-2 were constructed during the first phase of the experiment. These wells contained three thermocouples each with one at the top, center and bottom of the coal seam. The other instrument wells, I-3 through I-8, each contained seven thermocouples distributed as shown in Fig. 3.

Each instrument well also contained a stainless steel tube used for water level measurement. This was accomplished by bubling air through and measuring the hydrostatic pressure. Several of these plugged with coal fines but enough were available to satisfactorily complete the hydrology measurement program. During the gasification period the bubbler tubes were used as gas pressure indicators and to extract gas samples from the burn zone.

Three wells, CB-1, CB-2, and CB-3, had a stainless steel tube sealed in place for use with a movable thermocouple. Only well CB-2 ever showed a substantial temperature rise and that only near the end of the gasification period.

The fixed thermocouples were 1/8" diameter stainless steel sheathed chromel-alumel. They were enclosed in a stainless steel housing to provide mechanical protection. The thermocouples all operated satisfactorily until the burn front actually reached the well. Most of the thermocouples that were exposed to high temperatures (approximately 1000°C) eventually burned out. The failure indication was a change in resistance as they shorted out and formed new junction points. The time of failure was determined by inspection of the temperature records for erratic behavior or, in most cases, when all thermocouples in a well indicate the same temperature.

Coring and Hydrologic Testing

Examination of cores taken after the blast showed moderate to heavy fracturing in the upper few feet of the coal bed, then a lesser fractured zone in the middle, and a highly pulverized zone at the bottom 5-10' of the coal bed. Core from the holes between the two explosive charges showed the most fracturing while core from the holes farthest out the least. Correspondence of the degree of fracturing with one and two dimensional explosive code calculations is building confidence in our ability to calculate the extent of fracturing. However, a review of flow behavior pre and post explosion led to the conclusion that permeability is not a simple function of the degree of fracturing.

We found, in general, that postshot wells completed in the lower part of the coal bed showed that the coal in these regions was of lower permeability than preshot. Well P-1, when initially completed, produced an order of magnitude less water than a preshot well, until extensive cleaning operations finally opened up a connection from it to well I-5. (6,8)

Analysis of the drawdown measurements (9) shows three major regions of permeability; a native region of 0.3 darcy permeability at radial distances greater than 50 feet, a high (10-20 darcy) inner core region within 10 feet of the HE wells and an intermediate enhanced region (1/2 to 3 darcy). These values of permeability represents averages over the coal thickness.

Slug and pulse test showed similar patterns but also indicated a considerable degree of heterogeneity in these three regions.

Our interpretation of the hydrology and coring data is the following. The fracturing resulting from the explosive charges enhanced the average permeability in the vicinity of the charges, when the seamed is viewed in a two dimensional areal perspective. However, when viewed in cross section it appears that at certain vertical locations near the explosive charges, the permeability is below preshot levels. This is believed to be a result of plugging by coal fines produced by the intense close-in fracturing. Consequently although the explosives were emplaced at the bottom of the coal bed, much of the permeability enhancement apparently tended to be near the top of the seam.

Dewatering

Dewatering rates were in good agreement with estimates. (10) After a few hours of higher flow rates a relatively constant rate of water withdrawal of approximately 10 gpm was observed. This withdrawl rate was maintained until pressurization during air flow tests cut the rate to near zero.

Figure 4 shows the actual water levels observed at various observation points in the fractured coal. Water levels indicated at the right-hand side of the figure were measured 3-5 days after start of dewatering. Wells DW-1 through 6 and P-1 were pumped below the coal seam bottom. Wells EM-4 and EM-5 were approximately 50 feet east of the HE wells and EM-1, 2, and 3 were 100 feet east.

The local variations in permeability are evident from this figure. The water level in I-5, I-7, and the HE well dropped to within a few feet of the bottom within one hour while the level in 8-OW, which is only a few feet away from P-1, remained well above the top of the coal.

Air Flow Tests

Air flow tests were begun by injecting air into well I-0 at about 15 psig. The pressure was gradually raised to 60 psig and the flow allowed to stabilize. No leakage to the surface was observed but pressures of up to 40 psig were observed in wells 100 feet away. Air losses to the underground system were approximately 40% for this mode of operation.

The I-0 well was drilled and cased to the top of the coal seam. The rubble filled explosion cavity extends completely through the coal. Thus, with the cavity dewatered, injecting air into I-0 puts high pressure on the entire cavity leading to many possible paths for leakage to the surroundings. The hydrology data suggests that good communication paths exist from the I-0 well to DW-6, DW-1 and presumably to the environmental wells EM-1 through 6.

Reversing the air flow and injecting in well P-1 put high pressure at the bottom of the seam. This reduced the pressure in the I-0 well and also reduced the air losses. About 95% of the injected air was recovered in this mode of operation.

Because of the large air loss found when injecting in I-0 we decided to reverse our original intention and gasify from well P-1 to well I-0.

Two SF_6 tracer runs were made, one for each flow direction. These tests were quite successful and implied an accessible void volume of about 600 ft^3.

GASIFICATION

Ignition

Electrical resistance heating (1 Kw) was used to ignite the coal. Two electric barbeque charcoal lighters were strapped together and lowered down the P-1 well along with a thermocouple. Several bags of charcoal briquets were dumped down the well until the lighters were covered. Once all valves were properly set and the air flow turned on, the charcoal ignited in a few minutes, as indicated by the thermocouple. Ignition took place at 16:30 on Oct. 15, 1976 (Julian day 289.7). The injection and production flow rates are shown in Fig. 5 for the entire experiment.

Gasification History

As mentioned previously a good communication path was established through the bottom part of the coal seam between well P-1 and well I-5, in the center of the zone as shown in Fig. 2. We expected that the burn would progress along this path and then travel upward and go along the top of the seam to well I-0. At first this seemed to be the case. Operating with an input pressure of about 60 psig, the flow dropped from 130 scfm to 100 scfm during the first two hours after ignition, and then the flow rose steadily for the rest of the day. Thermocouples in two of the wells, I-7 and I-5 responded within a hour of ignition. Temperature of about 100°C were recorded at the 142 foot level, two-thirds of the way into the coal seam at both wells. This situation is illustrated in Fig. 6. Here, the thermocouple wells and injection and production wells are shown in their relative positions with the top of the coal seam indicated by a tic mark to the left of the vertical scale. (The vertical distance scale factor is twice the horizontal scale factor.) Injection and production flows are indicated by arrows where the length of the arrow is proportional to the flow rate.

On the second day of gasification (day 290) temperatures began to rise in wells I-1, I-6, I-8, and DW-4 as shown in Fig. 7. At about 290.6 the output flow increased sharply to 1300 scfm and a large quantity of water was produced. The injection pressure was lowered several times to control the flow. After a few hours of controlled production the flow increased suddenly to over 2400 scfm accompanied by the emission of coal fines mixed with tar. All of the pressure and gas sampling lines were quickly plugged as well as the production flow meter orifice plate. The bypass line around the flow meter section was opened to shunt the gas flow while repairs were being made. The temperature distribution given in Fig. 8 clearly shows the override at this time.

The heating value of the produced gas is shown in Fig. 9. The steady decline in the days following the breakthrough is evident. The temperature distribution on day 291.7 and 292.9 are shown in Figs. 10 and 11. The increase in temperature near the top of the seam in wells I-4, I-6, and I-7 is indicative of the creation of an override path along the top of the coal seam. The distribution on day 294.9, Fig. 12 shows that although the burn is predominently near the top of the coal, there is some indication of burning in the bottom half of the seam especially at I-1.

A high flow test was run on day 295.5 - see Fig. 5. However, as can be seen in Fig. 9 the heating value did not change appreciably except for a temporary dip at the end of the test. No major changes in temperature were noted during this test.

During the high flow test we tried a period of water injection into the input well, P-1. From 1 to 2 gpm of water was injected which is almost equal to the natural influx. No measurable effect on any parameter was found. This is further evidence that the burn was near the top of the coal at this time.

By day 297, the burn front was close enough to the production well, I-0 so that the output gas temperature had reached 400°C and was still climbing. A small leak had developed in the grout seal around the well casing and the valve gaskets were being seriously overheated. An attempt was made to cool the gas by flooding wells DW-1 and DW-6. Although a slight decrease in well head temperature was noted, the main effect was to increase the production flow rate and to increase the heating

value of the gas to 150 Btu/cuft. This caused the flare stack temperature to climb so the attempt was stopped and the pumps turned back on.

Reducing the flow rate by cutting the input pressure helped to reduce the output temperature but it also caused a serious deterioration in the heating value of the gas. Raising the pressure did not restore the heating value to its original point and the deterioration continued. The compressor was shut down and the gasification experiment terminated on day 300. Figure 13 shows the temperature distributions at this time.

Gasification Results

Gasification proceeded for 11 days. During this time approximately 10 MMSCF of air were injected and 19 MMSCF (13.2 MMSCF dry) of gas were produced. Initial air injection pressure was approximately 70 psia which fell rapidly on the second day of operation to a value of 25-30 psia. Production pressures were generally about 5 psi lower. The rapid decrease in injection pressure was a result of the rapid increase in flow conductance of the formation.

The rapid change in conductance during the initial portion of the gasification is shown in Fig. 14. Just after ignition the relative conductance fell rapidly and then recovered to approximately 70% of its pregasification level and maintained this level for approximately 1/2 a day. At this point the rapid rise occurred and during the course of most of the gasification the conductance was 50 to 100 times its pregasification value.

Gas loses during the gasification were only significant during the early high pressure operations. Figure 15 shows the integrated gas recovery (based on a nitrogen balance) as a function of time. It shows an ultimate recovery of 93% of the injected nitrogen.

The dry gas composition, as measured by gas chromatograph, for the primary gas components are shown as a function of time in Figs. 16 and 17. A higher percentage of pyrolysis gases were apparently present during the first two days of the test resulting in a higher methane concentration. During the central portion of the tests gas composition was relatively stable. This was followed by a marked decline in CO, H_2, and CH_4 levels occurring near the end of the test as the oxidation zone approached the exhaust well. No influence on composition can be seen as a result of the high flow test. However, a definite change in the composition is indicated during and after the injection of the water slug. This consists of a rapid rise in hydrogen concentration followed by a rapid decline in H_2, CO, and CH_4.

Considerable quantities of water were produced from the area in the form and liquid and gas during the gasification test. Liquid water was produced by pumps located in the DW wells. Steam was produced from the gasification production well. The steam accounted for 30% of the total produced gas volume (see Fig. 18).

The burn geometry as deduced from the thermocouple data and coal consumption estimates is shown in Fig. 19a (plan view) and Fig. 19b (elevation view). The burn started at the bottom of well P-1 and was progressing horizontally towards well I-5 and also vertically toward the top of the seam. After the blow-out the burn went mostly along the top of the seam but also continued along the central line at lower elevation in the coal.

The total energy recovery in the form of combustible gas was 65% of that available from the estimated 128 tons of consumed coal. The total energy balance is shown in Fig. 20. Note that if the combustion energy estimated to be present in the produced tars is included as useable energy the total useful energy recovery becomes approximately 73%. The underground losses of heat energy were quite small. The largest energy loss from the system was due to the production of a considerable amount of steam.

Conclusions — A. Explosive Fracturing

Hoe Creek experiment No. 1 is probably one of the most thoroughly diagnosed fracture experiments ever performed by our laboratory. We feel that the general agreement between experiment and our one and two dimensional codes SOC and TENSOR is quite good in predicting the degree of fracture. There are still some details that are not clear. The layered appearance of the fracturing and the rather large scale asymetries as a function of azimuth from the shot points are hard to understand in what appears to be a very homogeneous coal seam.

Our knowledge of the relationship of degree of fracture to permeability is much less satisfactory. In fact, comparing the results from the Kemmerer and Hoe Creek experiments, it is obvious that total failure strain, (shear plus tensile), is not a reliable predictor of permeability. We are looking into the possibility that tensile failure (11) may be more directly related to permeability.

The results from the Hoe Creek experiment indicate that spherical HE shots placed at the bottom of the coal seam will not produce a permeability distribution that is suitable for gasification. Other geometries and types of explosive fracture are under consideration for future experiments. (12)

Conclusions — B. Gasification

Forward combustion gasification was achieved without any problem of plugging of the formation. After two days of operation, flow conductivity was an order of magnitude above pre-gasification levels. However, even before this short circuit condition was reached, plugging did not seem to be serious.

Injecting air at well I-0 resulted in unacceptably high losses. Reversing the flow direction for gasification so that well I-0 was kept as close to atmospheric pressure as possible reduced the overall loss rate to 7%.

The short circuiting of the flow which occurred after 28 hours of gasification, limited the total volume of coal gasified.

The gas composition, gas heating value and oxygen utilization were all fairly constant during the course of the burn. Marked change occurred only at the end of the experiment. Gas composition was not influenced by doubling the air injection rate.

The total water influx into the gasification region was about 65% of the pre-gasification level. About 30% of this amount entered the hot zone. However, this water influx did not appear to influence the product gas composition, indicating that it mixed with the hot gas after the reactions were completed. However, the influx of water into the system may have limited the amount of coal recovered by limiting the lateral spreading of the burn zone.

Energy recovery in the form of produced products amounted to 75% of the energy in the consumed coal. There were essentially no losses to the subsurface formation. The greatest energy loss took the form of the production of steam.

"Reference to a company or product name does not imply approval or recommendation of the product by the University of California or the U.S. Energy Research & Development Administration to the exclusion of others that may be suitable."

NOTICE

"This report was prepared as an account of work sponsored by the United States Government. Neither the United States nor the United States Energy Research & Development Administration, nor any of their employees, nor any of their contractors, subcontractors, or their employees, makes any warranty, express or implied, or assumes any legal liability or responsibility for the accuracy, completeness or usefulness of any information, apparatus, product or process disclosed, or represents that its use would not infringe privately-owned rights."

REFERENCES

(1) G. H. Higgins, "A New Concept for In Situ Coal Gasification," Lawrence Livermore Laboratory, Rept. UCRL-51217 (1972).

(1a) D. R. Stephens, F. O. Beave and R. W. Hill, LLL In Situ Coal Gasification Program, Lawrence Livermore Laboratory, Rept. UCRL-78308 (1976); also in Proceedings 2nd Underground Coal Gasification Symposium, Morgantown, W. Va., August, 1976.

(2a) J. R. Hearst, T. Butkovich, E. Laine, R. Lake, D. Leach, J. Lytle, J. Sherman, D. Snoeberger, R. Quong, "Fractures Induced by a Contained Explosion in Kemmerer Coal," Int. J. Rock Mech. Min. Sci. & Geomech. Abstr. Vol. 13, pp. 37-44, Pergamon Press 1976. Printed in Great Britian.

(2b) T. Butkovich, "Correlation Between Measurement and Calculations of High Explosive Induced Fracture in a Coal Outcrop," Lawrence Livermore Laboratory, Rept. UCRL-76984 (1975).

(3) LLL In Situ Coal Gasification Program, Quarterly Progress Report, July through September 1975, Lawrence Livermore Laboratory, Rept. UCRL-50026-75-3 (1975).

(4) Randolph Stone, David F. Snoeberger, "Evaluation of the Native Hydraulic Characteristics of the Felix Coal (Eocene, Wasatch Formation) and Associated Strata, Hoe Creek Site, Cambell County, Wyoming, Lawrence Livermore Laboratory, Rept. UCRL-51992.

(5) LLL In Situ Coal Gasification Program, Quarterly Progress Report, October through December 1975, Lawrence Livermore Laboratory, Rept. UCRL-50026-75-4 (1976).

(6) R. W. Hill and C. B. Thorsness, UCRL (in preparation).

(7) LLL In Situ Coal Gasification Program, Quarterly Progress Report, January through March 1976, Lawrence Livermore Laboratory, Rept. UCRL-50026-75-4 (1976).

(8) LLL In Situ Coal Gasification Program, Quarterly Progress Report, July through September 1976, Lawrence Livermore Laboratory, Rept. UCRL-50026-76-3 (1976).

(9) D. F. Snoeberger, Field Hydroles, Test of Explosively Fractured Coal, Lawrence Livermore Laboratory, Rept. UCRL-78957 (1977).

(10) LLL In Situ Gasification Program, Quarterly Report, April through June, 1976, Lawrence Livermore Laboratory, Rept. UCRL-50026-76 (1976).

(11) T. R. Butkovich, Calculation of Fracture and Permeability Enhancement from Underground Explosions in Coal, Lawrence Livermore Laboratory, Rept. UCRL-77945.

(12) T. R. Butkovich (in preparation).

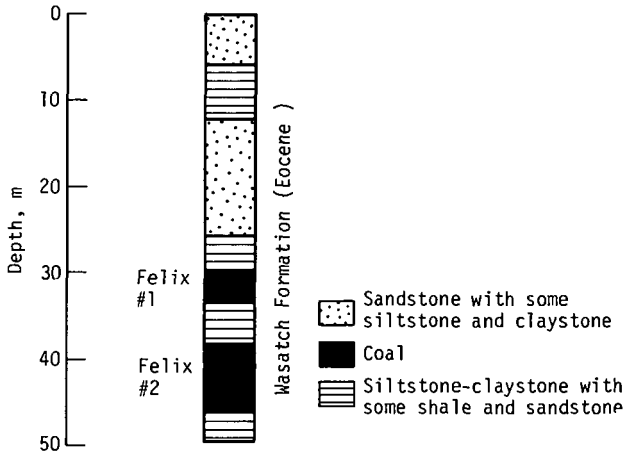

Fig. 1 Site stratigraphy obtained from cored wells.

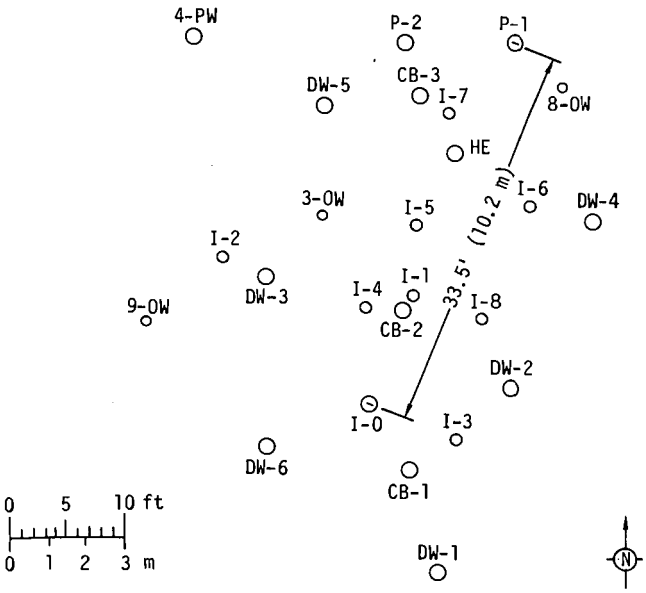

Fig. 2 Hoe Creek Experiment I plan view showing bottom hole locations. Well 3-OW was sealed off before gasification.

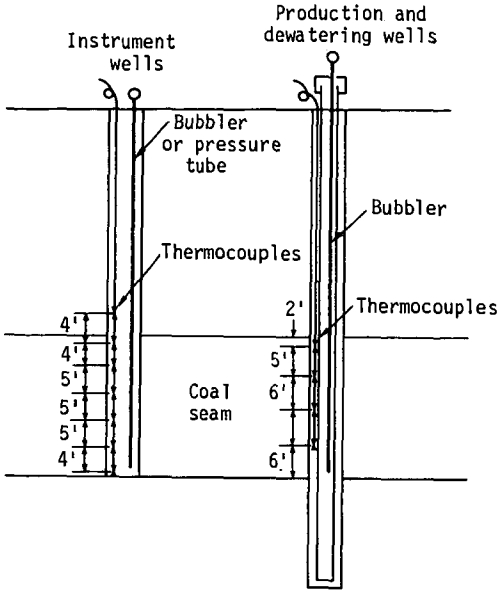

Fig. 3 Typical subsurface instrument placement.

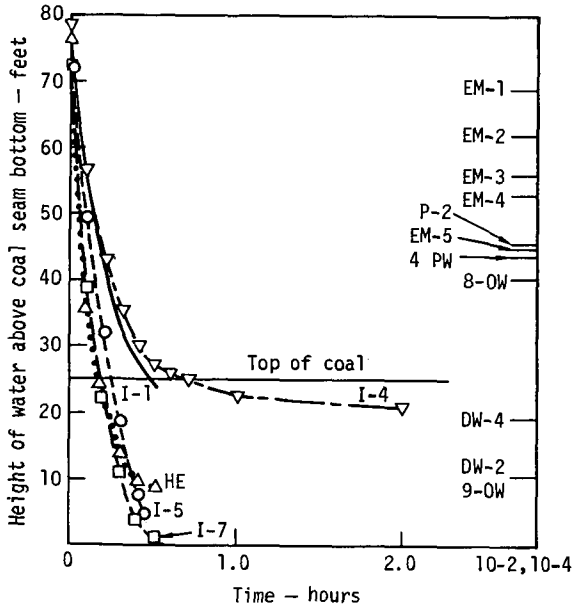

Fig. 4 Water levels at several locations within the fracture zone as a function of time after the start of dewatering. The levels indicated on the right are those reached after three to five days of pumping.

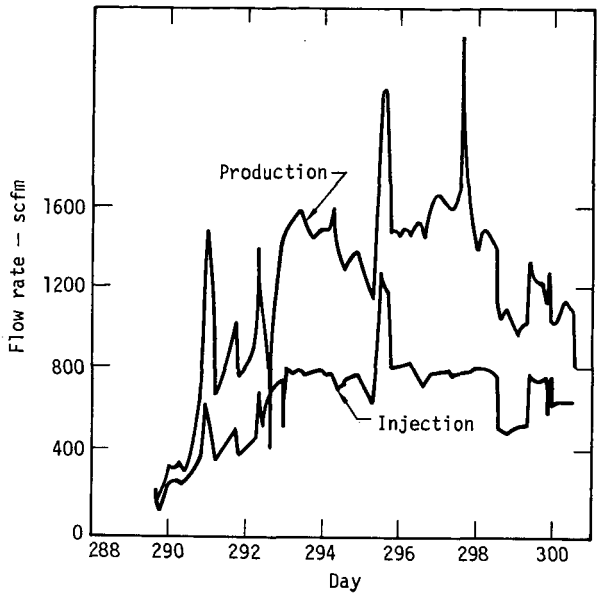

Fig. 5 Injection and production flow rates for the entire gasification experiment. The production flow was calculated from a nitrogen balance for the period 291.4-292.2 when the production flow meter was bypassed.

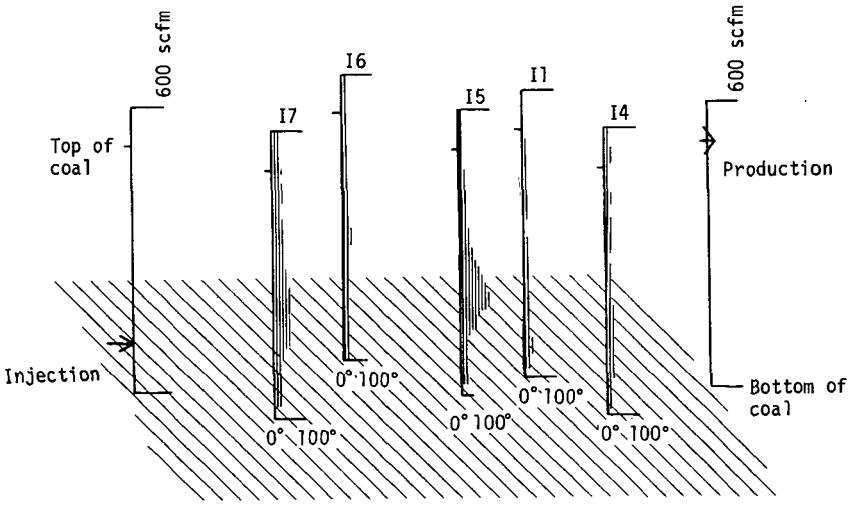

Fig. 6 Temperature profiles in the instrument wells on day 289.74. The wells are shown in relative positions in the coal seam. The vertical distance scale factor is twice the horizontal scale factor. The length of the arrows marking injection and production points are proportional to the flow rates.

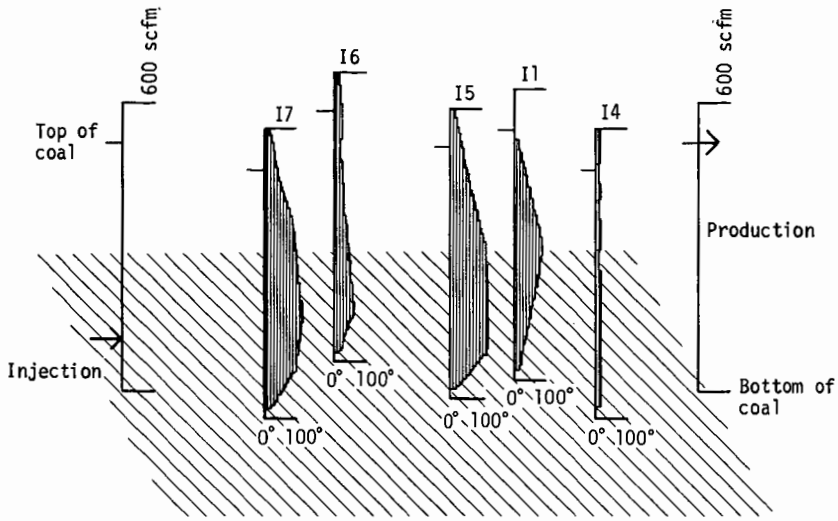

Fig. 7 Temperature profiles in the instrument wells on day 290.60. The wells are shown in relative positions in the coal seam. The vertical distance scale factor is twice the horizontal scale factor. The length of the arrows marking injection and production points are proportional to the flow rates.

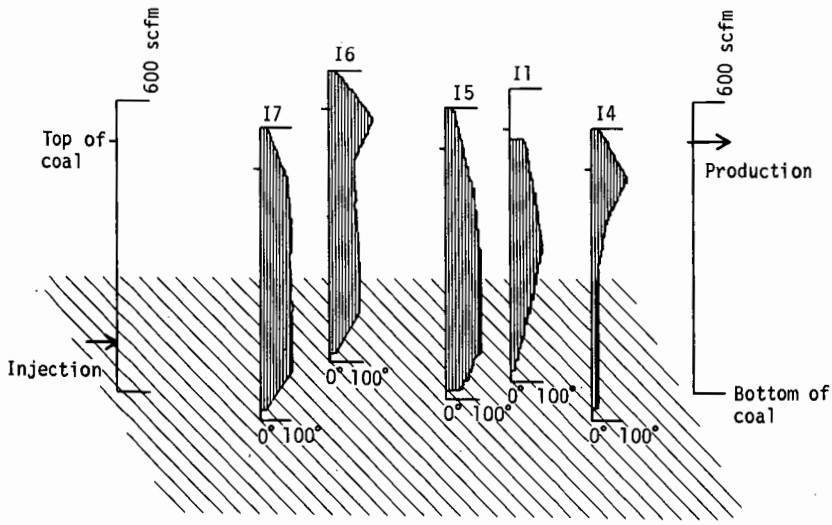

Fig. 8 Temperature profiles in the instrument wells on day 291.2. The wells are shown in relative positions in the coal seam. The vertical distance scale factor is twice the horizontal scale factor. The length of the arrows marking injection and production points are proportional to the flow rates.

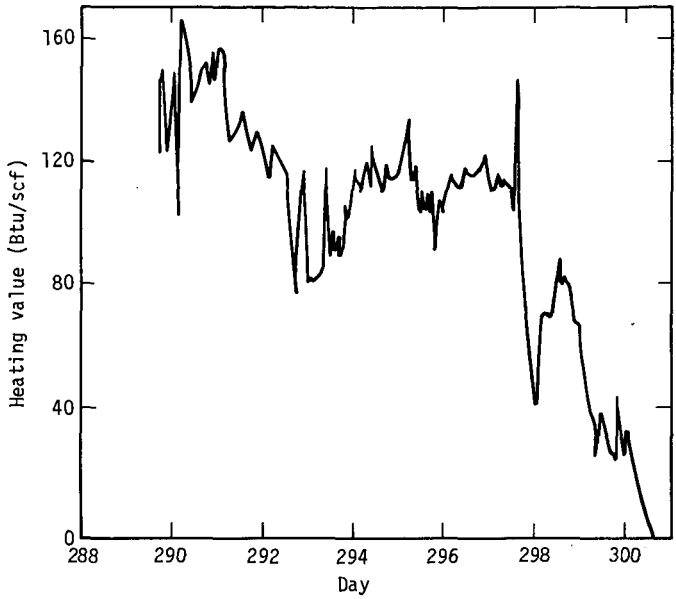

Fig. 9 Dry gas heating value during gasification.

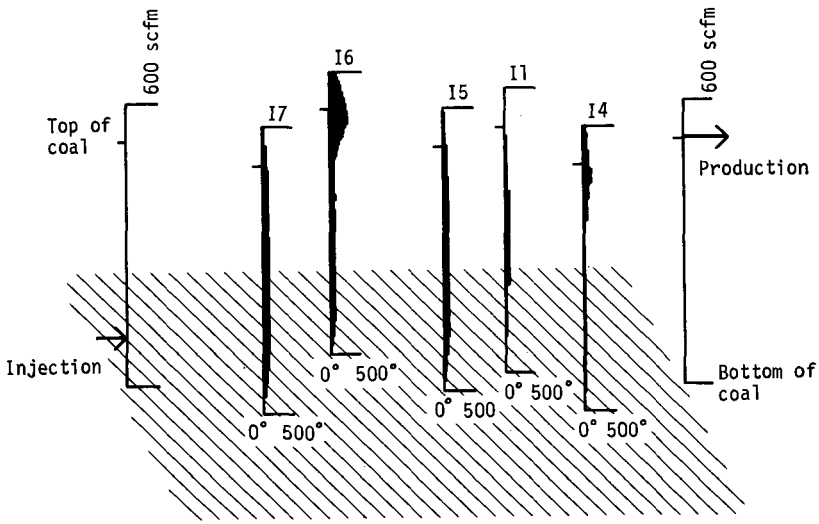

Fig. 10 Temperature profiles in the instrument wells on day 291.70. The wells are shown in relative positions in the coal seam. The vertical distance scale factor is twice the horizontal scale factor. The length of the arrows marking injection and production points are proportional to the flow rates.

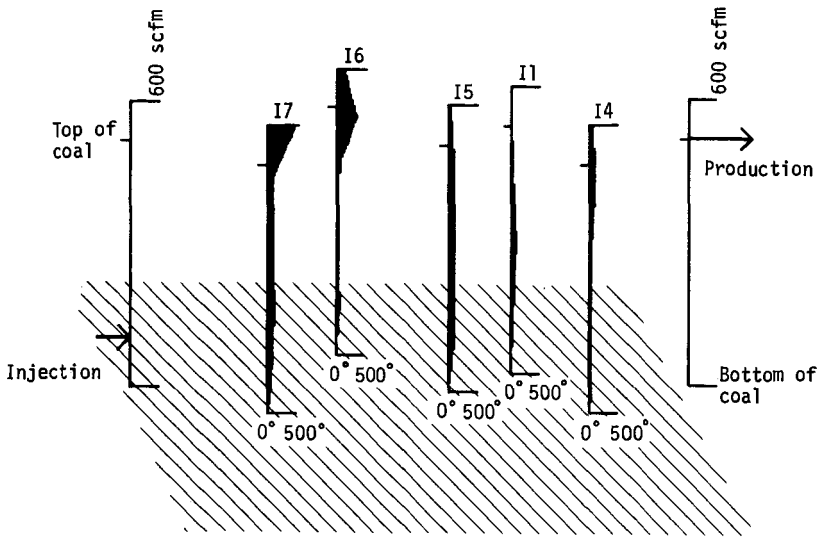

Fig. 11 Temperature profiles in the instrument wells on day 292.94. The wells are shown in relative positions in the coal seam. The vertical distance scale factor is twice the horizontal scale factor. The length of the arrows marking injection and production points are proportional to the flow rates.

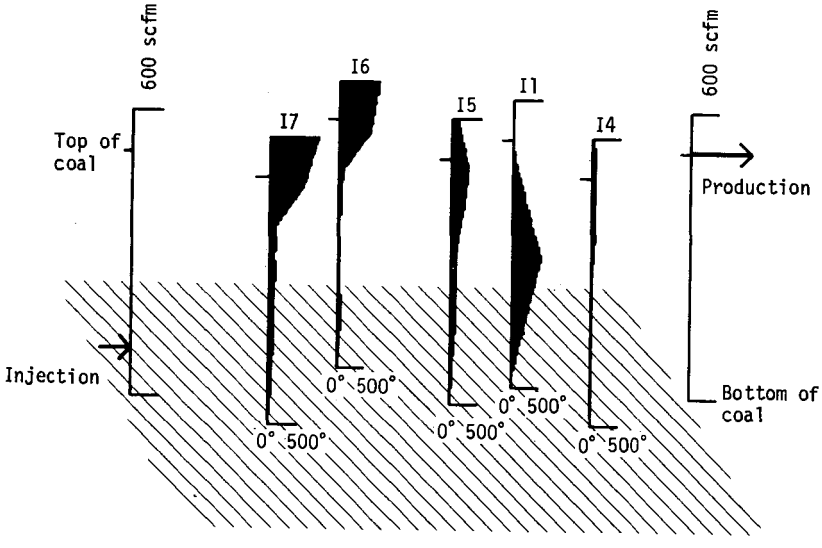

Fig. 12 Temperature profiles in the instrument wells on day 294.94. The wells are shown in relative positions in the coal seam. The vertical distance scale factor is twice the horizontal scale factor. The length of the arrows marking injection and production points are proportional to the flow rates.

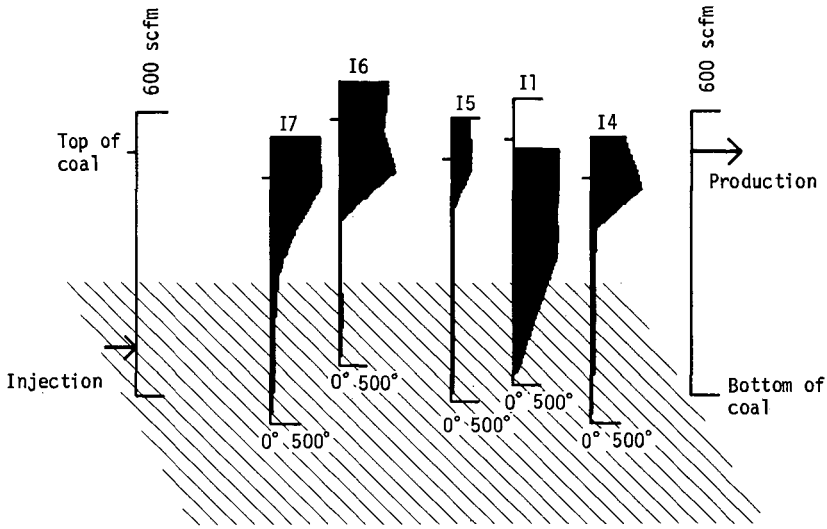

Fig. 13 Temperature profiles in the instrument wells on day 300.26. The wells are shown in relative positions in the coal seam. The vertical distance scale factor is twice the horizontal scale factor. The length of the arrows marking injection and production points are proportional to the flow rates.

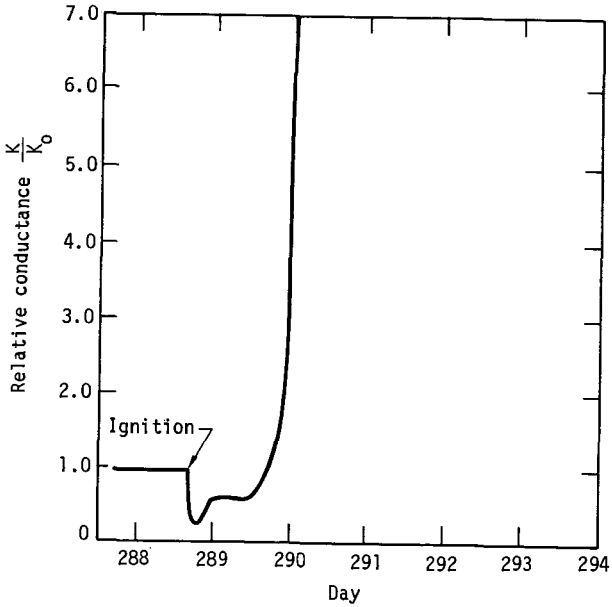

Fig. 14 Relative formation conductance between injection and production well.

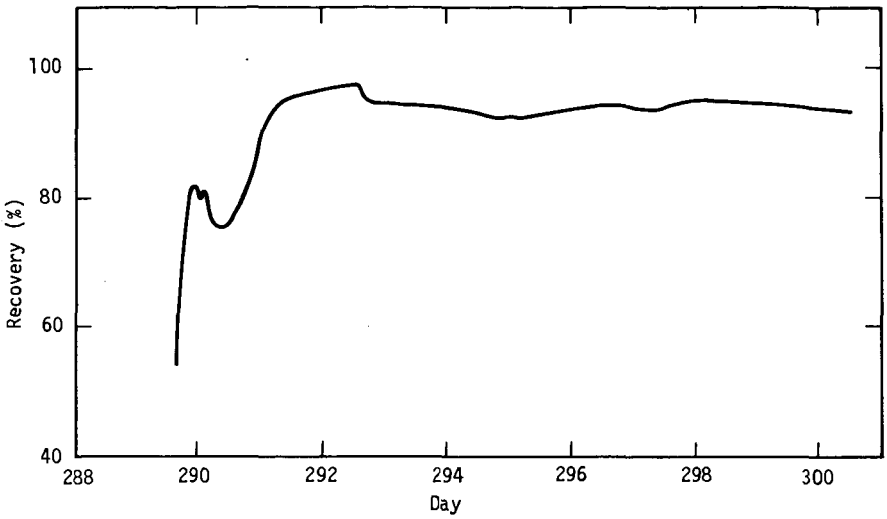

Fig. 15 Integral percent gas recovery during gasification.

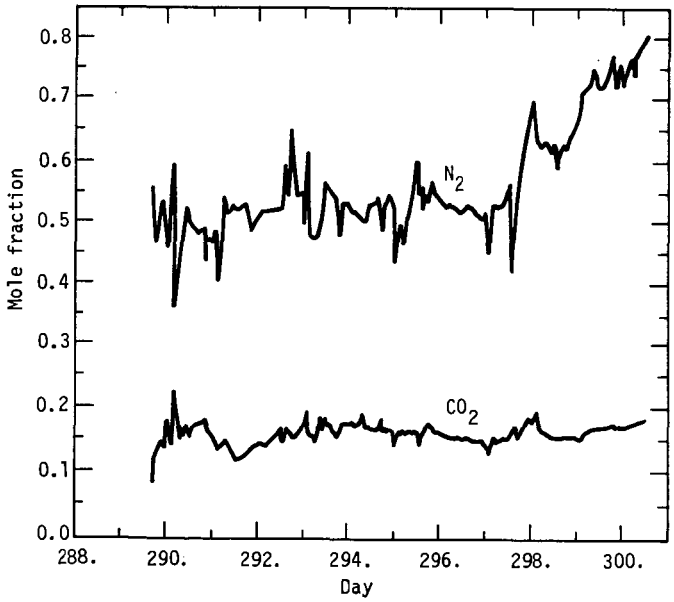

Fig. 16 Dry gas mole fractions of N_2 and CO_2 in product gas.

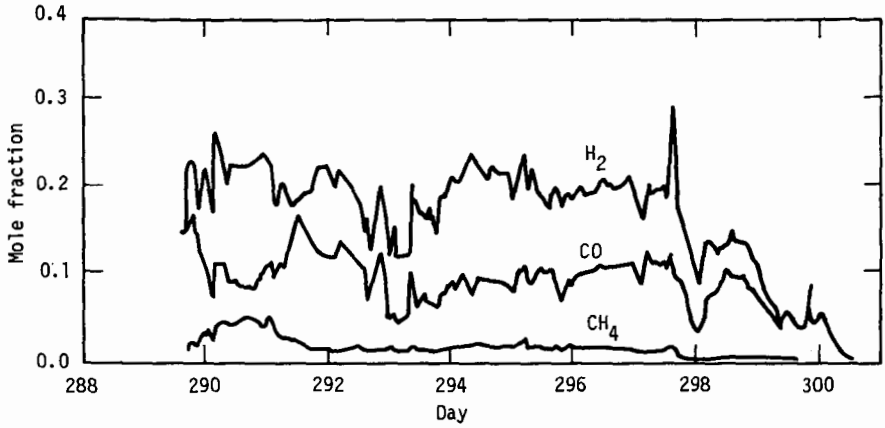

Fig. 17 Dry gas mole fractions of H_2, CO, and CH_4 in product gas.

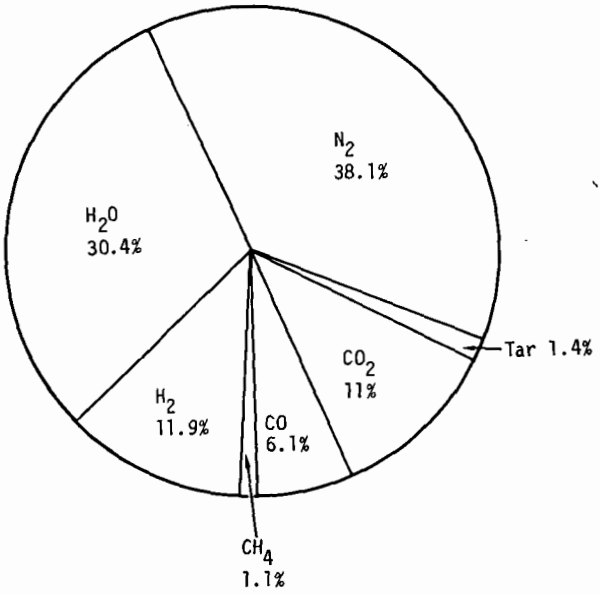

Fig. 18 Major gas product distribution on a mole basis.

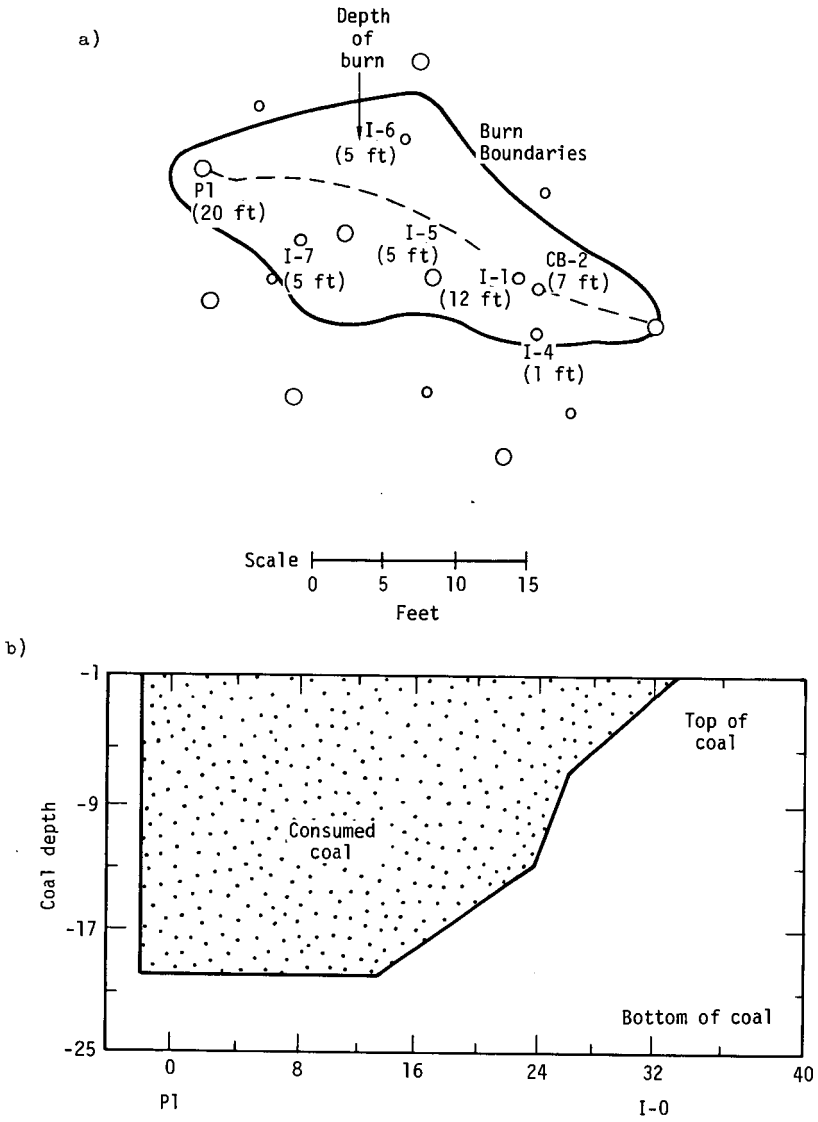

Fig. 19 a) Plan view, and b) centerline elevation view of gasified volume as estimated from temperature measurements. The depths given in parentheses indicate burn depth at that point.

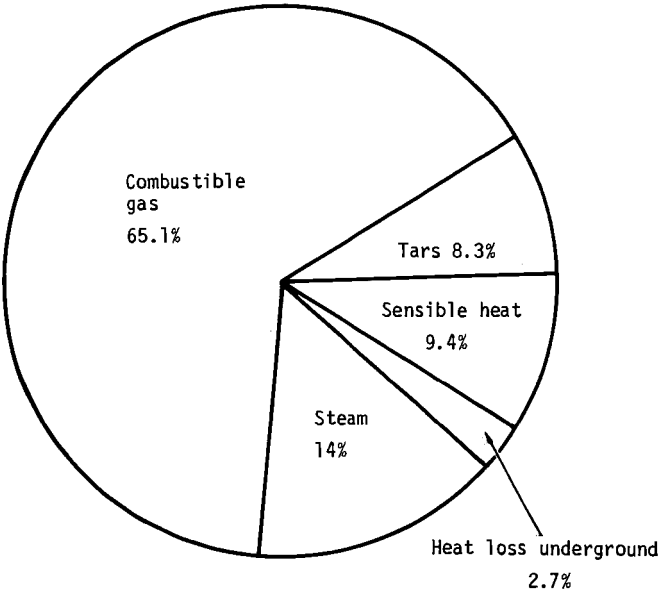

Fig. 20 Energy distribution in the gasification as a percent of consumed coal energy.

FIELD HYDROLOGICAL TESTS OF EXPLOSIVELY FRACTURED COAL*

D. F. Snoeberger

Lawrence Livermore Laboratory, University of California
Livermore, California 94550

INTRODUCTION

Hydrologic tests were made in the explosively fractured Felix No. 2 coal seam on part of the Lawrence Livermore Laboratory in-situ coal gasification experiment at the Hoe Creek site 24 km SW of Gillette, Wy. (1) The purposes were to evaluate wells and regions to be gasified and to gain information for improvement of explosive effects predictions.

In this paper related prior work is summarized and preliminary interpretations of the post-fracturing hydrological tests are given.

REVIEW OF PRIOR FIELD WORK

Hydrogeology (2,3)

The subbituminous Felix coal occurs within the Eocene Wasatch Formation and at the experimental site consists of two nearly horizontal seams, Felix No. 1 and Felix No. 2 in descending order. They are of nearly constant thickness, 3 m and 7.6 m respectively, and separated by approximately 5 m of siltstone-claystone unit. The Felix No. 2 is underlain by at least 3 m of a claystone-shale unit. A typical lithologic sequence of near-surface strata is shown in Fig. 1.

The water table is approximately 23 m above the top of the Felix No. 2 coal which can be characterized as a leaky anisotropic aquifer. Its average horizontal fracture permeability is 0.3 darcy. Its axis of maximum permeability (0.4 darcy) trends N59°E corresponding approximately to the average bearing, N70°E, of the most prominent set of vertical fractures (face cleat). Table 1 lists these and other results for the coal and associated strata. Surface locations of test wells are shown in Fig. 2.

Explosive Fracturing and Permeability (4)

Two charges, each of 340 kg of explosive, were fired simultaneously on Nov. 5, 1975, in the bottom 1.5 m of the coal (Wells HE and INJ,** Fig. 3). The horizontal separation was 7 m.

At this time, predicted pattern of permeability enhancement in the horizontal plane of the charges showed a joined region of 100 darcies or greater at the charge locations and a decrease of permeability with distance out to the native coal (0.3 darcy) at approximately 13 m. Other possible effects combinations were recognized including compaction at a distance around each charge and decreases in permeability due to generation of finely sized particles.

*This work was performed under the auspices of the U.S. Energy and Research Development Admin. Contract W-7405-Eng-48.

**Later redesignated I-O.

Table 1. Hydraulic characteristics[a] of Felix coal and associated strata, Hoe Creek site, pre-shot.

Stratum	Horizontal permeability darcy	Coefficient of storage	Vertical permeability darcy
Felix No. 1	0.47 to[b] 1.42[c]	2×10^{-2}	—
Strata between Felix No. 1 and No. 2	0.12[c]	2.24×10^{-3}[d]	0.022[d]
Felix No. 2	0.41[e] 0.23[f]	1.18×10^{-3}	—
Strata below Felix No. 2	—	—	<0.0015[g]

[a]Dashes indicate that no measurement was made.

[b]A range of values is given for two different-type single-well tests in the same well.

[c]Results from slug-injection tests.

[d]Values are averages for the total thickness of strata between Felix No. 1 and Felix No. 2 coals.

[e]Value along the axis of maximum hydraulic conductivity, which trends N 59° E.

[f]Value along the axis of minimum hydraulic conductivity, which trends N 31° W.

[g]Refers to average values for first 2.1 m of strata below bottom of Felix No. 2 coal.

Initial Post Fracturing Hydrologic Tests (4,8)

We tried pulse tests and sustained constant-rate pumping (drawdown) tests to measure permeability in the heterogeneous explosive-fractured region. Both showed average enhanced permeabilities of 2-4 darcy for assumed radially symmetric regions. Definition was limited by number of observation wells and locations. Analysis of pumping tests was by drawdown difference between wells after the rate of change had slowed (quasi-steady-state). A repeated pumping test gave higher results but within a factor of 2 for most observation wells. Results are shown in Table 2.

Observation of unchanging hydraulic head in the Felix No. 1 coal (Well 12-OW) during testing indicated that there had been no major change in vertical leakage into the Felix No. 2 coal attributable to the explosive fracturing.

These results along with air-flow tests and new computer calculations of fracturing were the base for field modifications for a gasification test.

Table 2. Results of initial post-fracturing permeability tests. Analysis was by drawdown difference at a fixed late time except as noted.

Pumped well	Observed well	Permeability darcy
9-OW	3-OW	3.0
	8-OW	2.2
9-OW (2 min pulse)	3-OW	2.3
	8-OW	2.3
INJ (NOV)	I-1	1.5
	3-OW	1.7
	9-OW	3.3
	HE	1.6
	8-OW	1.7
	4-PW	0.7
INJ (DEC)	I-2	3.3
	3-OW	4.2
	HE	2.7
	8-OW	3.4

Modified Well Pattern, Completions and Instruments (5,6,7)

In preparation for gasification along the INJ-HE axis, a pattern of dewatering wells, production well* and instrument wells was provided. Figure 4 shows the locations as completed. Figure 5 shows the surface locations of 5 environmental monitoring wells placed at 2 distances, approximately 15 m and 30 m out. Well completions were such that the injection and dewatering wells could be approximated as fully penetrating the Felix No. 2 coal and well P-1 as partially penetrating, open in the bottom 1.5 m of the coal. Typical wells are shown in Fig. 6. The dewatering, production and environmental wells were cleaned and developed by methods similar to those used for the pre-shot hydrology wells. (2) Bubbler tubes ended near the base of the coal. Bubblers were equipped with metered nitrogen gas supplies and pressure transducers for hydraulic head measurement and transmission. All available wells and instrument holes were provided bubblers with the exception of the five environmental wells in which we used well sounders manually. Pumps, piping and instruments were arranged to provide for hydraulic testing as well as gasification use. Data recording equipment consisted of strip chart recorders and a data acquisition computer with magnetic and printed paper-tape outputs, all in parallel.

Post Explosion Core Sampling (7)

In order to obtain more information on fracturing, four cores had been taken completely through the Felix No. 2 coal seam at locations 1.8 m to 2.7 m from shot sites. All were found to be similar in appearance, with moderate to heavy fracturing in the top of the coal, followed by a less fractured zone, and then by a heavily

*Designated PROD-1 initially and changed to P-1 later.

fractured zone in the bottom 1.5 m to 3 m. The core between the explosives locations showed the most fracturing, the core farthest away from either exhibited the least fracturing.

PRE-GASIFICATION HYDROLOGICAL TESTS (7)

Summary of Results and Discussion

During development we found an unacceptably low water flow rate into well P-1, 0.006 ℓ/sec (0.1 gpm). We reviewed possible causes and made contingency plans for remedial work on P-1 and drilling of a diagnostic and potential replacement well, P-2. We suspected cement intrusion or completion in a low permeability region.

Consideration of the fracturing pattern as shown by the core samples and of flow behavior in upper and lower portions of the Felix No. 2 coal during drilling and earlier well tests before and after explosive fracturing led to the interpretation that although flows in the native coal were reasonably homogeneous vertically, post-explosion flow conditions were not uniform. While cracks created by the explosion may promote high flows in the upper regions, fines generated by the explosions tend to restrict or plug flow in the lower regions.

We enlarged P-1 to 1 m diameter in the bottom 1.5 m of coal and found that it produced 0.06 ℓ/sec (1 gpm), still less than desired. This work required removal of the screen and sump liner. We next drilled well P-2 in three stages of depth in the Felix No. 2 coal for flow measurements. The top half produced 0.4 ℓ/sec (7 gpm); the next quarter produced 0.02 ℓ/sec (0.3 gpm), the bottom half 0.03 ℓ/sec. This indicated lower permeability in the bottom part of the coal at least in the vicinity.

We then reinstalled the sump liner in P-1. While washing the liner in place a path opened hydraulically. Test flow was 0.63 ℓ/sec (10 gpm). A short pumping test of P-1 drew the water levels in I-5 and P-1 well into the coal, indicating a channel in the lower half of the coal (Fig. 7) across the shot region at HE. We could proceed with hydrological tests of the overall region and wells.

The specific capacity of the dewatering wells ranged from 0.7 to 7 gpm per ft of drawdown. Wells DW-1 and DW-6 showed the highest capacities. Results are in Table 3.

Graphical interpretations of drawdown tests by pumping I-0 and P-1 at constant rates show two regions of enhanced permeability, one about each of the explosion centers out to 3 m and a region of intermediate enhancement on out to the native coal at 15 m. The permeabilities obtained are: 14 darcy and 7 darcy respectively for regions at I-0 and P-1; and 1.5 darcy for the intermediate region. Figures 8 and 9 show these graphs.

Table 3. Relative performance of dewatering wells.

Well No.	Specific capacity (gpm/ft)
DW-1	0.71
DW-2	0.15
DW-3	0.07
DW-4	0.19
DW-5	0.07
DW-6	0.59

The apparent discontinuity shown in Fig. 9, for the data within 10 ft, may be due to the channel opened in final work on P-1 and to its non-symmetrical location.

The same method of analysis of drawdown tests of dewatering wells gave lower results for the inner (core) regions and higher values for the intermediate region. This is apparently a result of nonuniformity of flow field about the dewatering wells.

Late time drawdown data indicated some vertical leakage from the unit above the coal but again, approximately the same as pre-shot. Estimated vertical permeability values of 3 to 5 md were obtained.

Short, simultaneous injection-withdrawal tests (2-well recirculation) were made to investigate the permeability in the I-O and HE regions. These tests were analyzed utilizing flow net techniques. Drawdown equipotentials were plotted on a plan view and selected flow lines drawn perpendicular to the equipotentials. Permeabilities of different areas were calculated by the gradient method wherein the gradient was obtained from the equipotential surface and the flow was apportioned via the flow net construction. An areal or field permeability K is calculated from the equation $K = Q/iA$, where Q is the flow in a region, i is the hydraulic gradient in that region, and A is the vertical section of the region through which the flow passes. Figures 10 and 11 are flow nets drawn for pumping P-1 to I-O and DW-4 to DW-6.

Figure 12 is a composite prepared from results of flow net analyses and drawdown tests. The estimates of permeability for the inner core regions, 10 d at HE and 20 d at I-O, and the near native zone, 0.5 d, between the explosion centers are from the flow nets. The flow net and drawdown results for the inner enhanced permeability regions are consistent. The dashed lines on Fig. 12 connect well pairs in which the closeness of movement of water level during drawdown testing indicate a fracture or flow channel between them. The P-1 to I-O test does not show the low permeability zone between explosion centers seen in the DW-4 to DW-6 test because of the symmetrical placement of the zone with respect to pumping from P-1 to I-O.

Analysis of the hydraulic response of the explosive-fractured coal is complicated by the strong radial variation of permeability and the presence of many relatively large sized well casings. In addition some of the fractures have become conduit-like in their ability to equalize pressure between certain observation well pairs or cause an uneven distribution of flow when one of the pair is a pumped well.

Figure 13 shows an outline of the gasification path indicated by thermocouple data on a simplified version of the composite sketch. The composite suggests a more westerly veering path to avoid the intermediate near native zone of coal.

Further evaluation and interpretation of the hydrological data are needed and a comparison with post burn core sample results when available.

The critical importance of permeabilities and their distribution is that the in-situ flow paths and thus the reaction zone configuration are determined by them. A given permeability net tends to determine ultimate resource recovery efficiency. In view of the importance of the deduced permeability net, it is important to further develop field tests and analysis techniques. Simple methods for measurement of the absolute or relative local permeabilities at several depths through a fractured seam are needed.

REFERENCES

(1) Charles B. Thorsness, Richard W. Hill, and Douglas R. Stephens, "Preliminary Results from an In-Situ Coal Gasification Experiment Using Explosive Fracturing," Preprint, Joint ACS-CIC Conf., Montreal, Canada, May 29, 1977.

(2) Randolph Stone and David F. Snoeberger, "Evaluation of the Native Hydraulic Characteristics of the Felix Coal (Eocene, Wasatch Formation) and Associated Strata, Hoe Creek Site, Campbell County, Wyoming," Lawrence Livermore Laboratory, Rept. UCRL-51992, Jan. 8, 1976.

(3) Randolph Stone and David F. Snoeberger, "Cleat Orientation and Areal Hydraulic Anisotropy of a Wyoming Coal Aquifer," Lawrence Livermore Laboratory, Rept. in preparation.

(4) LLL In-Situ Coal Gasification Program Quarterly Progress Report, October through December, 1975, Lawrence Livermore Laboratory, Rept. UCRL-50026-75-4 (1976).

(5) LLL In-Situ Coal Gasification Program Quarterly Progress Report, January through March, 1976, Lawrence Livermore Laboratory, Rept. UCRL-50026-76-1 (1976).

(6) LLL In-Situ Coal Gasification Program Quarterly Progress Report, April through June, 1976, Lawrence Livermore Laboratory, Rept. UCRL-50026-76-2 (1976).

(7) LLL In-Situ Coal Gasification Program Quarterly Progress Report, July through September, 1976, Lawrence Livermore Laboratory, Rept. UCRL-50026-76-3 (1976).

(8) Albert E. Sherwood, R. Quong, and D. F. Snoeberger, "Permeability of Explosive Fractured Coal — Aquifer Modeling and Analysis of Field Hydraulic Data," Lawrence Livermore Laboratory, Rept. in preparation.

NOTICE

"This report was prepared as an account of work sponsored by the United States Government. Neither the United States nor the United States Energy Research & Development Administration, nor any of their employees, nor any of their contractors, subcontractors, or their employees, makes any warranty, express or implied, or assumes any legal liability or responsibility for the accuracy, completeness or usefulness of any information, apparatus, product or process disclosed, or represents that its use would not infringe privately-owned rights."

"Reference to a company or product name does not imply approval or recommendation of the product by the University of California or the U.S. Energy Research & Development Administration to the exclusion of others that may be suitable."

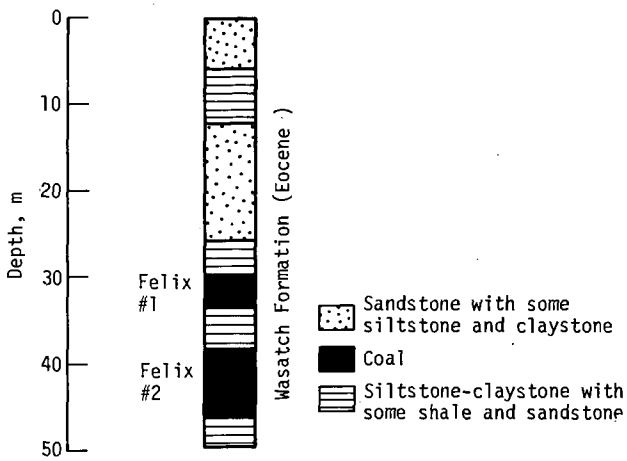

Fig. 1 Typical sequence of near-surface strata of the Hoe Creek site.

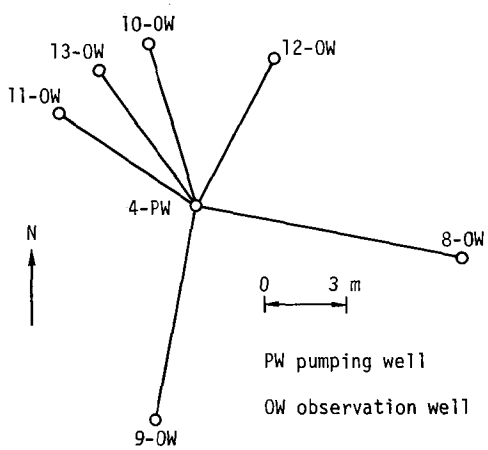

Fig. 2. Surface locations of test wells

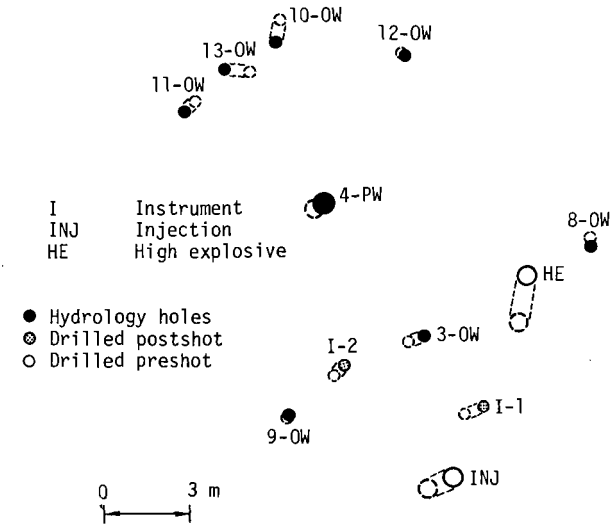

Fig. 3. Hole locations related to explosive fracturing. Dashed circles indicate positions of hole bottoms.

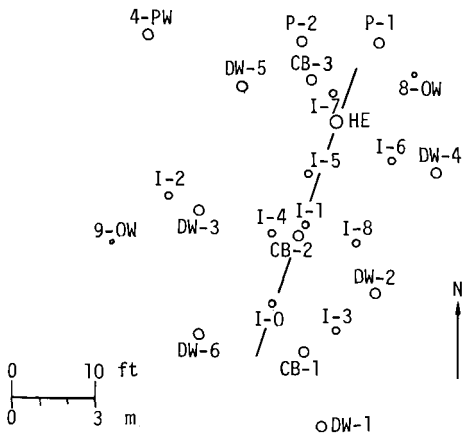

Fig. 4. Locations of wells and core holes (I-8, CB-1, -2, -3).

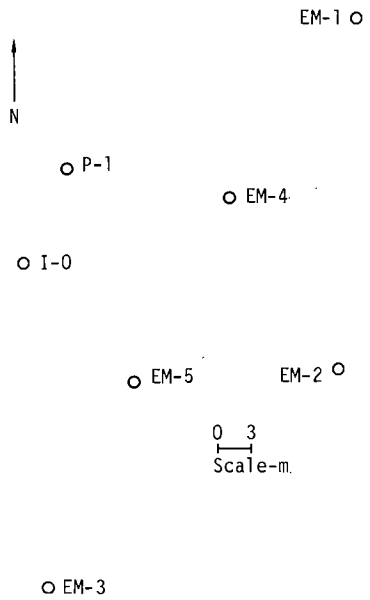

Fig. 5. Surface locations of environmental monitoring (EM) wells, 15 m and 30 m out from I-O and P-1.

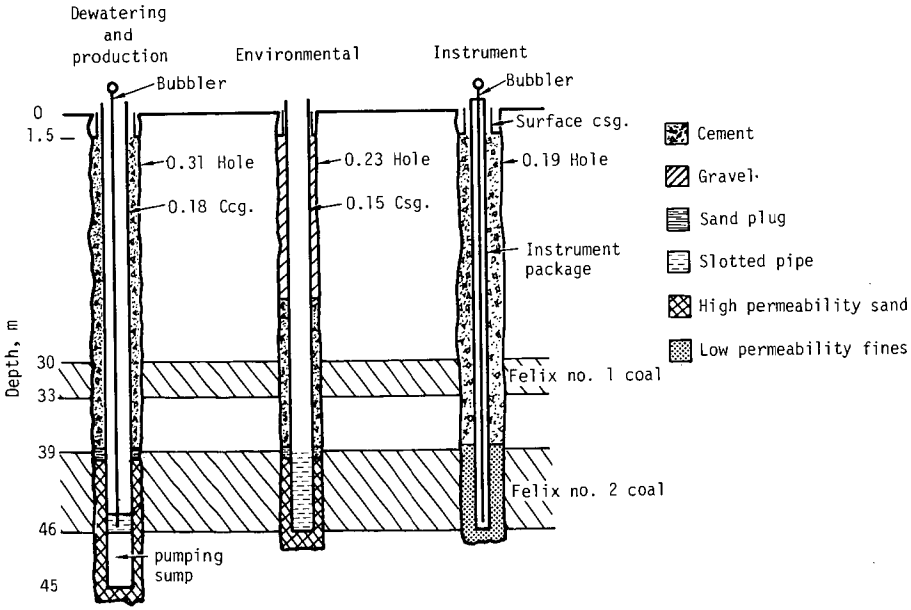

Fig. 6. Typical well and instrument completions. Dimensions are in meters.

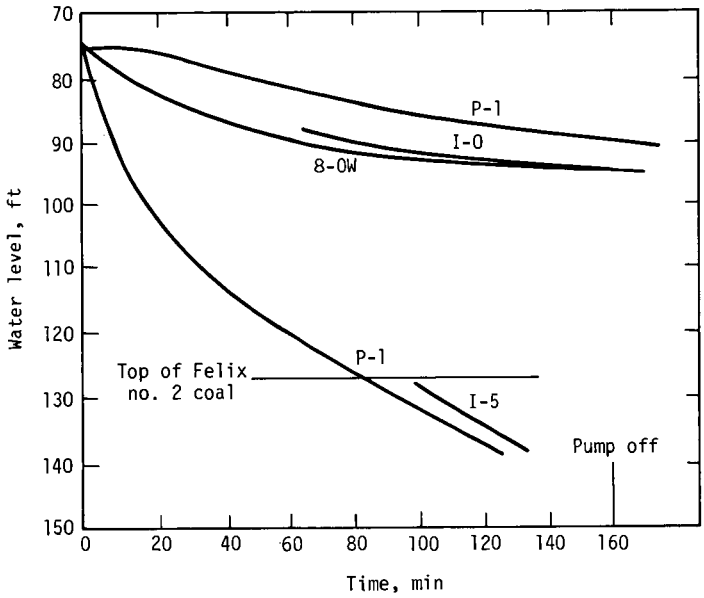

Fig. 7. Water level drawdowns by pumping well P-1 at 0.63 ℓ/sec (10 gpm).

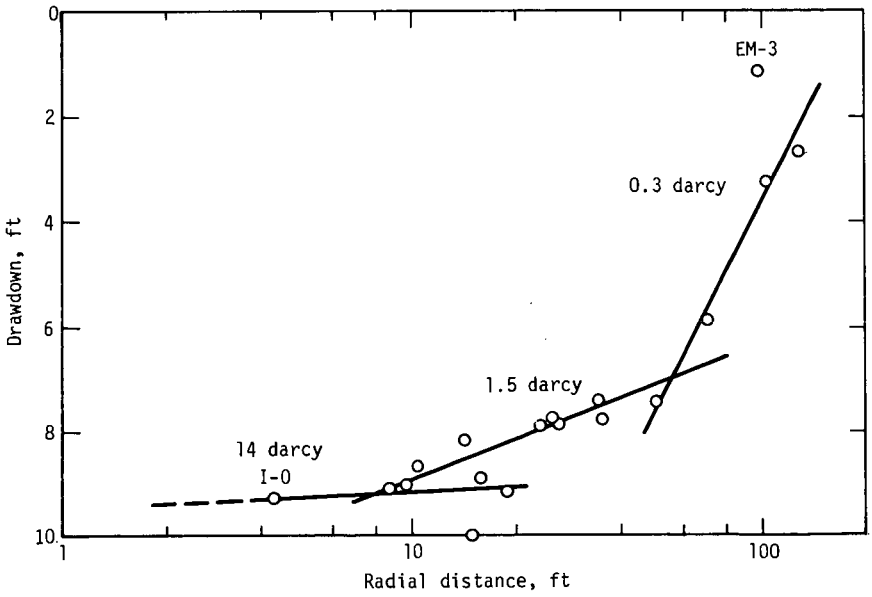

Fig. 8. Drawdowns, by pumping I-0 at 3 gpm, versus radial distance from I-0.

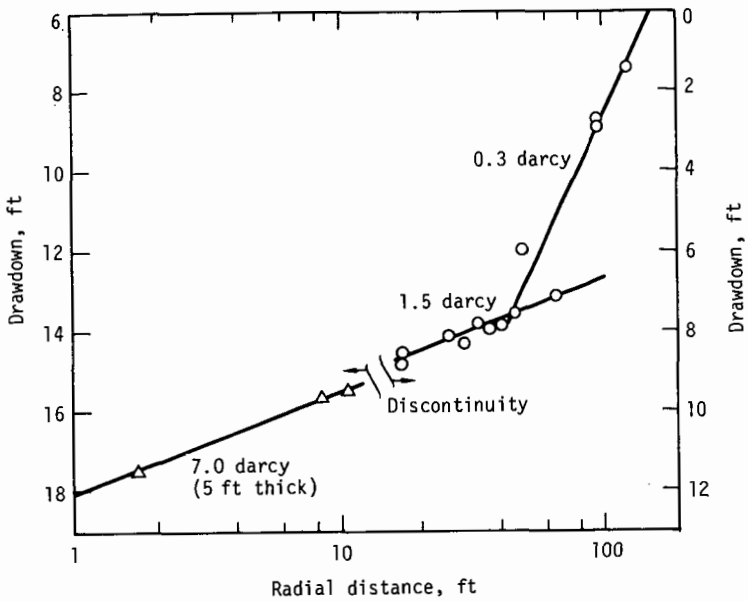

Fig. 9. Drawdowns, by pumping P-1 at 3.2 gpm, versus radial distance from P-1.

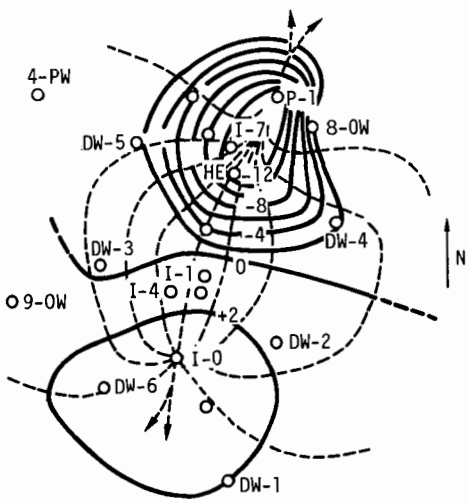

Fig. 10. Flow net. Hydraulic head (potential) contours and flow lines indicated by pumping 15 gpm from P-1 into I-0.

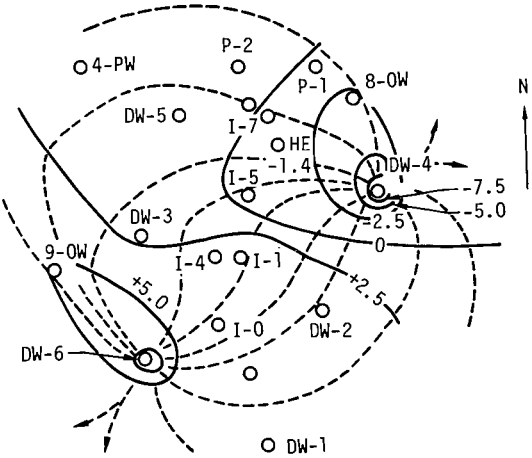

Fig. 11. Flow net. Hydraulic head (potential) contours and flow lines indicated by pumping 7.2 gpm from DW-4 into DW-6.

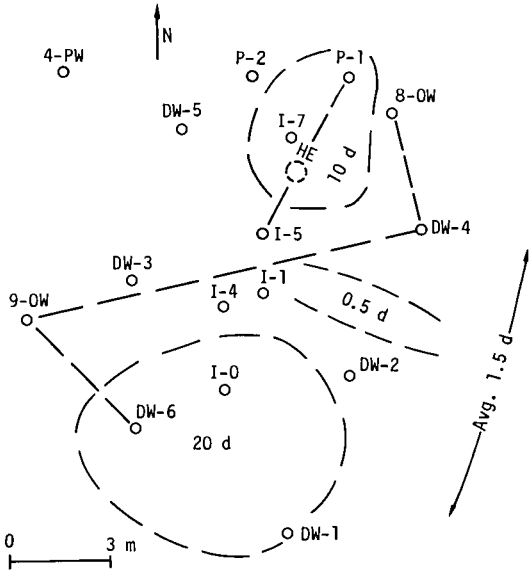

Fig. 12. Heuristic composite of channels or fractures (dashed lines), inner enhanced regions and near native zone between the explosion centers.

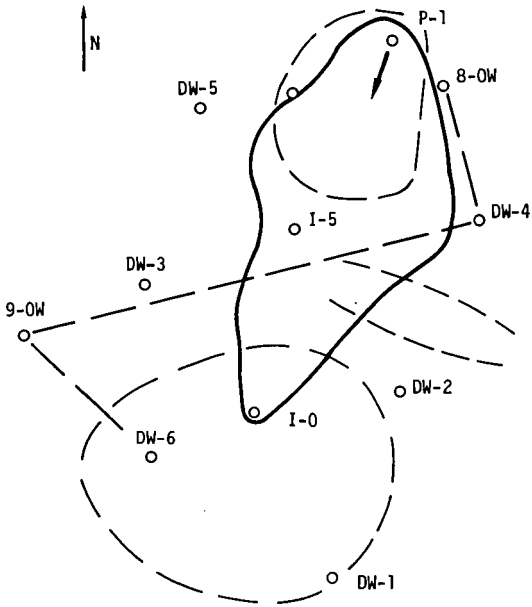

Fig. 13. Gasified region overlain on hydrology composite. Burn progressed from P-1 to I-0, overriding coal in final stages.

COMBINED CO_2-O_2 UNDERGROUND PYROLYSIS-GASIFICATION FOR SOUTHWESTERN COALS

N. E. Vanderborgh, E. M. Wewerka, W. J. Trela, J. M. Williams, Jr.
and G. R. B. Elliott

Abstract

Although vast quantities of subbituminous coals are located in the Southwestern U. S., severe technical problems exist in utilizing this resource. Much of these coals occur at depths where surface mining is not feasible. Even if this were not the case, a combination of limited water availability and environmental controls suggests that rapid expansion of coal utilization is not feasible. New technologies must be developed to exploit the known, vast coal resources in this region.

Details will be given on one such proposed process that involves a preliminary pyrolysis step followed by CO_2-O_2 gasification. This process is designed to yield both a hydrocarbon and a medium -Btu gas product stream. Arid, southwestern subbituminous coals appear well suited for an initial hydrocarbon removal step. Studies suggest that CO_2 is an adequate reagent to efficiently remove some 35% of the available carbon by reductive pyrolysis. The resulting semi-char has been shown to maintain adquate reactivity for eventual gasification.

Preliminary laboratory and engineering analyses for this underground coal conversion technology are described.

COMBINED CO_2-O_2 UNDERGROUND PYROLYSIS-GASIFICATION FOR SOUTHWESTERN COALS

Large enough coal resources have been identified in the Southwestern regions of the United States to permit planning for increases in coal utilization to meet the significant energy needs of the Western states. (1,2) This reemphasis upon coal is timely as proven reserves of both oil and gas are declining. (3) Yet, marked increases in coal utilization are limited by a variety of environmental and technological factors.

Only a small fraction, probably less than 5%, of the known coal resource can be extracted using surface mining technology. (4) Identified seams show dip, falling rapidly out of surface mining reach. Lenticular, thin and multiple seams of considerable depth suggest that underground mining may not be attractive.

Increased coal utilization using the remaining surface-minable coal may also be difficult to realize. (5) Opposition to increased strip mining is appearing. Stack cleaning of combustion gases from these high ash, low surfur materials has proven difficult. There remain serious questions about the advisability of increased combustion facilities. Any significant increase in coal utilization within the arid Southwestern region will also be limited by water availability. (Although limited brackish aquifers have been identified, it is not obvious that this water can be readily consumed for industrial processing.)

These factors, a combination of technological and environmental concerns, have already slowed a series of projects that were designed to increase coal utilization in the Southwestern United States. (5) It is becoming ever more obvious that the unique mixture of regional conditions leads to problems that are not readily addressed with existing technology. There is only a limited quantity of coal, using surface mining, that can be extracted and that coal is not easily used in combustion facilities. The concept presented in this paper is one approach that appears to have promise in expanding coal production in the Southwestern United States without moving into difficult and possibly restraining factors.

"Chemically mining" coal, underground conversion to gaseous or liquid fuels, is hardly a new idea (6). The thought of utilizing coal without the coincident societial and environmental costs of conventional mining has intrigued mankind for decades. (7,8) Partial underground combustion,"underground coal gasification," has been actively explored in the Soviet Union during the last fifty years (7). After some disappointing results in Alabama during the 50's, underground coal gasification programs are again active in the United States. (9) The Laramie Energy Research Center currently is demonstrating underground coal gasification in thick, subbituminous coals in Wyoming. (10) Lawrence Livermore Laboratory is exploring a concept of

oxygen-steam gasification, again in the coal fields of Wyoming. (11) The Morgantown Energy Research Center has begun studies exploring gasification in Eastern bituminous coals. (12) Initial commercial tests are being evaluated using lignite beds in Texas. Concurrently, tests are also planned in Canada and in Belgium. However, none of these other experimental programs are turned to address the particular technical problems that now exist in the Southwestern region of the United States.

TWO STAGE PYROLYSIS-GASIFICATION

The underground coal extraction process proposed here is shown schematically in Figure 1. On the lower left-hand-side, gasification occurs in a previously treated, underground coal seam. This reaction, fed by an oxygen rich feed and moderated with CO_2, produces a continuous supply of a low-Btu gas. Carbon dioxide replaces the more conventional steam injection. This gas stream exits from the underground generator at elevated temperatures. Anticipated levels of sulfur, nitrogen and particulate matter in this gas dictate that gas cleaning is essential prior to utilization. This process is more easily accomplished at lower temperatures. Consequently, the gas is first fed through a heat exchanger and then into a gas cleaning operation. In the cleaning process, the gas is also stripped of CO_2 and sulfur leaving a combustible gas for utilization. In order to maintain reasonable sizes of the cleaning equipment, the gas is first pressurized. Exiting gas steams are also at pressure and might be transported some distance prior to final usage. Utilization of this cleaned product gas should cause no more environmental degradation than methane combustion.

Carbon dioxide, extracted during the gas cleaning process, is heated using the sensible heat from the gasification process and is then used for two purposes. Part of the gas is fed back into the gasifier for regenerative control. The remainder is fed into another, adjacent coal seam. This process, a hot gas preconditioning step, dries and partially pryolyses the virgin coal leaving a seam of open and uniform porosity with controlled reactivity. Pyrolysis products, moisture, liquid and gaseous hydrocarbons, are brought to the surface, collected, and shipped to a hydrocarbon processing plant. Following adequate reductive pyrolysis (with hot CO_2), the gas stream is changed to a mixture containing oxygen and the hot coal bed is gasified. Another, adjacent seam, following manifolding and seam opening, is then used for the site of the next pyrolysis section.

The overall process is designed to initially convert coal, using hot gas flows, into a stream of liquid hydrocarbons that could partially supplyment existing sources of petroleum feed stocks. During this process the mass transfer properties and the chemical reactivities of the coal seam are modified leaving a highly porous bed for subsequent gasification. This type of process is designed for the high volatile content, subbituminous coals found in the Southwestern United States.

DRYING AND PYROLYSIS OF SOUTHWESTERN COALS

Coals located in the Southwest are typically of subbituminous rank. (4) However, unlike the majority of such low-rank coals, these seams contain only a modest amount of water. Ten per cent moisture, is perhaps an average value although analyses of core segments can show values near 3%. (13) Previous underground coal gasification shows that water plays a key role in underground processing for this compounds acts as a major chemical reactant that can easily degrade gas quality. (14) Water is also an important heat transfer agent. Equally important, however, is the fact that water is a key factor in seam permeability. Consequently, moisture control underground must be a major consideration in any underground gasification process.

Permeability of underground coal seams is a difficult parameter to accurately determine. It appears that many of these subbituminous coals naturally show low permeabilities in the range of 0.1 mD. Removing moisture from these coals enchances the permeability by at least three orders of magnitude. (15) This behavior is readily understandable if one considers coal a solid, perhaps a hardened gel, with various-sized interconnecting pores and capillaries. We assume that the majority of these pores are less than 50 nm ($5x\ 10^{-8}$ cm) (16) and that these pores give coal a molecular-sieve property. Certain molecules appear to be able to penetrate the coal structure while other, not necessarily larger ones, are excluded. Temperature plays an important role in gas transport within pore structures of this type.

Moisture in pore structures of these coals effectively fills pores, due to the tetrahedral bonding capabilities of water, in a three-dimensional manner efficiently closing the material to mass transport. (17) (These low rank coals, due to their high heteroatom content, typically show hydrophillic behavior.) Removing the moisture effectively requires an agent that opens pore structure. Carbon dioxide is effective in doing this for like water, CO_2 also firmly adsorbs onto coal surfaces but unlike water, CO_2 is not capable of filling pore interiors. Rather one can assume that once a monolayer of this gas has adsorbed, the interior of the pore remains open. Consequently, the first important reason for moisture removal is to gain enchanced permeability both to move liquids and to cut down on pumping work requirements during the gasification process.

Moisture also degrades the gasification process. First steam formation lowers process temperatures increasing CO_2 production. (14) Secondly, the reaction of carbon monoxide with moisture is not advantageous for then CO is converted into a mixture of gases (H_2 and CO_2) with approximately the same total heat content but twice the volume. Lastly, moisture in the reduction zone should cool that zone, decreasing the effective residence time for CO production. All of these reasons suggest that one will be far ahead if water is first removed from the gasification process prior to CO generation. Such water removal seems feasible in Southwestern subbituminous coals by hot gas treatment.

Hot gas drying-pyrolysis requires the transport of significant quantities of gases - first calculations suggest that approximately one liter of hot gas is needed to pyrolyze one gram of coal. Moreover, that 1 gram of coal (volume approximately 0.65 cm^3) is converted to gaseous products with a volume, at STP, of 250 cm^3. Moving these quantities requires that the seam have reasonable flow characteristics. It seems unlikely that virgin coal will show high enough permeability to readily move sufficiently large quantities of gases. Consequently it may be necessary to develop seam opening techniques such as long range explosively driven penetrators, electrolinking, directed chemical leaching, etc. Evidence suggests that initial opening is feasible. (18) Moreover, carbon dioxide appears especially suitable for additional seam opening. This gas exhibits a high thermal conductivity and a low gas viscosity suggesting that for a primary heat transfer agent, CO_2 can be delivered with minimum pumping costs. Once a segment of the seam has been pyrolyzed to enhance flow parameters, then additional flows can be maintained.

However, even if enchanced permeabilities can be obtained, seam heating using hot gas flows cannot be done rapidly without large pumping costs, large quantities of heat and CO_2. Since gasification is a slow process, and the pyrolysis step is tied to that gasification, then pyrolysis must also be done slowly. One can assume that the heating process may take several months to accomplish. Should coal not be an efficient insulator, heat losses would prove prohibitive. However, unlike convective heat transport which will be promoted during the drying process, conductive heat transport is inefficient in coal. Thermal conductivities near 0.1 W/MK are well known. (19) In the absence of convection, heated coal will remain at high temperatures for long periods of time. Such data is shown in Figure 2. These data show the thermal waves measured at three different distances (five, ten and 20 feet) from a 950° F wall as a function of time. Heat, under these conditions, will be contained for years in a coal volume and will remain there until convective processes extract it. This heat will be available to increase process temperatures during the gasification step. Since necessary temperatures need be near 1000° C, this is an important energy contribution.

GASIFICATION OF DRIED SOUTHWESTERN COALS

Following the pyrolysis step, some 35% of the initial mass of the coal (as received) might be removed in a hydrogen-rich fraction. Laboratory studies suggest that the remaining semi-char will exhibit low and interconnected permeability. (13) Other studies show that the reactivity of this hydrogen-depleted material with oxygen is decreased somewhat from that over the virgin material; however this decrease (reaction rates are slower by less than a factor of two) should still leave sufficient reactivity for the gasification process. (20)

Gasification on a hydrogen-depleted char leads, primarily, to a stream of CO. The utilization of this gas presents many possibilities especially so since utilization can be in a controlled industrial atmosphere with little

concurrent health hazards. There seem to be no reason to convert this product gas to other materials, e.g., methane, methanol, etc., although certainly these options exist.

ENGINEERING ANALYSIS OF THE COMBINED PYROLYSIS-GASIFICATION PROCESS

Initial engineering analyses have been completed on this underground coal gasification process. This combined-cycle process is somewhat similar to other above-ground facilities. For instance, there is good similarity between this underground process and a low-Btu gas generator/gas cleanup/electricity generator system. However, in the present case, the majority of the processes occur underground. Underground processing offers some distinct advantages-residence times can be extended without changing costs - as well as some distinct advantages - pumping work can well be excessive and control can be difficult - over conventional coal processing facilities.

The results for these studies are based on the engineering flow diagram shown in Figure 3. This figure shows two separate, interconnected processes, the gasification path, heat removal, pressurization, gas cleanup and then utilization. (The cost projections are scaled to supply a 1,000 MW_e plant.) Waste heat and carbon dioxide are stripped from the gasification process to run the lower cycle, the hot gas pyrolysis step.

Projected annual consumption and production figures are listed in Table 1 (Again, these are projected for a 1,000 MW_e plant;hydrocarbon projections are taken from laboratory pyrolysis data.). One can see that such an operation would consume some 4×10^6 tons of coal annually and produce electricity, low molecular weight hydrocarbons, higher molecular weight hydrocarbons (pyrolyzed liquids), sulfur and pressure-volume work. (This latter results from pressurization of the output stream. The work equivalent contained in this gas volume is 50 MW. Most probably this work would be expended in operating plant utilities.)

There are two different resource recovery aspects to consider. The first is the fraction of the total coal contained in the seam that is recovered; the second is the cost of recovering a particular quantity of energy contained in a segment of the coal. Obviously, both of these recovery considerations are important. It is unrealistic to think that underground coal processing will ever show recovery efficiencies that approach 100%. However, these data do suggest that underground pyrolysis-gasification can lead to a favorable financial and energy return.

Resource recovery considerations are interrelated to a wide variety of different topics. For instance, subsidence in previous underground coal gasification has been a major problem. Pipes sever, ruining expensive manifolding installations. Cracks open, allowing excessive gas escapages. Above ground buildings tilt, causing structural damage. It appears that the optimum system for underground coal pyrolysis-gasification may well

leave enough coal underground to minimize subsidence. (This would not be unlike current room-and-pillar techniques of underground mining, a technique used for exactly the same reason.) These and other site specific questions need to be answered before one can accurately define the economics of resource recovery. What is now clear, however, is that without careful control of the underground process, the optimization of resource recovery may not be possible.

Another important consideration is the cost of the produced fuel gas. Preliminary data are shown for this projection in Table 2. Costs projections were taken from similar studies estimating costs for above ground surface gasification to produce a low-Btu gas. (21) The operating and maintenance cost charge nothing for the cost of the fuel; $12.3 million is the anticipated annual field development charge. Bottom line projections must be altered to include taxes-royalty on the coal consumed. These projections show that each $1.00 ton or royalty increases the cost of the final product by about $10¢/10^6$ BTU. Thus a $3.50/ton of coal consumed increases the final fuel costs to $\$1.56/10^6$ Btu. This projected favorable cost should remain stable over the lifetime of the plant.

The data lend to several interesting conclusions. Foremost of these is that the field development charges are not an important factor. (These projections were calculated for a 7.6 m (25 foot) seam located 152 m (500 ft.) below the surface using 7.6 m (25 ft.) well spacing. Charges for increased field development are, however, most influenced by changes in the pumping work. Large amounts of energy are expended in moving gases underground. Costs are reflected in the high annual capital charges. Increases in underground permeability gained, for instance, in decreasing well spacing may be a wise investment. Second, the difficult technology is, to a large extent, below ground. Gas handling and cleaning systems, if one accepts the eventuality of low temperature gas cleaning, are all off-the-shelf systems. This is also true for electricity generating systems - conventional gas turbines can be incorporated without concern for high temperature corrosion and abrasion. These data also suggest that gas leakage, concurrent subsidence, and water influx, factors that can uncontrollably change the underground chemistry and rheology are the things that really most influence the economics of the process. Therefore, the program at Los Alamos Scientific Laboratory has been designed to carefully investigate these several aspects of the underground process.

TECHNOLOGY DEVELOPMENT PROGRAM

Studies are now exploring the processes of concurrent heat and mass transfer through Southwestern subbituminous coals. Central to these initial studies is the problem of moisture removal and permeability modification by hot gas treatment. Laboratory data will be obtained on representative coal blocks to identify necessary kinetic parameters of concurrent heat and mass transfer. These data are essential for mathematical modeling of these

underground processes. These modeling activities will predict flow profiles and lead to suggest manifolding techniques.

Studies also will explore the interrelated problems of resource recovery and environmental impact. An appreciation now exists that environmental degradation due to gas leakages, to various subsidences and to groundwater contamination is interrelated with resource recovery. The economic trade-offs between a "contained" underground operation and recovery efficiency are also under study.

These laboratory and analytical studies will serve as input into planning for a series of controlled field tests using Southwestern subbituminous coals. These tests will operate on a segment of coal somewhat close to the surface, perhaps near 15 m (50 feet) deep. First a defined region of the coal will be isolated from the rest of the seam. One feasible way to perform this isolation is to construct a concrete-pier wall from the surface, through the seam and part way into the underburden. A representation of a section of this containment wall is shown in Figure 4. Concrete piles will be laid in a rectangular pattern defining a coal section 15 m x 15 m (50 ft x 50 ft). Feed and control pipes will then be inserted into the coal. Important here are pipes placed behind the wall, "water cooling" pipes, to maintain the integrity of the wall and assure that the fire can't move out of the contained section. Undoubtedly, some sort of subsidence control will be essential.

Although this experimental arrangement has some similarity to laboratory block tests, several important features suggest that this approach is necessary to learn which really takes place underground. One needs to work with virgin coal, with underground moisture and gas content intact. Yet one needs to be assured of defined mass balances. The thrust behind these studies is to obtain definitive answers about flows, chemical and heat balances and resource recovery. Two separate tests are planned. The first of these will study the drying and pryolysis of a coal section. Following seam opening, directed flows of hot gases will pass through a coal section. Pyrolysis will be carried on for a fixed period and then quenched. Detailed postmortem analyses will be made on the block. A second test will again study the drying and pyrolysis of a second block; however, this test will be carried through a gasification stage prior to the final post mortem. These field tests will provide data for subsequent planning and large-scale commercialization.

ACKNOWLEDGEMENT

The authors wish to thank F. P. Schilling, G. A. Baca, J. W. Barnes and G. E. Cort for their helpful discussions and assistance.

REFERENCES

(1) F. E. Kottlowski, E. C. Beaumont and J. W. Shomaker, "New Mexico" in 1975 Keystone Coal Industry Manual, McGraw-Hill, Inc., New York, p. 585, 1975.

(2) C. D. Kolstad, "The 1975 Energy Production System in the States of the Rocky Mountain Region", Los Alamos Scientific Laboratory, LA-6624, December 1976.

(3) E. C. Arnold, et al., "New Mexico's Energy Resources '75", Bulletin 107, New Mexico Bulletin 107, New Mexico Bureau of Mines and Mineral Resources, Socorro, NM 1976.

(4) anon, "Outlook for Coal: Bright, but with Problems", Chem. Eng. News., 55, Feb. 14, 1977.

(5) J. W. Shomaker, et al., "Strippable Low-Sulfur Coal Resources of the San Juan Basin in New Mexico and Colorado," Memoir 25, New Mexico Institute of Mining and Technology, State Bureau of Mines and Mineral Resources, Socorro, NM, 1971.

(6) G. R. B. Elliott, "Chemically Mining Coal," Mining Engineering, Sept., 1973.

(7) J. L. Elder, "Underground Gasification of Coal", in Chemistry of Coal Utilization, H. H. Lowry, Editor, John Wilen and Sons, Inc., New York 1963, pp. 1023-1041.

(8) National Coal Board, The Underground Gasification of Coal, Sir Isaac Pitman and Sons, Ltd. 1964.

(9) R. Raimondi, P. L. Terwiliger, and L. A. Wilson, Jr., "A Field Test of Underground Combustion of Coal," J. Petroleum Technol., Jan. 1975, pp. 35-41.

(10) G. C. Cambell, C. F. Brandenburg and R. M. Boyd, "Preliminary Evaluation of Underground Coal Gasification at Hanna, Wyo., Bureau of Mines, Laramie, Wyo. BM-TPR-82, Oct., 1974.

(11) G. H. Higgins, "A New Concept for in-situ Coal Gasification," Lawrence Livermore Laboratory, Rept UCRL-51217, Rev. 1, Sept. 27, 1972.

(12) W. K. Overbey, Jr., C. A. Komar and J. Pasini, III, "Underground Combustion of Coal: Proposed Concept for Direction Control of the Combustion Zone," paper presented at the Annual Meeting of the Geological Society of America, Dallas, TX, Nov. 11-14, 1975.

(13) H. E. Nuttall, W. G. Stoddart and W. J. Chen, "Reactivity and Kinetics of Sub-bituminous New Mexico Coal," 51th Annual Conference of S.P.E., New Orleans, Oct. 3-6, 1976. Paper No. SPE 6154.

(14) N. Z. Brushtein and V. S. Za'grebalnaya, "The Influence of Moisture on the Process of Underground Gasification," Podzemnaya Gasifikatsiya Uglei, 3, 33 (1957).

(15) R. N. Pitkin, I. V. Eremin and K. I. Cheredkova, "Permeability of Yuzhno-Abinsk Coal From Kuzbass", Trudy Inst. Goryuckikh Iskopaemukh, Akad. Nauk S.S.S.R., Otdel. Tekh. Nauk, 7, 85 (1957).

(16) J. Thomas, Jr., H. H. Damberger, "Internal Surface Area, Moisture Content, and Porosity of Illinois Coals: Variations with Coal Rank," Illinois State Geological Survey, Circular 493, 1976.

(17) P. Cinche, H. Marsh and S. Pregermain, "Absorption of Carbon Dioxide, Methanol and Water Vapor on Cokes-Determination of Micropore Volume," Fuel, 46, 341, 1967.

(18) W. J. Carter, Los Alamos Scientific Laboratory, Los Alamos, NM, private communication.

(19) I. L. Faberov, E. S. Avdonina, and N. P. Turevskaya, "Effects of Preheating on the Thermal Conductivity of Blocks of Moscow Coal and of Oil Shale," Trudy. Inst. Goryuchikh, Akad. Nauk S.S.S.R., Otdel Tekh. Nauk., 7, 94 (1951).

(20) N. E. Vanderborgh, Los Alamos Scientific Laboratory, unpublished results.

(21) Second Supplement to the Application of El Paso Natural Gas Co. for a Certificate of Public Convenience and Necessity, FPC Docket No. CP 73-131, October 8, 1973.

TABLE 1: RESOURCE FLOW AND PRODUCTION PROJECTIONS FOR TWO-STAGE PYROLYSIS GASIFICATION UNDERGROUND COAL UTILIZATION FACILITY

A. INPUT STREAMS (ANNUAL RATES)

Coal Consumed	3.51×10^6 tons[a]
Air Consumed	8.03×10^9 scf
Water Consumed	negligible net input

B. OUTPUT STREAMS (ANNUAL QUANTITIES)

Electricity 8.77×10^9 KWh	\$0.03/KWh	$\$ 2.63 \times 10^8$
Low MW HC's[b] 1.08×10^{13} Btu	$\$1.50/10^6$ Btu	$\$ 1.62 \times 10^7$
High MW HC's[c] 1.26×10^6 Bar.	\$ 10/barrel	$\$ 1.26 \times 10^7$
Raw Sulfur 9.70×10^7 lbs.	\$ 50/ton	$\$ 2.43 \times 10^6$
PV Work 4.38×10^8 KWh	\$0.03/KWh	$\$ 1.31 \times 10^7$
	Annual Value	$\$ 3.07 \times 10^8$
	Per Ton Coal	\$88.55

[a] Assuming a 25' coal seam, annual area of seam addressed is (20/f acres) where f = fraction recovered, i.e., if half of the coal is consumed, then coal under 40 (20/0.5) acres would be consumed.

[b] Low molecular weight hydrocarbons, mainly C_1 - C_4 hydrocarbons, gases

[c] High molecular weight hydrocarbons, mainly C_5 - C_9 hydrocarbons, liquids

Other potential products, especially ammonia, are not listed.

TABLE 2: LASL TWO STAGE CO_2-O_2 UNDERGROUND COAL EXTRACTION-ECONOMIC PROJECTIONS

	ANNUAL COST (K$)	BASIS
OPERATION AND MAINTENANCE		
Coal Feedstock	0	
Field Development[a]	12,300	25 ft. well spacing
Plant Operation	10,440	
Administration	5,760	
Misc. Taxes	4,160	1.1% of plant investment
	$32,680	
DEPRECIATION	17,860	4.7% of plant investment
CAPITAL CHARGES	57,000	15% of plant investment
BYPRODUCT REVENUES	(11,000)	estimated market value
TOTAL ESTIMATED COSTS	$96,540	
ESTIMATED COSTS PER 10^6 BTU	$1.21	
ESTIMATED COSTS INCLUDING ROYALTY OF $3.50/ton coal	$1.56	

Costs calculated assuming mid 1975 completion of construction.

Costs do not include capital or operating costs for electricity generation or hydrocarbon separation facilities. Potential revenues from hydrocarbons are likewise neglected.

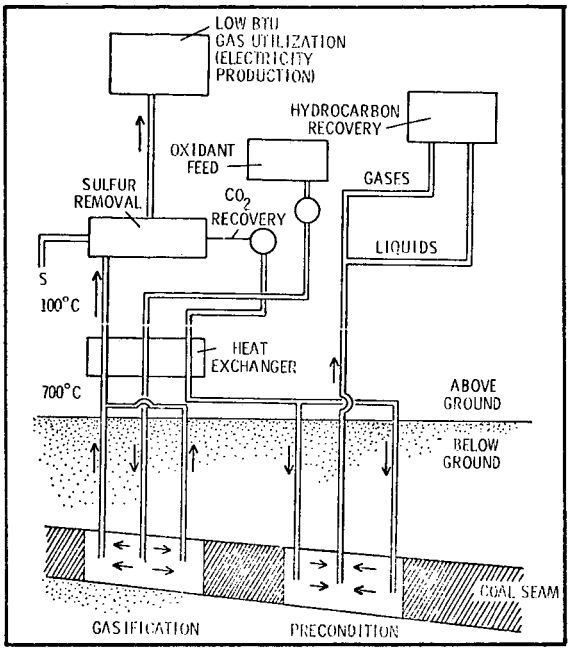

Figure 1: Two Stage Underground Gasification and Pyrolysis Facility For Utilization of Deeply Lying Southwestern Subbituminous Coals.

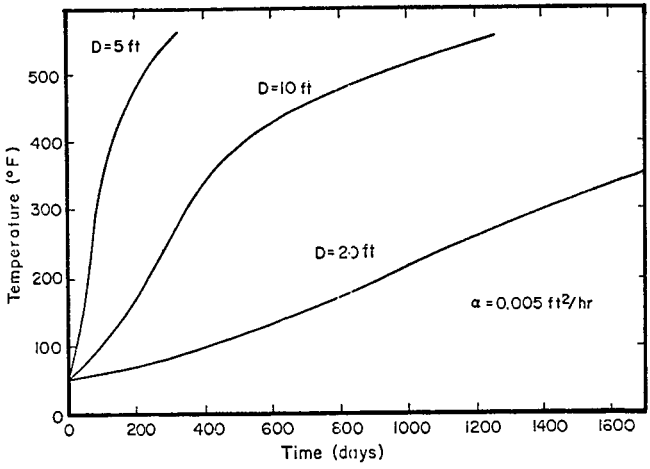

Figure 2: Thermal Waves Resulting from 950°F Wall 5, 10 and 20 feet In Coal with $\alpha = 0.005\ ft^2/hr$. Conduction Only.

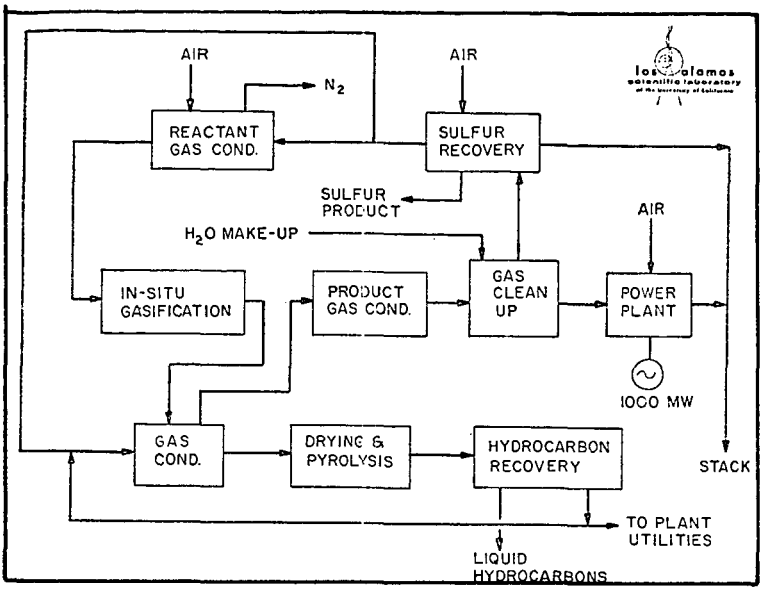

Figure 3: Flow Diagram of Above Ground and Below Ground Processing Facilities for Two-Stage CO_2-O_2 Process. (All process steps except in in-situ gasification and drying and pyrolysis are above ground)

Figure 4:

Cross Section of Mass Control Wall for Underground Experiments

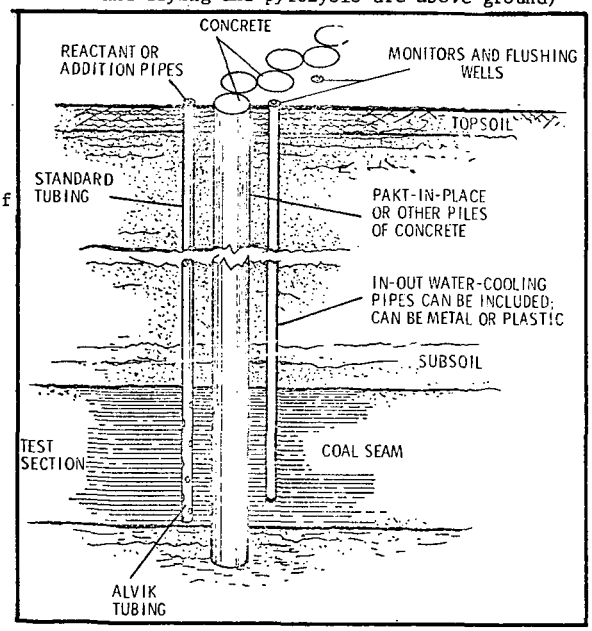

A REPORT ON THE SUCCESSFUL DEVELOPMENT OF UNDERGROUND COAL GASIFICATION AT HANNA, WYOMING

D. D. Fischer, S. B. King, and A. E. Humphrey

Energy Research and Development Administration
Laramie Energy Research Center
P. O. Box 3395, University Station
Laramie, Wyoming 82071

INTRODUCTION

Previous authors have reported the results of several field tests of underground coal gasification (1). Prominent among these are the Russian work (1, 2) (which has included commercial utilization of UCG), the British tests (3), and early U.S. experiments (4-7). In 1973 the Bureau of Mines initiated the first of a series of field experiments near Hanna, Wyoming. This first test was designated Hanna I and has been previously detailed (8-11). The first Hanna experiment (Hanna I) was conducted from March 1973 through March 1974. Approximately 4000 tons of coal were utilized. During six months of optimum operation 1.6 MM scfd of 126 Btu/scf gas were produced.

Based upon the encouraging results of Hanna I, a second experiment, designated Hanna II, was initiated in 1975. This experiment was divided into three parts, called Phases I, II, and III. Phase I has already been reported (12) and will only be referred to as a basis of comparison. Phase I was conducted from June through August 1975. It yielded an average production of 2.7 MM scfd of 152 Btu/scf gas during 38 days of gasification between two wells on a 52.5 feet spacing. Approximately 1260 tons were utilized during the experiment. The results of Phases II and III are the subject of this report.

Description of the Process

The UCG process being tested by the Laramie Energy Research Center (LERC) is known as the Linked Vertical Well (LVW) technique. It involves two major steps: preparation of the coal seam followed by gasification as depicted in Figure 1. The preferred preparatory step is reverse combustion linking. The steps involved in reverse combustion linking are shown in Figure 1 A, B, and C. Wells are drilled and completed to the coal seam. A downhole electric heater is positioned in one well to ignite the coal. Air at a pressure slightly less than lithostatic pressure is injected at the ignition well to sustain a combustion zone. Then air injection is switched to an adjacent well. The injected air percolates through the coal seam to the ignition well and the combustion zone proceeds from the ignition well to the injection well, i.e., toward the source of oxygen. Because of this countercurrent movement of the injected air and the combustion zone, the process is, at

this point, called reverse combustion. As this combustion zone proceeds to the injection well, a localized, highly permeable pathway of carbonized coal is left behind. When the combustion zone reaches the injection well, the system is ready for high volume, low pressure air injection which allows efficient gasification.

This preparatory step is extremely important because its location within the seam and its successful completion determine the future course of the gasification period. In addition, it is essential because coal in its natural unprepared state has insufficient permeability to enable air injection rates necessary for efficient coal gasification.

Figure 1 D, E, and F shows schematically the gasification step. Upon initiation of high volume, low pressure air injection, the gasification zone expands around the injection well until it encompasses the full seam thickness. The gasification zone then proceeds back toward the ignition well. Thus this step is a forward combustion process, i.e., reaction zone movement and gas flow in the same direction. In this manner the full seam thickness is gasified between two adjacent wells with high thermal efficiency.

Description of Hanna II

Phase I of Hanna II has been described in a previous paper (12). Phases II and III were conducted using the well pattern shown in Figure 2. The instrumentation wells were drilled and instrumented by Sandia Laboratories of Albuquerque, New Mexico, under ERDA funding (13).

The seam being utilized is the Hanna #1, a 30-feet thick subbituminous coal seam at a depth of approximately 275 feet at the Hanna II site. Wells 5, 6, 7, and 8 were completed 10 feet through the coal seam and perforated over the bottom 6 feet of the coal seam.

The original plan for conducting Hanna II, Phases II and III consisted of the following steps:

Phase II

1. Reverse combustion link Wells 7 and 8.
2. Reverse combustion link Wells 5 and 6.
3. Gasify from Well 6 to Well 5.

Phase III

1. Reverse combustion link from the 5-6 line to the 7-8 line.
2. Gasify in a line drive from the 7-8 line back toward the 5-6 line.

The main advantage of operating such a line drive system would have been improved areal sweep efficiency. Success of the technique was dependent upon the ability to form the broad reverse combustion link from the 5-6 line to the 7-8 line. This broad front link was not achieved and Phase III was modified to another two-well gasification system with gasification proceeding from Well 8 to Well 7. Phase II was completed as planned.

RESULTS OF HANNA II

Phase II

Reverse combustion linkage of Wells 7 and 8 was conducted during December 1975. Linkage of Wells 5 and 6 was completed in April and May 1976. No instrumentation was available along the 7-8 line to determine the location of the link, but as seen in Figure 2, the 8 wells between Wells 5 and 6 gave an accurate picture of the linkage path. Figure 3 shows the path of the link from Well 5 to Well 6 based on thermal data gathered during the linkage process.

Much more important is the location of the link within the coal seam relative to the bottom of the seam. The most advantageous position is within the bottom third of the seam. As the link proceeded from Well 5 to 6, the initial temperature rise observed at thermocouples in Wells D, O, G, E, and B always occurred at levels 0 or 5 feet above the bottom of the seam. Thus, placement of the link low in the seam was extremely successful. Positioning the link low in the seam allowed the gasification front to undercut the coal as it moved from Well 6 back to Well 5 after completion of the link. This resulted in fresh coal falling into the reaction zone yielding high resource utilization efficiency and producing a packed bed system.

The link was completed on May 4, 1976. Gasification from Well 6 to Well 5 was conducted from May 5 through May 30. Injection rates used were 1700, 2500, and 3500 scfm, respectively, in a programmed fashion as shown in Figure 4. Production rates, product gas gross heating value, and gas composition for the five major components are shown in Figures 4-6. As can be seen the step function increases in air injection rate had no effect on gas composition or gross heating value. Until the last eight days when the gasification zone approached Well 5, the heating value was extremely constant.

The total tonnage of coal utilized during both the linkage and gasification of the 5-6 system was 2520 tons. This value is based on a carbon balance using a weighted average composition determined from a core taken at the Hanna II site (14). This compares to 1260 tons utilized during gasification between two wells on a 52.5 feet spacing during Phase I. The improved utilization during Phase II is postulated to result from the higher injection rates, the positioning of the link at the bottom of the coal seam, and from holding 30 to 50 psig back-pressure on the production side. The estimated gasified area based on thermal data from the instrumentation wells and on modeling efforts conducted at LERC (15, 16) is shown in Figure 7. Thermal data indicates

that at the midpoint of the 5-6 line the gasification zone was almost as wide as the 5-6 spacing.

Phase III

As previously stated, Phase III was modified from the proposed line drive system to another two-well experiment with gasification proceeding from Well 8 to Well 7. Again three pre-planned injection rates were used. These rates were 2500, 3500, and 4500 scfm, respectively. In addition, backpressuring the system was conducted to determine the effects of reservoir pressure changes on the gas composition.

Figures 8-11 show the injection and production rates, injection and production pressure, product gas gross heating value, and product gas composition for the five major components. Significant differences are seen in the heating value and composition when compared to data from the 5-6 system. The heating value dropped off much more rapidly during the lifetime of the 7-8 system.

The explanation for this difference is shown in Figures 12 and 13. Figure 12 shows the gross heating value, cold gas thermal efficiency, and ratio of water produced to coal utilized during the 5-6 gasification period. As can be seen, the heating value and cold gas efficiency were stable until Julian Day 142 (May 21, 1976) followed by a gradual decline.

In contrast, Figure 13 shows the same variables for the 7-8 gasification period. The heating value and cold gas efficiency show a steady decline from the beginning of the 7-8 gasification period with the most dramatic drop occurring around Julian Day 196 (July 14, 1976). That drop coincided with a planned decrease from 80 to 30 psig in the backpressure held on the system. The ratio of water produced to coal utilized increased sharply at that time. Compared to the 5-6 period, this ratio was approximately twice as high during the early stages of the 7-8 burn and six times as high after relieving the backpressure on Julian Day 196. This dramatic increase in water would be expected because groundwater influx should increase as the surface area of the cavity in the seam increases. In addition, decreasing the reservoir pressure further increased the water influx rate.

Increasing the air injection rate toward the end of the 5-6 burn would have stabilized the product gas heating value and cold gas efficiency since excess water does not appear to have been the cause of the decline in those two values. Also, an increased injection rate and higher backpressure during the last 20 days of the 7-8 burn would have improved the results of the 7-8 burn, but maximum air compression capacity had already been achieved.

The unique character of Phase III was the excellent resource utilization. The tonnage of coal utilized during Phase III was 4200 tons (Figure 14).

Overall, Hanna II is considered extremely successful even though the line drive process was unsuccessful. The total tonnage of coal utilized was 6690 tons, of which 680 tons were utilized during the unsuccessful line drive attempt. This is compared to the available 4600 tons contained within the 60 by 60 feet square of the 5, 6, 7, 8 well pattern. Obviously, coal was utilized outside that arbitrary boundary but exceeding this artificial total by such a margin indicates high resource utilization efficiency. Determination of the actual efficiency awaits coring and seismic surveys of the gasified area to finalize the true boundaries of the gasification zone, but there can be little doubt that UCG can achieve high resource utilization efficiencies under controlled conditions.

Energy Balance Calculations

Three different calculations have been previously reported (17). The first, defined as the energy return ratio, is simply the ratio of total usable energy produced from the process to total energy consumed in operating the process. This value must, of course, be somewhat greater than one for the process to be worthy of commercialization.

The second, defined as overall process efficiency, is the ratio of total usable energy produced from the process to total energy input to the process, i.e., the total energy consumed in operating the process plus the latent energy available in the amount of coal utilized. This value can, of course, never exceed one.

The third, defined as thermal efficiency, is the ratio of total usable energy from the process to total energy available in the amount of coal utilized. Again, this value can never exceed one.

The total energy produced from the process is the sum of five individual terms. These are the heat of combustion of the dry product gas, the heat of combustion of the liquid hydrocarbon byproducts, the sensible heat of the dry product gas, the latent and sensible heat of water vapor contained in the wet product gas, and the heat loss to ash and strata surrounding the coal seam.

For the purposes of this paper, the total usable energy produced from the process is defined as the sum of the heats of combustion of the dry product gas and of the liquid byproducts. No credit is taken for either the latent or sensible heats. The results of these calculations are shown in Table I.

Table I. Energy Balance Results for Hanna II

	Phase		
	I	II	III
Energy Return Ratio	5.3	4.5	4.5
Overall Process Efficiency (%)	71.5	74.3	65.3
Thermal Efficiency (%)	82.7	89.0	76.3

Accomplishments of Hanna II

Hanna II yielded several outstanding accomplishments in the field of UCG using air injection. These were the following:

1. Production of the highest gross heating value product gas over the longest duration ever reported.

2. Operation at the highest thermal efficiencies ever reported.

3. Highest production rate from any UCG test in the Free World.

4. High overall sweep efficiency for parallel two-well patterns.

5. The most thoroughly instrumented UCG test ever conducted.

CONCLUSIONS

Based on the results of Hanna II, a large number of predicted problem areas attributed to in situ coal gasification technology do not appear to be of significance. Stable operation at high production rates with relatively constant gas quality and composition have been achieved. Overall process and thermal efficiencies were high and resource recovery was excellent. No detectable gas leakage occurred based on nitrogen and argon balances. No shutdown due to equipment or process failure was encountered. Process control based on adjustment of air injection rate to maintain the optimum air/water ratio appears feasible. Future tests planned at Hanna will concentrate on further demonstration of these conclusions and will address the major unknowns still associated with the in situ coal gasification process, i.e., the effects of subsidence and the determination of optimum and maximum well spacings.

REFERENCES

1. A. D. Little, Inc., "A Current Appraisal of Underground Coal Gasification," Report No. C-73671 (Dec. 1971), 121 pp.

2. Skafa, P. V., Underground Gasification of Coal, Translated from Gosudarstvennoe Hauchno-Tekhnicheskoe Izdatel'stvo Literatury Po Gornomu Delu, Moscow (1960), 324 pp.

3. Sir Alexander Gibb and Partners, The Underground Gasification of Coal, Sir Isaac Pitman & Sons, Ltd., London (1964).

4. Dowd, J. J., J. L. Elder and J. P. Cohen, "Experiment in Underground Gasification of Coal, Gorgas, AL," BuMines RI 4164 (Aug. 1947), 62 pp.

5. Elder, J. L., M. H. Fies, H. G. Graham, R. C. Montgomery, L. D. Schmidt, and E. T. Wilkins, "The Second Underground Gasification Experiment at Gorgas, AL," BuMines RI 4808 (Oct. 1951), 72 pp.

6. Capp, J. P., J. L. Elder, C. D. Pears, R. W. Lowe, K. D. Plants and M. H. Fies, "Underground Gasification of Coal - Hydraulic Fracturing as a Method of Preparing a Coalbed," BuMines RI 5666 (1960), 50 pp.

7. Capp, J. P., and K. D. Plants, "Underground Gasification of Coal with Oxygen-Enriched Air," BuMines RI 6042 (1962), 14 pp.

8. Campbell, G. G., C. F. Brandenburg, and R. M. Boyd, "Preliminary Evaluation of Underground Coal Gasification at Hanna, Wyoming," BuMines TPR 82 (Oct. 1974), 14 pp.

9. Schrider, L. A., J. W. Jennings, C. F. Brandenburg, and D. D. Fischer, "An Underground Coal Gasification Experiment, Hanna, Wyoming," SPE 4993, presented at the SPE Fall Meeting of AIME, Houston, TX (Oct. 6-9, 1974), 25 pp.

10. Brandenburg, C. F., D. D. Fischer, G. G. Campbell, R. M. Boyd, and J. K. Eastlack, "The Underground Gasification of a Subbituminous Coal," presented at the Div. of Fuel Chem., Am. Chem. Soc. National Spring Meeting, Philadelphia, PA (Apr. 1975), 11 pp.

11. Schrider, L. A., C. F. Brandenburg, D. D. Fischer, R. M. Boyd, and G. G. Campbell, "The Outlook for Underground Coal Gasification," presented at the 1975 Lignite Symposium, Grand Forks, ND (May 1975), 32 pp.

12. Brandenburg, C. F., R. P. Reed, R. M. Boyd, D. A. Northrop, and J. W. Jennings, "Interpretation of Chemical and Physical Measurements from an In Situ Coal Gasification Experiment," SPE 5654, presented at the SPE Fall Meeting of AIME, Dallas, TX (Sept. 28-Oct. 1, 1975), 28 pp.

13. Stoller, H. M., L. A. Schrider, and D. A. Northrop, "The Status of Instrumentation and Process Control Techniques for In Situ Coal Gasification," presented at the 22nd ISA International Instrumentation Symposium, San Diego, CA (May 25-27, 1976).

14. Estep-Barnes, P. A., and J. J. Kovach, "Chemical and Mineralogical Characterization of Core Samples from Underground Coal Gasification Sites in Wyoming and West Virginia," RI-75/2, Morgantown Energy Research Center, ERDA (Dec. 1975), 16 pp.

15. Gunn, R. D., and D. L. Whitman, "An In Situ Coal Gasification Model (Forward Mode) for Feasibility Studies and Design," RI-76/2, Laramie Energy Research Center, ERDA (Feb. 1976), 39 pp.

16. Gunn, R. D., and D. L. Whitman, "A Predictive Model for In Situ Coal Gasification by the Permeation Method," Society of Petroleum Engineers Journal, submitted for publication.

17. Fischer, D. D., J. E. Boysen, and R. D. Gunn, "An Energy Balance for the Second Underground Coal Gasification Experiment, Hanna, Wyoming," presented at the SME of AIME National Meeting, Atlanta, GA (Mar. 6-10, 1977), 17 pp.

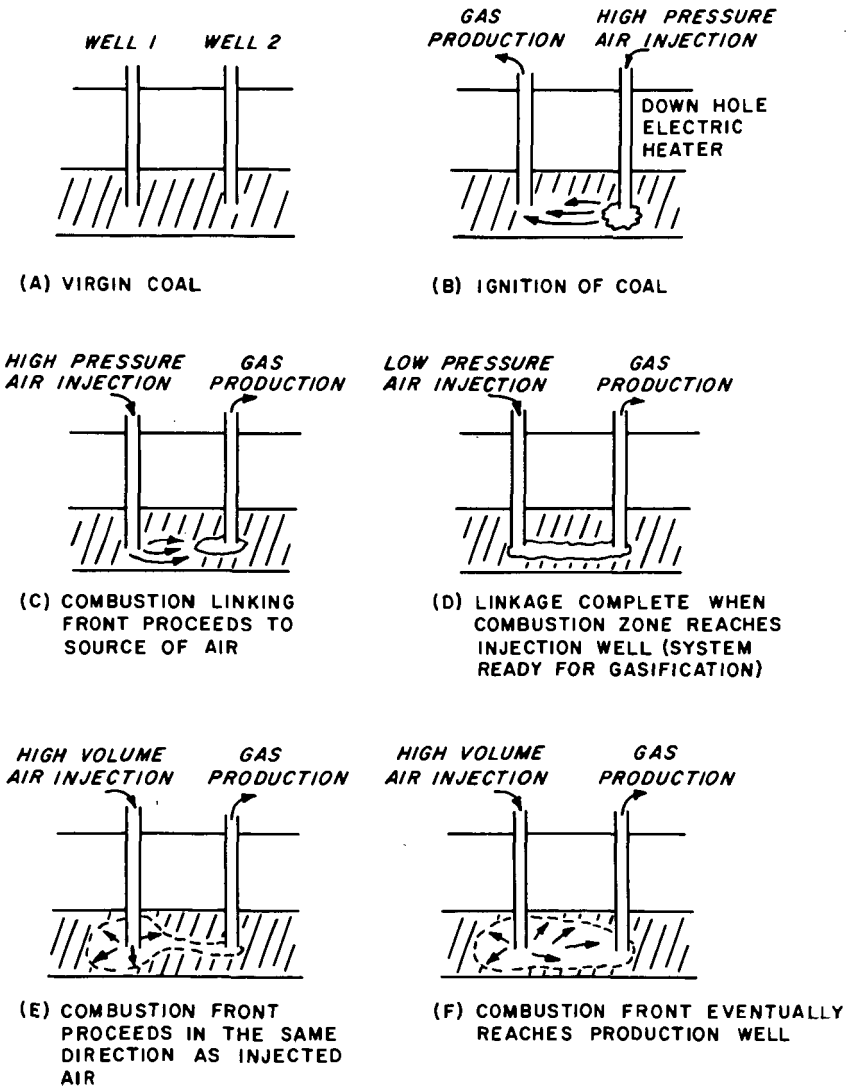

Figure 1 - Schematic of the LVW UCG Process

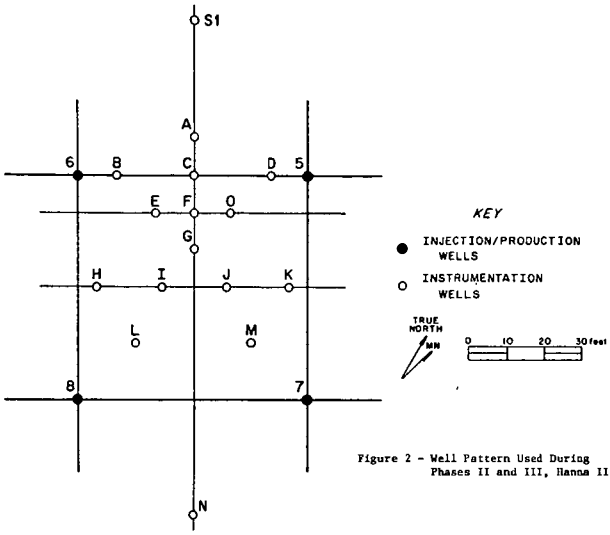

Figure 2 - Well Pattern Used During Phases II and III, Hanna II

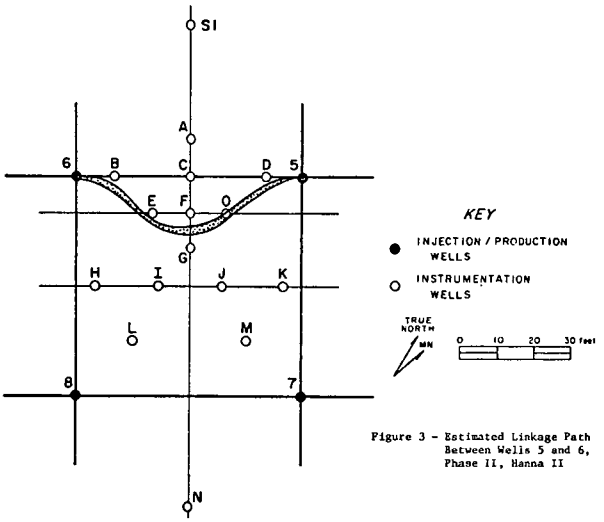

Figure 3 - Estimated Linkage Path Between Wells 5 and 6, Phase II, Hanna II

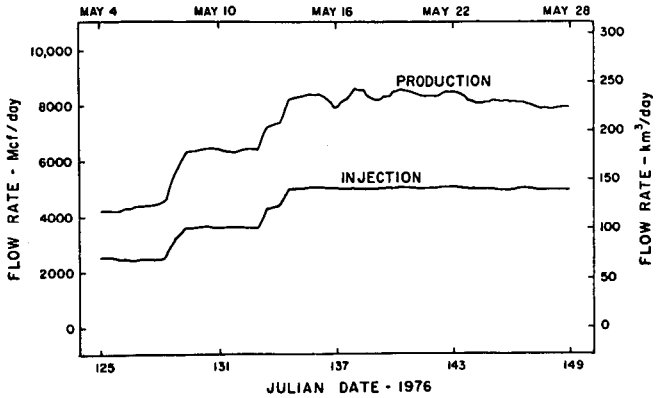

Figure 4 - Injection and Production Rates, Phase II, Hanna II

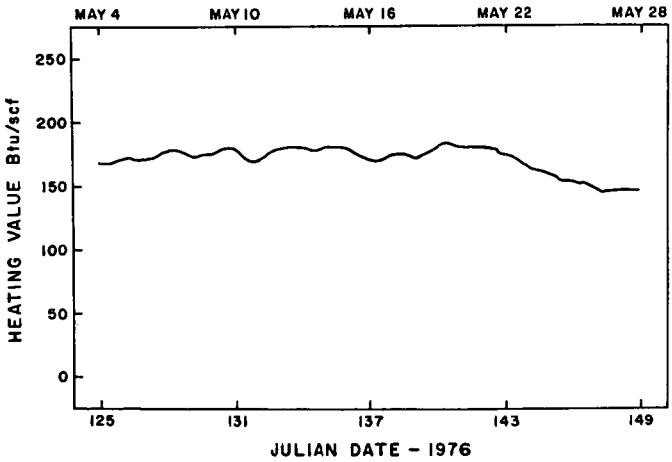

Figure 5 - Product Gas Gross Heating Value, Phase II, Hanna II

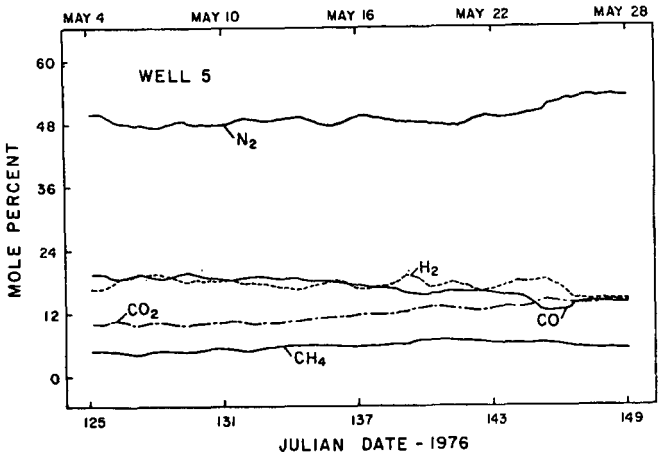

Figure 6 - Product Gas Composition, Phase II, Hanna II

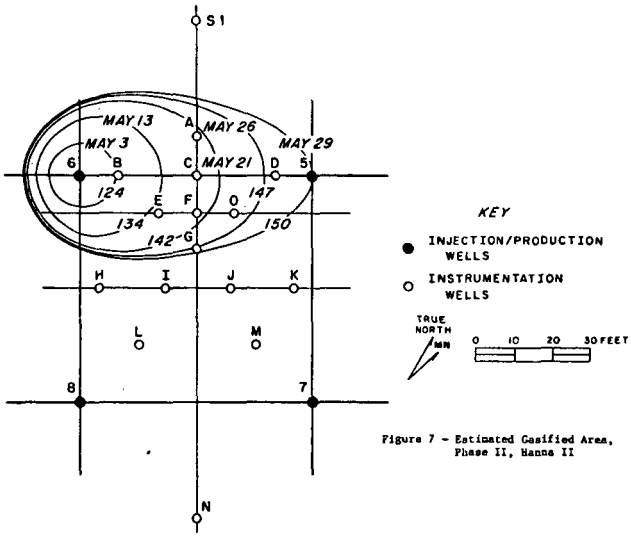

Figure 7 - Estimated Gasified Area, Phase II, Hanna II

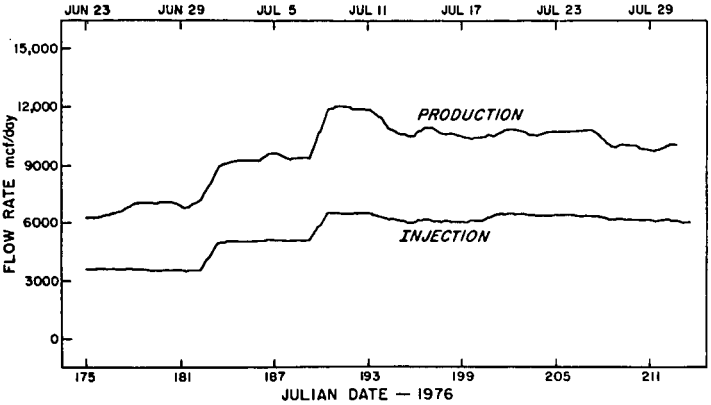

Figure 8 - Injection and Production Rates, Phase III, Hanna II

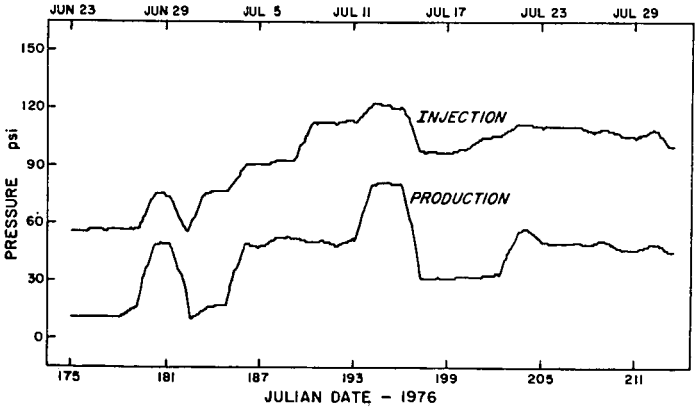

Figure 9 - Injection and Production Pressures, Phase III, Hanna II

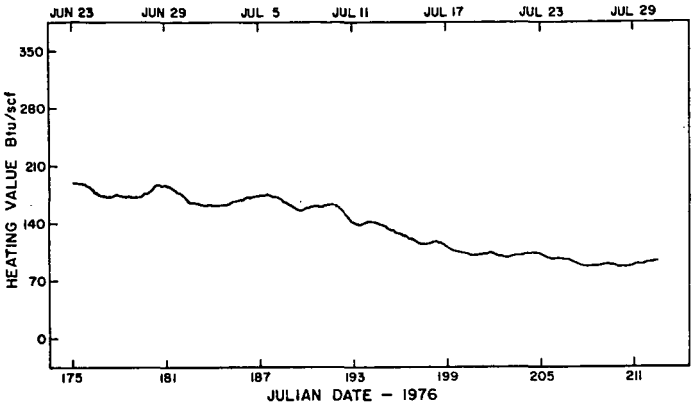

Figure 10 - Product Gas Gross Heating Value, Phase III, Hanna II

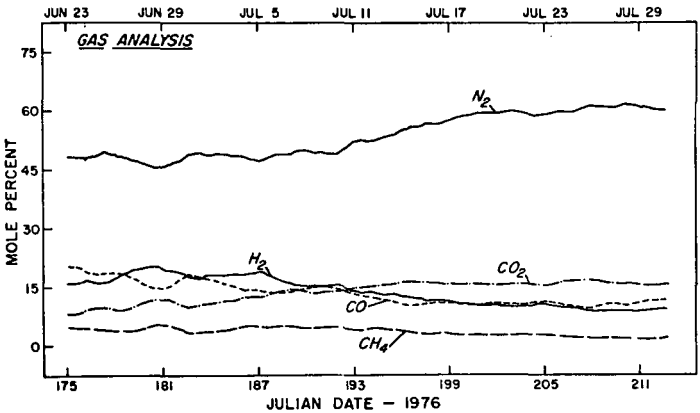

Figure 11 - Product Gas Composition, Phase III, Hanna II

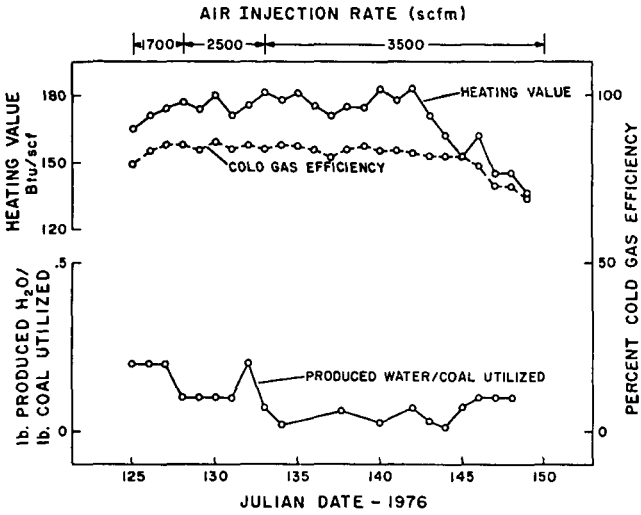

Figure 12 - Effects of Water Influx on Phase II, Hanna II, Results

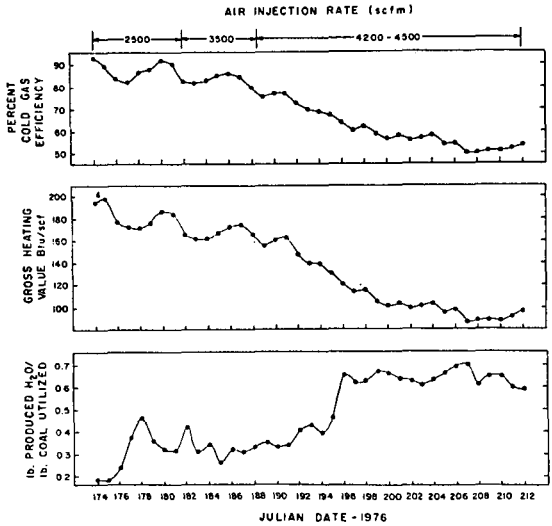

Figure 13 - Effects of Water Influx on Phase III, Hanna II, Results

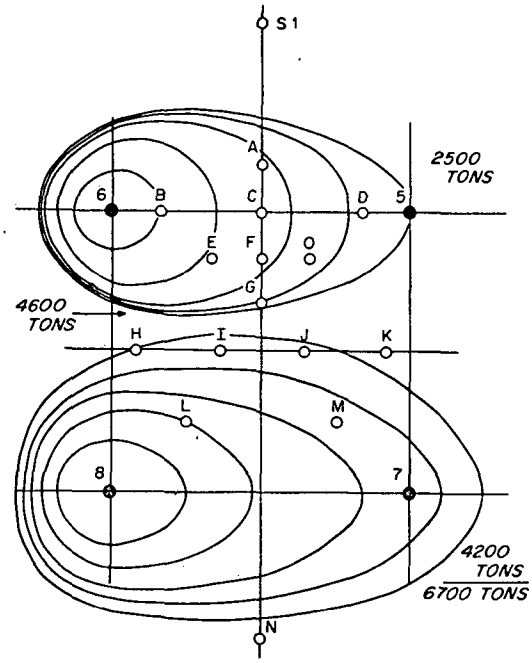

Figure 14 - Estimated Gasified Area,
Phases II and III,
Hanna II

PROBLEMS SOLVED AND PROBLEMS NOT SOLVED IN UCG

Robert D. Gunn

University of Wyoming and the
Energy Research and Development Administration
Laramie Energy Research Center
P. O. Box 3395, University Station
Laramie, Wyoming 82071

INTRODUCTION

Several different processes of UCG (Underground Coal Gasification) are being investigated in North America. Of these, the linked vertical well process, developed by the Laramie Energy Research Center, has been field tested most extensively and is closest to eventual commercialization. There is, consequently, substantial participation in further field testing of the linked vertical well process or minor variations of it. Partial or complete industrial participation is involved in the field testing programs of the Alberta Research Council, Texas A&M University, and Texas Utilities.

Problems, some solved and some not solved, which are associated with UCG are discussed in this work. Discussion of these problems outlines the current status of the linked vertical well process. The purpose is to provide perspective concerning what has been accomplished already and what remains yet to be done on the road to commercialization of UCG.

PROBLEMS SOLVED

1. Low Gas Quality

An appraisal of world-wide research efforts in UCG through 1971 showed that no field experiments using air injection had consistently produced gas with a heating value of more than 4.7 - 5.1 MJ/m^3 (120-130 Btu/scf). In most cases the gas heating values averaged less than 3.9 MJ/m^3 (100 Btu/scf) (1). In contrast all experiments conducted at Hanna, Wyoming, have resulted in heating values above 4.7 MJ/m^3 (120 Btu/scf). During the best controlled of all of the Hanna experiments, the Phase II Hanna II test, the gas heating value averaged 6.7 MJ/m^3 (171 Btu/scf) at production rates exceeding 215,000 m^3/day (8 million scf/day).

The favorable results at Hanna stem from three well defined conditions:

1. Favorable geological conditions (2, 3). An impervious shale overlies the Hanna No. 1 coal seam. The seam is relatively thick, 9 m. It lies at sufficient depth, 82-122 m, so that gas leakage to the surface has not occurred. A single aquifer, of very low productivity, overlies the coal seam.

2. Subbituminous coal. Mathematical model calculations show that the heating value of gas produced from either lignite or bituminous coal should be lower than the heating value of gas from subbituminous coal. Gases produced by carbonization of the coal make up a substantial part of the fuel gases produced by UCG. Subbituminous coal has a high volatile content; in addition, the carbonization gases are rich in methane.

In boreholes and large channels, probably the most critical chemical reaction is the steam-carbon reaction

$$C + H_2O \longrightarrow CO + H_2$$

which requires a long residence time compared to simple combustion. In an open borehole, or a borehole partially filled with rubble and large pieces of coal, there is poor contact between the solid coal char and the mixture of water vapor and hot combustion gases.

In contrast in the linked vertical well process, no open borehole exists between the air injection and gas production wells. Instead gases permeate through the dried, partially devolatilized coal. Average particle size, at least for the Hanna No. 1 Seam, is on the order of one millimeter. Because there is intimate contact between gases and solid, the gasification reactions are more extensive; and gas heating values, consequently, are higher. Bituminous coal contains less volatile matter and, therefore, produces a lower heating value gas. Lignite has a high volatile content, but on devolatilization relatively little methane is produced and a lower quality gas is obtained.

3. Control of water influx. Soviet data from field tests and commercial operations (4, 5), mathematical model calculations (6, 7, 8), and experimental results from Hanna, Wyoming, (9, 10) all verify that a too high water influx can produce a major deterioration of gas quality. The physical reasons for the deleterious effect of water have been discussed elsewhere (5, 6, 8, 10). Most western Tertiary coal seams are aquifers. The Hanna No. 1 coal seam, however, is a relatively unproductive aquifer. Therefore, it is relatively easy to adjust air injection rates to maintain a near optimum air/water ratio.

2. Decreasing Heating Value

In many field tests the gas produced started initially with a reasonable heating value which then declined gradually to unacceptable values. Two mechanisms are known which can cause this behavior:

1. Use of boreholes. One method of coal gasification involves the drilling of boreholes to connect the injection and the production well. The coal is ignited then and gasified along the length of the borehole. In this process the coal burns radially outward, and the borehole increases in size. As the borehole grows in size, more gas by-passes the coal; and the gas heating value deteriorates correspondingly.

2. Higher water influx for larger burned areas. Since many coal beds in the West are aquifers, water influx tends to increase as more and more surface is exposed by the combustion front. In addition, for larger burned out areas subsidence occurs establishing communication with overlying aquifers within the subsidence zone.

With an exception discussed later in this paper, a drastic decline in gas heating value has not occurred during the Hanna field tests. The major reason is that the linked vertical well process used at Hanna is not a borehole method but a permeation method, that is, it is essentially a packed bed process. Packed beds are widely used in the chemical process industries. A principle, well known among process chemists and engineers, is that for satisfactory results channeling must be avoided in packed bed equipment such as chemical reactors, liquid-liquid extraction columns, and distillation towers. None of the Hanna field tests have yielded any definite evidence that open channels have been created.

Thermal data from instrumented observation wells (11), flow rate and gas composition measurements (9, 12), and mathematical modeling (6, 7) have been used extensively in developing the foregoing description of the mechanics of the linked vertical well process. As more is learned about the process, it becomes increasingly clear that lignite and subbituminous coal properties are especially amenable to UCG. Both types of coal shrink on heating, and drying alone increases the coal permeability by about two orders of magnitude (13). It is these properties which permit reverse combustion linking and a permeation type gasification process to be used.

3. Variability in Gas Quality and Gas Production Rates

A wide variability in gas quality and production rates has been observed on an hourly or daily basis in many field experiments. The need for a constant gas flow rate, however, presents no real problem. It is readily achieved with a constant air injection rate and with the use of a flow control valve on the production line.

At Hanna variations in gas heating values on the order of $\pm$ 5 to 10 percent have been observed at a single well on a daily basis. This falls within the acceptable limits for the firing of large boilers. For a commercial operation, however, many production wells would be in use simultaneously and the variability in the gas composition would tend to average out. It is also noted that gas variability has been more extreme in the borehole or streaming methods of UCG.

4. Low Thermal (Cold Gas) Efficiency

In this work thermal efficiency is defined as the upper heating value of dry gas and liquids produced divided by the heating value of the coal consumed. Consistent with this definition, sensible heat is not included nor is the latent heat of any water vapor in the gas.

The instrumentation used during the Hanna field tests permits a accurate determination of the thermal efficiency. These efficiencies are the highest ever recorded. The Phase II Hanna II test achieved an

efficiency of 89 percent for the entire 25 days of the test during which 2300 tonnes (2500 tons) of coal were consumed.

Such high efficiencies are readily achieved under good operating conditions. The many feet of earth overlying and underlying the coal seam provide excellent insulation. In thick coal seams, therefore, the UCG process operates nearly adiabatically. Most of the thermal energy released from the combustion of coal char and air must be produced at the surface in the form of sensible and latent heat and in the heating value of the gas produced, i.e., chemical heat. The sensible heat is a less convenient form of energy because it can be transported only over very short distances.

In the borehole or streaming method of UCG a substantial portion of the hot combustion gases by-pass the coal and a considerable portion of the total energy released appears at the surface in the form of sensible heat. In permeation processes only a small portion of the energy goes into sensible heat. The combustion gases intimately contact the coal, and most of the sensible heat is used up for the highly endothermic steam-char reaction which produces a combustible gas.

A number of conditions can lead to lower thermal efficiencies as well as lower gas heating values.

1. Thin coal seams. A larger portion of the energy is lost to the surrounding rock formations.

2. Very high ash coal (over 50 percent). A substantial portion of the thermal energy is taken up by the ash.

3. Low air injection rates. Gas residence time underground is longer, and a larger portion of the energy is lost to the surroundings. Very low air flow rates also result in lower reaction zone temperatures.

4. Gas channeling. This results in poor contact between gases and coal.

5. Too high water influx. Vaporization of the water uses up much of the available thermal energy.

6. Gas leakage.

The mathematical model mentioned in this paper can be used to quantify individual effects listed above. It can also be used to quantify the synergistic influence of two or more of these effects acting simultaneously. More detailed discussions of the distribution of energy during the UCG process have been reported for the Hanna field tests (5, 6, 7, 10).

5. Low Resource Recovery

In the borehole or streaming method of UCG, the combustion front tends to travel down the borehole rather rapidly and to break through to the production well. Once this occurs the gas quality deteriorates very rapidly below acceptable levels. Under these circumstances, a large portion of the

coal is likely to be by-passed, and energy recovery is low. In all tests of the linked vertical well process at Hanna, Wyoming, the combustion zone advanced along a broad front, and most of the coal in place was consumed. For example, Figure 1 shows the well layout for Phases II and III of the Hanna II experiment. Wells 5, 6, 7, and 8 are production and air injection wells. Letters A to O indicate instrumented observation wells with thermocouples at several levels within the coal seam. With the thermal data it is possible to track the progress of the combustion zone. These data show that the combustion front burned through all wells within the 60 foot square pattern except well K. It is concluded, therefore, that the areal sweep efficiency is well over 80 percent.

The square well pattern shown in Figure 1 contained 4170 tonnes (4600 tons) of coal. Material balance calculations based on the carbon content of produced gases show that about 6070 tonnes (6690 tons) of coal were consumed (9, 14). Obviously considerable burning occurred outside the square pattern. In fact, the combustion zone burned through to well A but not to well N on the opposite side of the pattern. At the same time cores of coal taken near burned out regions have shown no real evidence of partial utilization of coal, i.e., cored coal samples indicate no substantial carbonization (15). It is inferred, therefore, that practically all coal contacted by the combustion front is completely gasified.

A two dimensional mathematical model developed for UCG shows reasonable agreement with field performance determined by thermal measurements and material balance calculations (16). When work on this model is completed, it will be possible to predict the shape of the combustion zone for any given well pattern.

6. Overall Process Efficiency

The overall process efficiency is defined here as the upper heating value of dry gas and liquids produced divided by the heating value of the coal consumed plus all energy consumed on site for gas compression, utilities, etc. All tests with the linked vertical well process at Hanna, Wyoming, have shown that UCG is an efficient method of energy recovery (10). Typically about 14 percent of the energy produced is consumed for gas compression and other purposes. Most of the energy consumption is for gas compression. Therefore, the 14 percent figure can be greatly reduced by optimizing the size of well casing and surface piping and utilizing efficient air compression equipment. Pressure measurements show that for a well spacing of 18 m (60 feet), pressure losses are only 0.7-2.0 N/m^2 (1-3 psi) even at air injection rates of 120,000 m^3/day (4.5 million scf/day). Thus, very little energy is lost in forcing air through the coal seam because of the great permeability of lignite and subbituminous coal after drying and devolatilization by reverse combustion. Overall process efficiencies range from 65 to 74 percent for the linked vertical well tests conducted at Hanna, Wyoming (10).

7. Control of Combustion Front

In a permeation type method of UCG such as the linked vertical well process, control of the direction and rate of progress of the combustion

front is achieved through selection of the pattern for production and injection wells and through control of the air injection rate. A two dimensional mathematical model described by Jennings et al. (10) has been used to predict location and shape of the combustion zone with satisfactory accuracy. The theory requires further verification with multiwell patterns.

8. Equipment Reliability

Equipment failures have severely plagued research on surface coal gasification processes. This has not been true with UCG (19). The high level of equipment dependability in UCG results from two conditions, the great simplicity of the surface installations required and the relatively low temperatures of gases produced.

9. Lack of Predictability

A frequent complaint has been that UCG is highly unpredictable; therefore, reliable engineering design was not possible presenting a major obstacle to commercialization of in situ coal gasification. In the past this has undoubtedly been true, but the results from the latest test at Hanna strongly indicate that the problem is close to solution.

Although UCG is not yet ready for commercialization, that time is approaching rapidly. At the present, understanding of the physical and chemical mechanisms controlling UCG is far more complete than of many competing coal gasification processes. This greatly increased understanding has resulted from three developments: extensive instrumentation of field experiments, availability of computers large and small (20), and the development of sophisticated models capable of predicting accurately field test performance.

10. Site Specificity

The very favorable results obtained from UCG field tests at Hanna, Wyoming, have not been duplicated anywhere else in the world. It might be concluded that success is specific to the Hanna site. This is not the case, however. Most of the parameters essential to successful UCG have been identified through the use of mathematical models and of massive amounts of data acquired during four years of field testing. Undoubtedly a number of favorable factors have contributed greatly to successful tests at Hanna, Wyoming; several of these factors have been discussed already (refer to item 1. Low Gas Quality). These factors, however, are by no means unique to the Hanna coal field but occur in many if not most areas of the West.

PROBLEMS NOT SOLVED

No attempt is made here to discuss all research problems which remain unsolved because, even with proven processes, new problems frequently arise. Instead problems which remain unsolved are classified as one of three types as a basis for discussion.

Critical problems. These are problems which, if not resolved favorably, will have a major harmful impact on the commercialization of UCG. Only two problems of this type are known, subsidence and excessive water influx.

Non-critical problems. These are problems which can have a major economic impact, but which will not prevent commercialization even if no favorable solution is found. Uncertainty concerning maximum well spacing is such a problem.

Developmental problems. These are problems which require application of off-the-shelf technology, or are problems which may require new technology but will not have a major economic impact on the process. Gas clean-up is such a problem.

11. Subsidence

Subsidence is probably the most important single obstacle to commercialization of UCG. Because of fiscal limitations, the tests at Hanna have been limited to two and four well patterns with 60 foot spacing. With this spacing no subsidence has been observed at the surface, although subsurface caving of the roof has occurred directly over areas of burned out coal.

When larger UCG patterns are used, subsidence of the surface will occur inevitably. At many locations in the western states this is not an insurmountable problem. Even with extensive subsidence, the surface is less disturbed than it would be by strip mining.

There are, however, three major problems associated with subsidence:

1. Disruption of overlying aquifers. A very sensitive political issue in arid regions.

2. Establishment of communication with overlying aquifers through subsidence and consequent flooding of the combustion zone.

3. Gas leakage to aquifers and possibly to the surface.

Only future field tests with large patterns can determine to what extent the foregoing harmful effects can be minimized.

Of course, if the effects of subsidence should prove intolerable in a given situation, it could be avoided entirely by utilizing small isolated burn patterns. This would be practical only if the rock overburden had sufficient structural strength as it does at Hanna. It would result also in an unfortunate reduction in the amount of recoverable coal.

12. Excessive Water Influx

Virgin coal in the Hanna No. 1 seam has low permeability and is a very unproductive aquifer. For this reason, it is possible to maintain a nearly optimum water/air ratio (moles water produced from the coal seam/moles air

injected) at reasonable air injection rates. This was true for Phases I and II of the Hanna II experiment. Both of these tests involved only two wells spaced 16 m apart for Phase I and 18 m apart for Phase II.

Both the heating value of gas produced and the thermal efficiency of the process were much lower for Phase III than for the previous two tests. Field data (9, 10) and calculations with the mathematical model (8) both confirmed that the deteriorating results obtained in the Phase III test resulted from an excessive influx of water. Physical limitations of the air injection system prevented adjustment of the water/air ratio.

Phase III involved a four well test pattern. Thus, the reaction zone was exposed to a much larger area of water drainage from the coal seam. Also the larger burn area may have promoted greater caving of the roof and communication with an overlying aquifer.

Excessive water influx can be controlled in four ways:

1. Use of dewatering wells.

2. Careful pressure control.

3. Adjustment of the air injection rate.

4. Gasification in an up dip direction.

The degree of success that can be achieved with these control measures can only be proven with the use of large well patterns in future tests.

13. Maximum Well Spacing and Depth

Factors affecting maximum well spacing and depth are largely conjectural and have not been investigated in field tests. Maximum depth at which the process is workable is an important indicator of the amount of coal that may be suitable for UCG. Maximum well spacing is important because the drilling and completion of wells is a major cost item in the operation of a UCG project. Neither is a critical problem, however. There are vast deposits of coal available at depths already tested successfully with UCG. Economic studies indicate that UCG even with the close spacing used at Hanna, Wyoming, may be competitive already with some intrastate natural gas prices (21).

14. Bituminous Coal

It has been emphasized earlier that the linked vertical well process is a permeation method and that this fact has been responsible for much of the success of the Hanna tests. Lignite and subbituminous coal shrink on drying and carbonization. This permits the use of reverse combustion linking, and the establishment of a permeation process during forward gasification. At this time it is not certain that the linked vertical well process can be used successfully in eastern bituminous coal which swells on heating. Because of the large population of the eastern states, it is important to test the viability of UCG in eastern coal. However, this is not classed as

a critical problem, that is, a problem critical to commercialization of UCG. Regardless of the outcome of eastern tests, UCG remains a workable process in lignite and subbituminous coal.

15. Gas Clean-Up

Gas treatment is classified as an unsolved problem because it has not been attempted or demonstrated in the field. Gas analyses, however, indicate that only existing technology is required for gas clean-up which is primarily a developmental problem.

Coal gas from coke ovens or Lurgi gasifiers contains heavy tars and much particulate matter. Extensive and relatively expensive clean-up is required for these gases, and the highly viscous coal tars tend to plug valves or other equipment.

In contrast gas from UCG is much cleaner. The condensed liquids cause fewer problems than typical coal tars because of the difference in their physical properties. The liquids from UCG have a low viscosity similar to that of oils. None of the material has a boiling point above 780 K (950° F). Almost a quarter of the more typical coal tar derived from the laboratory carbonization of Hanna No. 1 coal was composed of residue with a boiling point above 810 K (1000° F) (17).

Particulate concentrations and compositions have been reported as well as trace metal analyses (18). During forward combustion particulate loading has varied from 0.05 to 0.90 gm/m^3. About 1/2 to 2/3 weight fraction of the particulate matter collected falls in the submicron range. Analyses indicate that it consists of partially carbonized coal and coal char.

Sulfur is produced in the form of hydrogen sulfide and no sulfur dioxide has been measured. Hydrogen sulfide, of course, can be scrubbed much more easily from the gas than sulfur dioxide.

Gas production temperatures usually range between 510-590 K (450-600° F). Thus, high temperature clean-up is not needed, and existing technology appears to be adequate for gas treatment.

SUMMARY AND CONCLUSIONS

Fifteen major technical problems associated with UCG have been discussed. Ten problems have been largely solved, five remain unsolved. Of the five, it is believed that only two, subsidence and excessive water influx, can present potentially major obstacles to commercialization of UCG. The Laramie Energy Research Center has had virtually no field experience with either problem because they become major ones only with large well patterns which have yet to be field tested. However, proposed large area field experiments should determine within the next few years if these two problems can be resolved favorably.

ACKNOWLEDGMENT

Dennis Fischer and Mike Boyd of the Laramie Energy Research Center have reviewed the manuscript and provided many helpful comments.

REFERENCES

1. Arthur D. Little, Inc., "A Current Appraisal of Underground Coal Gasification," p. 38, 76, BuMines Rept. C-73671, 1971.

2. Campbell, G. G., C. F. Brandenburg, and R. M. Boyd, "Preliminary Evaluation of Underground Coal Gasification at Hanna, Wyo.," BuMines, TPR 82, Oct., 1974.

3. Schrider, L. A., and J. W. Jennings, SPE Preprint 4993, Soc. Petroleum Eng. Annual Fall Mtg., Oct. 6-9, 1974.

4. Gregg, D. W., R. W. Hill, and D. U. Olness, "An Overview of the Soviet Effort in Underground Gasification of Coal," Lawrence Livermore Lab., UCRL-52004, Jan. 29, 1976.

5. Gunn, R. D., D. W. Gregg, and D. L. Whitman, "A Theoretical Analysis of Soviet In Situ Coal Gasification Field Tests," Second Annual Underground Coal Gasification Symp., Morgantown, W. Va., Aug. 10-12, 1976.

6. Gunn, R. D., and D. L. Whitman, "An In Situ Coal Gasification Model (Forward Mode) for Feasibility Studies and Design," LERC/RI-76/2, U. S. E.R.D.A., Feb., 1976.

7. Gunn, R. D., D. D. Fischer, and D. L. Whitman, "The Physical Behavior of Forward Combustion in the Underground Gasification of Coal," SPE Preprint 6149, Soc. Petroleum Eng. Annual Fall Mtg., Oct. 3-6, 1976.

8. Gunn, R. D., D. L. Whitman, and D. D. Fischer, paper presented at Am. Nuclear Soc. Mtg., Energy Mineral Recovery Research, Golden, Colo., Apr. 12-14, 1977.

9. Fischer, D. D., C. F. Brandenburg, S. B. King, R. M. Boyd, and H. L. Hutchinson, "Status of the Linked Vertical Well Process in Underground Coal Gasification," Second Annual Underground Coal Gasification Symp., Morgantown, W. Va., Aug. 10-12, 1976.

10. Fischer, D. D., J. E. Boysen, and R. D. Gunn, "An Energy Balance for the Second Underground Coal Gasification Experiment, Hanna, Wyoming," presented at the 1977 National Meeting of SME of AIME, Atlanta, Ga., Mar. 6-8, 1977.

11. Beard, S. G., and R. P. Reed, "Some Insights from Temperature Measurements on Recent Underground Coal Gasification Experiments," Second Annual Underground Coal Gasification Symp., Morgantown, W. Va., Aug. 10-12, 1976.

12. Brandenburg, C. F., R. P. Reed, R. M. Boyd, D. A. Northrop, and J. W. Jennings, SPE Preprint 5654, Soc. Petroleum Eng. Annual Fall Mtg., Dallas, Tex., Sept. 28-Oct. 1, 1975.

13. Jennings, J. W., "Initial Results--Coal Permeability Tests Hanna, Wyoming," EPRI Grant No. RP 542-1, Quarterly Rept., Feb., 1976.

14. Brandenburg, C. F., D. D. Fischer, D. A. Northrop, and L. A. Schrider, "Results and Status of the Second Hanna In Situ Coal Gasification Experiment," Second Annual Underground Coal Gasification Symp., Morgantown, W. Va., Aug. 10-12, 1976.

15. Boyd, R. M., "Post Burn Analysis Techniques Applicable to Underground Coal Gasification," ibid.

16. Jennings, J. W., R. D. Gunn, C. F. Brandenburg, and D. L. Whitman, SPE Preprint 6181, Soc. Petroleum Eng. Annual Fall Mtg., New Orleans, La., Oct. 3-6, 1976.

17. King, S. B., "Preliminary UCG Tar Analyses," Second Annual Underground Coal Gasification Symp., Morgantown, W. Va., Aug. 10-12, 1976.

18. Fischer, D. D., "Monitoring of Emissions from an In Situ Coal Gasification Experiment," ibid.

19. Campbell, G. G., T. E. Sterner, and A. E. Humphrey, "Practical Considerations in Designing an UCG Test," ibid.

20. Eastwood, D. E., D. F. Moore, S. B. King, W. J. Lanum, J. K. Eastlack, and J. W. Jennings, "Real Time Process Monitoring in Underground Coal Gasification," ibid.

21. Moll, A. J., "The Economics of Underground Coal Gasification," ibid.

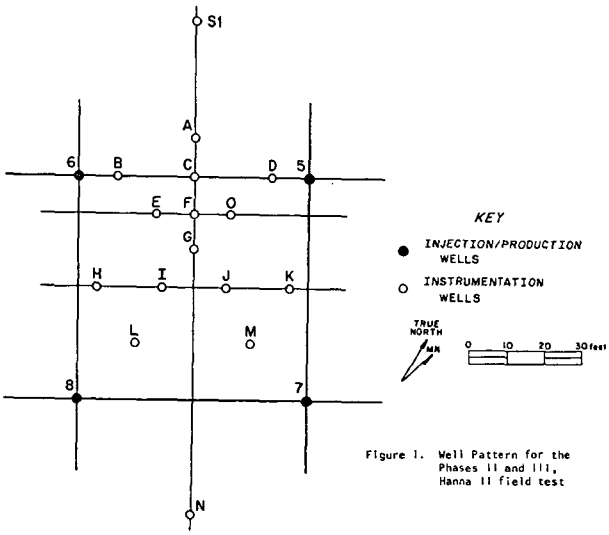

Figure 1. Well Pattern for the Phases II and III, Hanna II field test

DESCRIPTIONS OF REVERSE COMBUSTION LINKAGE AND FORWARD GASIFICATION DURING UNDERGROUND COAL GASIFICATION

P. J. Hommert and S. G. Beard

Sandia Laboratories
Albuquerque, New Mexico 87115

INTRODUCTION

From March to July 1976 the Laramie Energy Research Center (LERC) conducted Phases 2 and 3 of the Hanna II Underground Coal Gasification (UCG) Experiment in a 30-ft subbituminous coal seam located at a depth of 270 feet near Hanna, Wyoming (1). The test was extensively instrumented by Sandia Laboratories with the objectives of both measuring the in situ process directly and developing remote measurement techniques that would be appropriate for monitoring future large scale gasification projects. Primary among the remote techniques were passive acoustic, induced seismic and electrical (2). While the data in these areas are still undergoing analysis, the techniques appear promising in their ability to detect regions of affected coal and thereby provide real-time measurement of the process movement. In addition to these remote techniques, extensive thermal data were obtained during the test by thermocouples located within the coal seam. This paper presents information about this gasification test obtained from an analysis of a portion of these thermal data.

DESCRIPTION OF EXPERIMENT

The test utilized the linked vertical well concept for thick seam gasification. As applied at Hanna this involves essentially a two-step process. First, a high permeability link between the process wells is established by means of reverse combustion. This involves injection of high pressure air at one well and ignition at the other. A combustion front is then drawn from the ignition source against the air flow towards the injection well. Once the link is complete, air flow into the seam at lower pressures increases substantially, the direction of front movement reverses, and forward gasification proceeds from the injection well toward the production well.

Figure 1 indicates the process and instrumentation well pattern for the Hanna II experiment. The letter-designated Sandia instrumentation wells contained, along with other measurement devices, typically eight Chromel/Alumel thermocouples at different locations within the coal seam. Additional thermocouples were located in the overburden.

The experiment was conducted in two parts.* Phase 2 involved linkage and gasification between process Wells 5 and 6. Phase 3 was initially an attempt to drive the 5-6 burn as a line toward the 7-8 well line; however, this proved unsuccessful and the bulk of Phase 3 consisted of two-well gasification similar to the 5-6 burn. Most of the interpretations presented herein deal with the more heavily instrumented Phase 2 part of the experiment.

*Phases 2 and 3 were conducted between Days 96 and 152, and Days 152 and 213 (1976), respectively.

ANALYSIS

The majority of the thermal data obtained during the test show very rapid temperature rises. This is the result of sudden exposure to high temperature gas flows and/or the direct passage of the combustion front. There are, however, temperature rises seen during certain parts of the test which appear to be the result of conduction from a high temperature region. In particular, these responses were observed during reverse combustion linkage and the later stages of forward gasification. Such data can be analyzed by conduction models to provide information about the high temperature regions. The analysis constitutes the solution of an inverse problem; i.e., the source will be characterized by observations of its output.

The approach taken for solving the inverse problem in this paper is that of minimizing a least squares comparison of measured data and model calculations. This determines a solution range for the conduction model parameters. Both random search and simplex techniques are used to perform the optimization.

Linkage Analysis

During reverse combustion linkage, the affected coal is confined to a narrow region due to the low flow rates and the fact that thermal energy is propagated into the virgin coal predominantly by conduction (an inefficient transfer mechanism in coal). Thus, for analysis purposes, the linkage path is modeled as a cylindrical path of radius a and average temperature, T_H. Using this model, numerical finite difference calculations were made which included the effects of temperature dependent thermal conductivity and water vaporization. Results indicate that for responses below 200°F, the constant property analytical expression (3),

$$T(r,t) = (T_H - T_A)(a/r)^{1/2}\mathrm{erfc}((r/a-1)/2(\alpha t/a^2)^{1/2}) + T_A \quad , \qquad 1)$$

can fit the numerically generated results within ± 5% by adjusting the thermal diffusivity, α, as an empirical function of T_H. In Equation 1, T_A is the initial ambient temperature, r is the radial distance from the sensor to the center of the path and t is the time since the arrival of the path in the vicinity of the sensor. Equation 1 was used to analyze all the low temperature (< 200°F) responses seen during the Phase 2 linkage. During the period from ignition on Day 94 to Day 114, there were thermal responses of at least 5°F at 17 sensor locations with at least one in each of the eight wells nearest the line between process Wells 5 and 6. These data are shown in Figure 2 with the remainder of the responses in these eight wells during Phase 2. The thermocouple locations are expressed in feet from the bottom of the coal seam. For legibility the responses are truncated once a level reaches a temperature sufficient for gasification (taken here as 1500°F) or at an indication of thermocouple failure.

The optimization routines return values for a, T_H, and the position coordinates necessary to specify r. Least squares comparisons were made in four regions: near Wells D and O, between Wells F and G and between Wells A and C. The responses in Wells E and B indicate that the linkage path passed directly by these wells. Also, the speed with which it passed between them and the fact that the E-B line coincides with a major fracture direction makes it plausible that the path proceeded along a fissure near these two wells. Therefore, the data from these wells could not be appropriately analyzed with a conduction model.

The early responses shown in Figure 2 along the Well A-C-F-G line indicate the presence of two separate linkage paths. The leveling off seen in the 5-ft response

in Well C indicates that the path near this well probably did not fully develop. The temperature responses seen in the two levels in Well C and one level in Well A are consistent with a linkage path of equal size and temperature to that passing between Wells F and G but one that begins to cool rapidly after about Day 106. At approximately the same time, the F-G linkage path proceeded rapidly from Well E to B which would make this path the preferred flow direction.

Figures 3 and 4 summarize the results of the analysis of linkage data using Equation 1 where for the A-C path an additional term is added to account for cooling after Day 106. Figure 3 compares typical calculated and measured responses for a number of different sensor locations. Figure 4 shows the relative position and size of the linkage paths with respect to the instrumentation wells.

A number of statements concerning linkage can be made as a result of the analysis.

1. Typically, the initial temperature increase shown by the measured data is greater than that predicted. This is consistent with the idea that the initial pulse comes from the most active combustion zone whereas the long term response is indicative of the average temperatures in the path behind the combustion front. These temperatures are, of course, lower than the peak combustion temperatures.

2. The low thermal conductivity of coal results in large temperature gradients so that small changes in distance result in large temperature changes. Thus, the most accurate interpretations that can be made from the analyses are those relating to position.

3. Results consistently indicate effective diameters for the linkage path in the range 2.5 to 3.5 ft.

4. The analysis cannot determine accurately the temperature of the path, because temperature has a weak effect on response, and it is also sensitive to fluctuations in flowrate. Therefore, the responses result from heat sources whose strengths may vary widely over the measurement time. The analysis does indicate path temperatures of 900 to 1300°F.

5. The analysis places the center of the primary linkage path 5 ft from Well D, 3.5 ft from Well O, and 4 ft from Well G. Similarly, the other path is 4 ft from Well D and 4.5 ft from Well C.

6. In all the linkage data there is no evidence of thermal override in the coal seam. The Well A-C path remains about 6 ft from the bottom of the coal seam and the Well F-G path about 5.5 ft from the bottom.

7. None of the low temperature responses are inconsistent with either the analytical model itself or the interpretations resulting from the analysis. However, because of the nature of inverse problems (especially when there are many unknowns), these results do not preclude the possibility of other mechanisms or models accounting for the observed responses.

Gasification Analysis

In addition to the data obtained during linkage, the responses measured later by sensors outside the gasified zone can be analyzed with conduction models to determine the boundary of the affected coal zone in the vicinity of the sensor.

When analyzing thermal responses during forward combustion, it is important to recognize that certain regions of the virgin coal can be heated by convective gas flows in addition to possible conduction. In such regions a pure conduction analysis would not be appropriate. A number of factors, however, indicate that the initial temperature increases in Wells H, I, and J can be considered as primarily due to conduction. All these wells lie 20-30 ft away from the initial high permeability flow paths established during Phase 2, and two-dimensional isothermal compressible flow calculations indicate that at such distances there is very little gas flow in the virgin coal. Also, none of the thermocouples show any significant preheating prior to the upturn which has been characterized as due to conduction. Therefore, conduction models are appropriate for analyzing the responses in these wells as affirmed by the excellent agreement so obtained between calculations and measured data.

The model chosen to analyze these responses is that of a fixed wall which experiences a step jump in temperature to some typical gasified zone value at the initial time. In order to account for boundary movement a dummy initial time increment is used. This time increment allows for the establishment of a preheat zone which models the thermal profile preceding a slowly moving boundary. Two-dimensional calculations show that, due to the insulating properties of the coal, a one-dimensional expression can be used to determine the normal distance from the sensor to the boundary even if the boundary is vertically nonuniform.

For the one-dimensional case the appropriate analytical expression (3) is

$$T(x,t) = (T_H - T_A)\,\mathrm{erfc}(x/2\sqrt{\alpha t}) + T_A \quad . \qquad 2)$$

The variables here have the same meaning as in Equation 1 except that x is the distance from the sensor to the nearest point on the boundary. As was the case for the linkage analysis, for low temperature responses the analytical expression in Equation 2 provides good agreement with numerical calculations that include property variations and vaporization when α is an empirically determined function of T_H.

The data analyzed using this model were the responses seen late in Phase 2 in Wells H, I, and J. Plots of these data are presented in Figure 5. The agreement between the measured data and model calculations is quite good and better, in fact, than was seen in the linkage data analysis.

The analysis of the Well H, I and J responses lead to a number of conclusions concerning gasification in the later stages of Phase 2.

1. The final boundary at the end of Phase 2 (Day 152) for the 10-ft to 20-ft levels was approximately 4-5 ft from Well J and 3-4 ft from Wells H and I.

2. The vertical structure of the final boundary was such that it extended about 1 ft further out from the reaction zone center at the 10-ft level than at the 20-ft level.

3. The predominant reason for the time lag between the responses at the lower and higher levels is not the difference in final extent but rather the upper levels just reach the final position later in time. This conclusion implies that the combustion front, at least in the directions perpendicular to the process wells, at later times is not moving uniformly across the seam, but rather it is pivoting about the points of furthest extent near the bottom of the seam. This pivoting movement is illustrated more clearly in Figure 6 which shows a

schematic diagram of the gasified zone boundary movement during the later stages of Phase 2 in the vicinity of Well I. The lines drawn are approximations to the finite thickness boundary (~ 2 ft) containing pyrolysis and gasification regions. They are based on the information obtained from thermal data as to the final position, time of arrival at that position and minimum horizontal velocity just prior to reaching that position. Also, the boundary line on Day 135 is consistent with the contours drawn in Figure 7. The actual data used are for levels in the 10-ft to 20-ft region. The 30-ft and 0-ft responses are distorted by conduction in the over and underburden, respectively. None of the responses outside the 10 to 20 ft range are inconsistent with the extrapolated boundaries indicated by dashed lines in the figure.

4. Typical boundary temperatures necessary for good agreement between calculated and measured responses were in the range of 1150°F to 1600°F.

Data Interpretation

Having completed an analysis of the predominant conduction responses seen during Phase 2, it is of interest to correlate these analyses with the rest of the thermal data in an attempt to picture the structure of the gasified zone as a function of time. Figure 7 represents such an attempt. Figure 7a shows the gasified zone on Day 135 divided into two sections. The dashed line is an average extent for the 0-ft to 10-ft level within the coal seam. The solid line represents an average extent for the 10-ft to 30-ft levels. The reason for such a division is obvious from the considerable difference in areal extent between the two zones indicated in the figure. The primary inputs for constructing these contours are the responses at the lower levels in Wells A and D and the lack of such in the upper levels, extrapolation of the boundaries and arrival times indicated by analysis of the Well H, I, and J data, and the 20-ft responses in Wells F, G and O. The contours were also constrained to agree with LERC's material balance calculations as to the amount of coal gasified. Figure 7b shows the extent of the same two zones at the completion of Phase 2. These contours are more difficult to draw since the only hard data is the boundary near the H-I-J line and, of course, the need to agree with material balance calculations Therefore, it was necessary to extrapolate from the upper level responses in Wells A, D and G to draw the contours on Day 152. The effect of the assymetry in the primary linkage path is evident in the shape of the gasified region.

While continuous boundaries of a gasified zone can be drawn, it is important to recognize that the gasification mechanism probably varies along the boundary. For example, the rapid responses in the low levels of Wells A and C would seem to be characteristic of the advance of a combustion front and it's associated steep temperature gradients. In contrast, the more gradual rises seen in Well D are probably the result of expansion about the linkage path due to a high temperature oxygen depleted gas stream and reduction reactions.

Taken together, Figures 7a and 7b provide a picture of how the UCG process proceeded in the Hanna seam during forward gasification. There is an initial period of rapid horizontal growth at about the level of the linkage path perhaps due to higher in situ permeability in the horizontal direction. During this period the vertical growth is slower and is confined to the region near the injection well and adjacent to the linkage path. Then at some point the rate of horizontal extension low in the seam slows, and during the later stages of gasification the boundary "pivots" about the points of furthest extent and moves towards the roof of the coal seam aided by subsidence.

Three additional observations support this description of the process. First, if the gasified zone expands very rapidly in the lower third of the seam, then one might expect to see some combined convection-conduction heating to upper level thermocouples from below prior to their experiencing high gasification temperatures. Examination of the 15 and 20-ft responses in nearly all the wells shows just that trend. Almost without exception, the upturns at these levels are slower than those seen at the 0, 5, and 10-ft levels. Many of the responses are not unlike what would be calculated by conduction from a high temperature boundary 2 to 3 ft away. Second, induced seismic data (4) on Day 132 indicate a region of affected coal 4 to 6 ft beyond Well A at about the 5-ft level. This again indicates much more rapid expansion at the lower levels since it is clear from material balance considerations alone that at the upper levels the gasified zone can have nowhere near this extent. Finally, passive acoustic source locations in the overburden, which are indications of the zone extending to the roof of the coal seam, are predominantly located to the injection well side of the Well A-C-F-G line. This is consistent with the contours which show greater vertical extent in this region.

CONCLUSIONS

The thermal data analysis indicates the reverse combustion linkage path in the Hanna seam was approximately 3 ft in diameter. The position of the path with respect to the instrumentation wells was mapped and no evidence of vertical override was detected. The analysis of boundary thermocouple data combined with thermal responses from within the gasified zone indicate that the initial stages of forward gasification showed rapid horizontal expansion at about the level of the linkage path, whereas, at later stages vertical movement becomes more rapid and leads to final boundaries that are nearly vertical.

ACKNOWLEDGMENTS

The cooperation of L. A. Schrider, Dr. C. F. Brandenburg, and the many other members of the Laramie Energy Research Center staff in the Hanna experiment is greatly appreciated.

The contributions of R. P. Reed, who designed the thermal instrumentation system and with whom data interpretation was discussed many times are gratefully acknowledged. The Sandia personnel who fabricated and fielded the thermal sensors, operated and maintained the recording instruments, and reduced the data contributed significantly to this research.

This work was supported by the Division of Oil, Gas, and Shale Technology, United States Energy Research and Development Administration. Dr. Paul R. Wieber of that organization is manager of the in situ coal gasification program.

REFERENCES

1. C. F. Brandenburg, D. D. Fischer, D. A. Northrop, and L. A. Schrider, Results and Status of the Second Hanna In Situ Coal Gasification Experiment, Proceedings of the Second Underground Coal Gasification Symposium, Morgantown, WV, Aug. 1976, to be published.

2. D. A. Northrop, Editor, Instrumentation and Process Control Development for In Situ Coal Gasification, Sixth Quarterly Report, March through May, 1976, Sandia Laboratories Report, SAND76-0362, Albuquerque, NM, July 1976.

3. H. S. Carslaw and J. C. Jaeger, Conduction of Heat in Solids, Oxford University Press, London, 1959.

4. D. A. Northrop, Editor, Instrumentation and Process Control Development for In Situ Coal Gasification, Seventh Quarterly Report, June through August, 1976, Sandia Laboratories Report, SAND76-0612, Albuquerque, NM, October 1976.

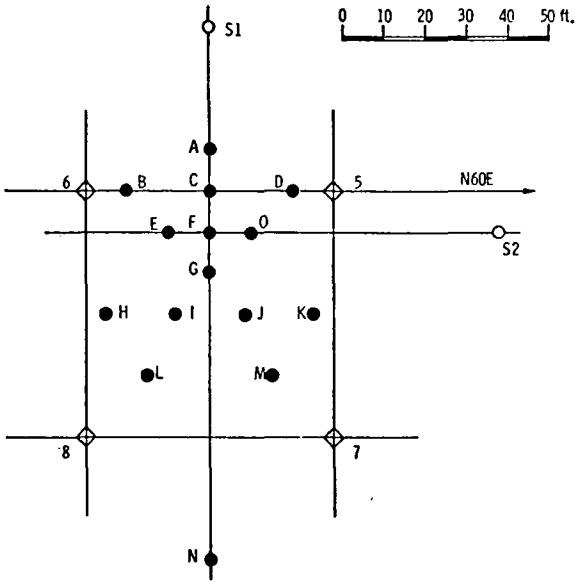

Figure 1. Well Pattern for Phases 2 and 3 of the Hanna II Experiment.

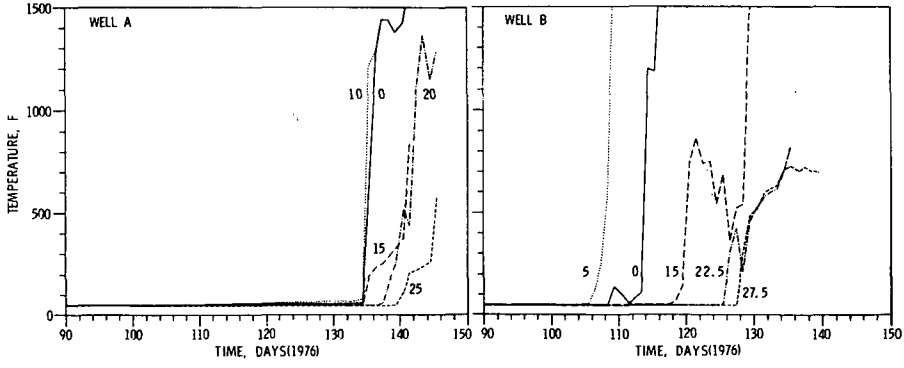

Figure 2a. Temperature-Time Profiles During Phase 2 in Wells A and B. (Thermocouple Locations (feet) Referenced to Bottom of 30-foot Coal Seam.)

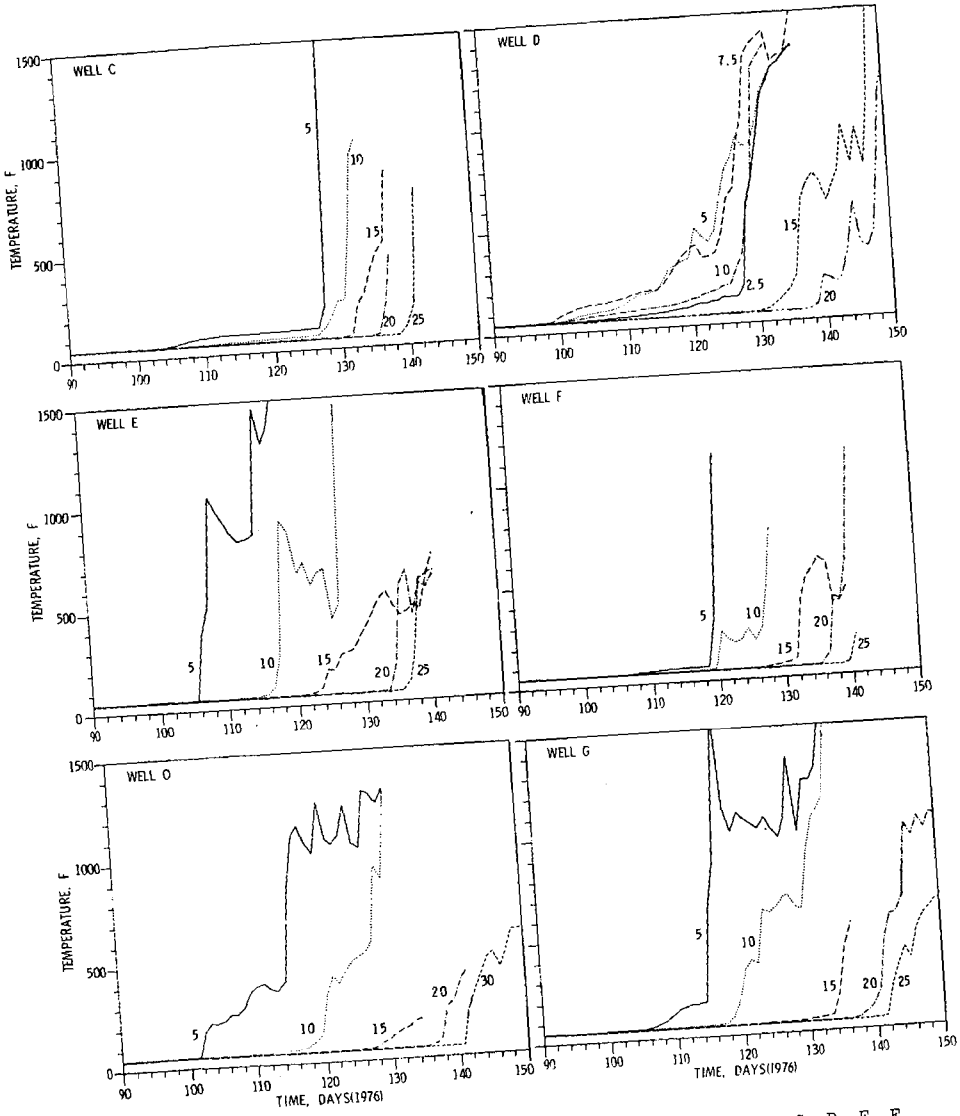

Figure 2b. Temperature-Time Profiles During Phase 2 in Wells C, D, E, F, O, and G. (Thermocouple Locations (feet) Referenced to Bottom of 30-foot Coal Seam.)

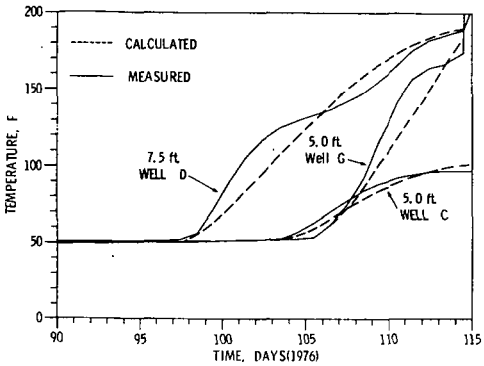

Figure 3.

Examples of Measured and Calculated Thermal Responses Utilized in Linkage Path Analysis.

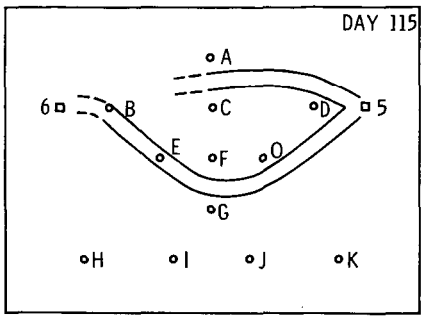

Figure 4.

Positions of Phase 2 Linkage Paths on Day 115 Based on Analysis of Thermal Data. Paths are Approximately 3 ft in Diameter and Located 5-6 ft Above Coal Seam Floor.

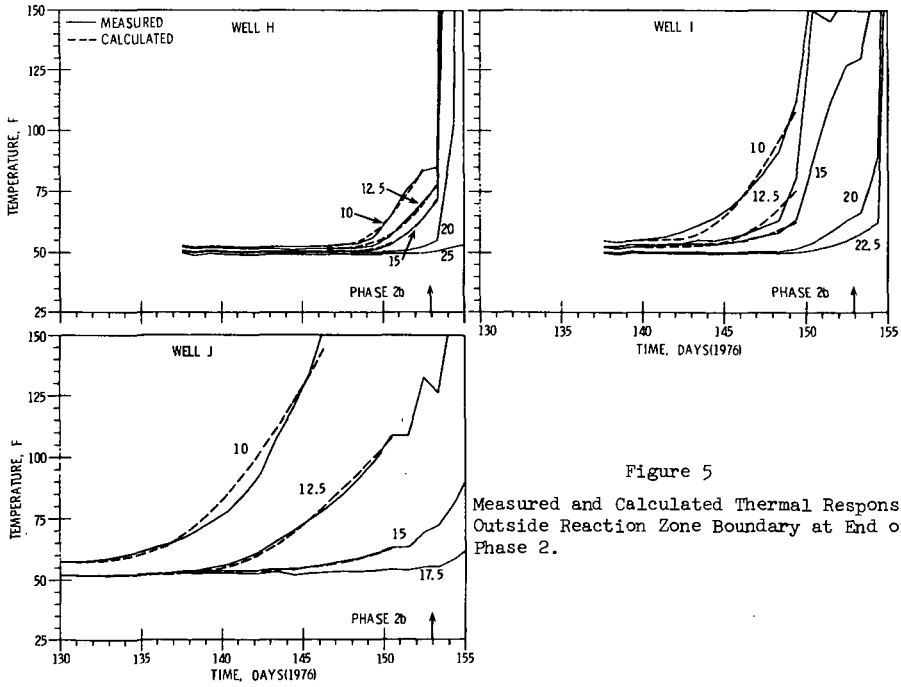

Figure 5

Measured and Calculated Thermal Responses Outside Reaction Zone Boundary at End of Phase 2.

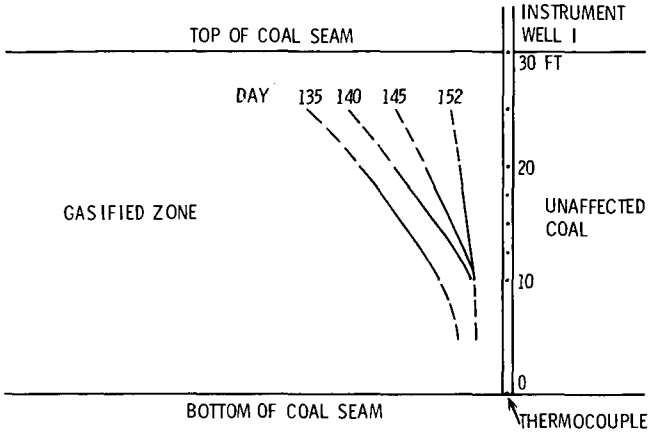

Figure 6. Schematic Diagram of Reaction Zone Boundary Movement Near Well I During Phase 2.

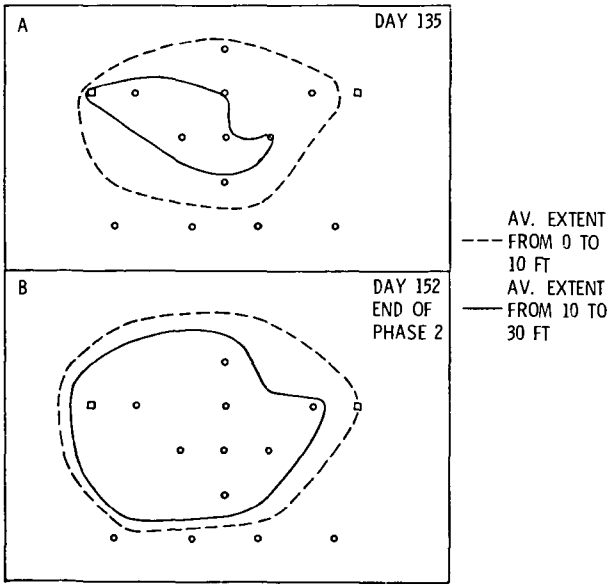

Figure 7. Delineation of Affected Coal Regions at 2 Times During Phase 2. Boundary Locations Based on Thermal Analyses and LERC Material Balance Calculations.

Investigations of Reverse Linking in Thin Bituminous Coal Seams

George W. Douglas
Marvin D. McKinley

The University of Alabama
College of Engineering
University, Alabama 35486

Introduction

This research project is being conducted as an investigation into the feasibility of underground (in-situ) coal gasification in the Warrior Coalfield of Alabama. It is sponsored by the National Science Foundation and is being carried out by the Mechanical, Chemical, and Mineral Engineering Programs of The University of Alabama in cooperation with the Geological Survey of Alabama. The Warrior Coalfield is the largest and most productive of the coalfields of the state. In addition to the seams that are now being stripped or deep mined, there are numerous thin seams less than 100 cm. in thickness which cannot economically be recovered by conventional technology. At present, the deepest underground mine in Alabama is 610 meters but recent deep disposal well drilling shows coal at 1370 meters. This suggests the presence of additional coal seams between these depths that cannot be economically mined but may have potential for production by in-situ gasification.

Laboratory Investigations

Several problems present themselves when one attempts to gasify thin seams of bituminous coal in-situ that are not evident for thick seams of lower rank coals. Eastern bituminous coals are largely swelling coals, a property which causes linking paths to swell short closing off air passages which are necessary for continuation of the gasification process. Further, it is suspected that heat losses to surrounding strata may cause serious problems in the economical gasification of thin seams. For these reasons it was decided that extensive laboratory and analysis work would be necessary before any field combustion tests would be feasible.

Laboratory tests to date have been conducted in a combustor shown in Figure 1. This combustor is designed to allow both forward and reverse combustion and the results of any particular run can be examined without disturbing the combustion residue. Instrumentation ports are available for thermocouple and gas sampling probes.

Early runs on solid blocks of coal were carried out with a single central crack being provided for linkage between inlet and outlet. Since it is expected that actual linking in the field will be done by hydraulic fracturing, resulting in narrow vertical cracks, such a model for the laboratory combustor seems reasonable. Forward combustion runs in the combustor verified that crack closure occurs due to coal swelling and, in addition, to tar condensation in the crack. Reverse combustion, on the other hand, proceeds quite satisfactorily and a typical result of reverse combustion is shown in Figure 2. Due to the physical properties of the eastern bituminous coal it seems that additional linking by reverse burning will be

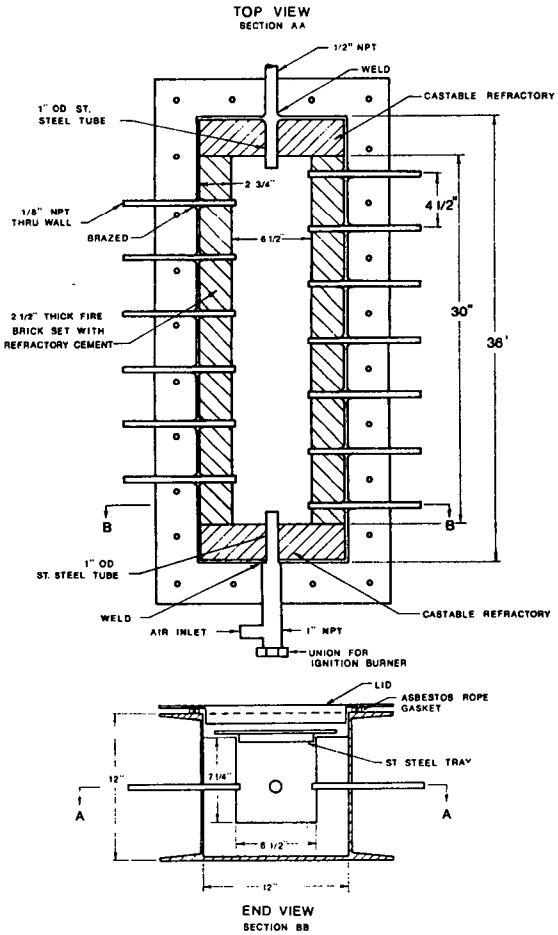

FIGURE 1

LABORATORY COMBUSTOR DETAILS

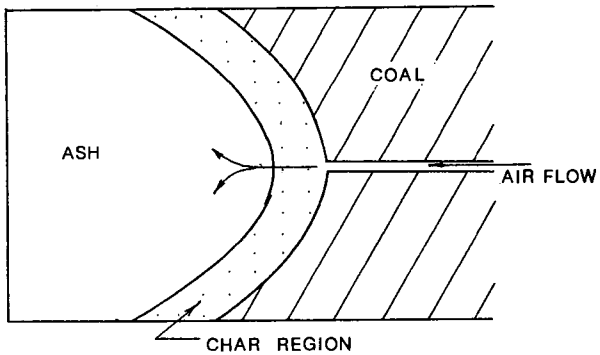

FIGURE 2

CONFIGURATION OF REVERSE BURN

necessary before a forward gasification process can take place. Primary concern is, therefore, presently being put on reverse linking procedures.

Early reverse combustion runs in the laboratory were made with high air flow rates and produced results similar to those shown in Figure 2. The burned-out region behind the thin carbonized zone is probably due to excess oxygen reacting with the carbon resulting in complete combustion. Since the objective of the linking process is to produce a carbonized zone which can then be gasified in the forward mode, it is important that the proper air flow be provided as that complete combustion is avoided. Further, the feasibility of the process will depend to a large extent on the radial extent of the carbonized zone and, since thin seams are being considered, heat losses to the surrounding strata will be important.

The approach to analyzing the reverse linking process will be two-fold. First, experiments in the laboratory combustor are currently being conducted to determine the relation between crack size, air flow rate and the extent of carbonization. During these experiments, measurements of temperature profiles within the coal are being made to provide estimates of temperature gradients. Past experiments have shown the gradients to be very steep so that coal within a few centimeters of the combustion zone shows little or no temperature rise. Secondly, a two-dimensional finite element heat conduction model is being adapted for use with the laboratory combustor. This program, written by Rohm and Haas Company for use with solid propellant rocket motors, can be used for thermally anisotropic, non-homogeneous bodies of complex geometry. The method of application will be to apply the model of Figure 3. Although the two-dimensional model will not strictly describe the three-dimensional case, it should provide some insight into the advance of the combustion zone. For example, when the program is applied to the model of Figure 3(a) it predicts isotherms as shown in Figure 4. Plans are to proceed stepwise into the coal moving the flame front and changing the boundary conditions as indicated by pyrolysis and air-flow experiments. The reasoning is that a portion of the heat that is produced by combustion is conducted into the coal seam raising its temperature thus pyrolyzing the coal at some distance ahead of the flame front. Further combustion occurs as a reaction between the pyrolysis products and air which has passed through the char to the reaction zone.

Laboratory pyrolysis experiments are presently being conducted to determine the rates at which various products are generated at different temperatures. The results of these pyrolysis experiments will be reported in a separate paper. The method of analysis will be to attempt to couple the combustion of the pyrolysis products and the resulting heat release with the conduction of heat into the coal and the consequent further pyrolysis. The finite element model allows a spatially variable boundary condition which will aid in this type of analysis. Actually, either of three boundary conditions may be used at the combustion front. These are constant temperature boundary, convection boundary, and constant heat flux boundary. Which of the three is to be used will depend on data obtained from this combustor and experience with the program. Since the oxygen supply will be greatest at the junction of the crack and the flame front, it is expected that this will be the region of greatest reaction and therefore the zone of fastest advance of the front. Thus, the hypothesis is that the carbonized zone will elongate as the pyrolysis reactions proceed and the question of interest becomes one of predicting the radial extent of the zone. Of course, multiple cracks will be present in the field case

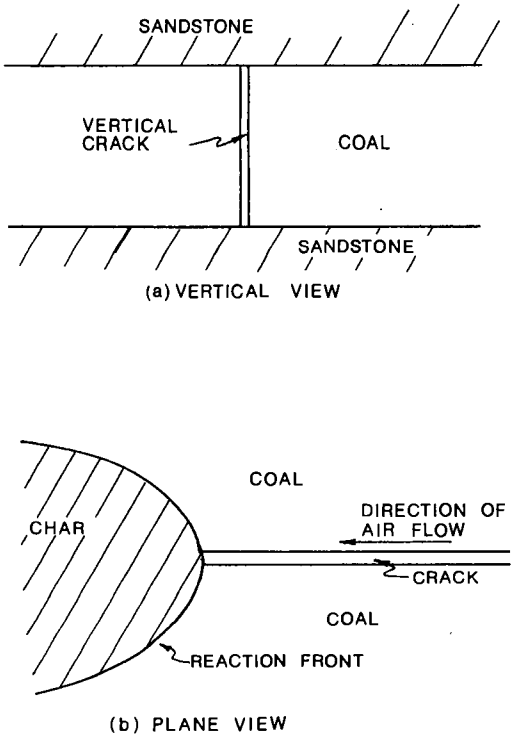

FIGURE 3
TWO DIMENSIONAL MODELS FOR APPLICATION OF THE FINITE ELEMENT HEAT CONDUCTION PROGRAM

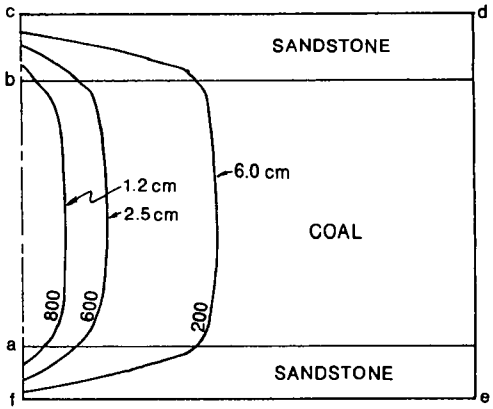

INITIAL CONDITIONS: 25° C

BOUNDARY CONDITIONS:

a-b: 1000° C
b-c: ADIABATIC
c-d: 25° C
d-e: 25° C
e-f: 25° C
f-a: ADIABATIC

COAL, $k = 2.16 \frac{cal}{hr\text{-}cm\text{-}°C}$

SANDSTONE, $k = 14.88 \frac{cal}{hr\text{-}cm\text{-}°C}$

FIGURE 4
RESULTS OF TWO DIMENSIONAL FINITE ELEMENT HEAT CONDUCTION PROGRAM AFTER ONE HOUR

but single cracks are considered here for analysis purposes. This method of analysis is expected to yield information on both rate and extent of the carbonization process as well as heat losses to the surrounding strata. The economics as well as as technical feasibility of the ultimate gasification process will depend in large part on the reverse linking process and our ability to predict its path and extent.

UNDERGROUND COAL GASIFICATION FIELD TEST IN ALBERTA - 1976

A.A. Roehl, R.A.S. Brown and E.J. Jensen

Alberta Research Council, Edmonton, Alberta, Canada

INTRODUCTION

Coal gasification is the processing of a solid fuel - coal - to generate a gaseous fuel. This has been practiced for many years in above-ground gasifiers using mined coal. The process involves primarily the reaction of the carbon in coal with water to generate hydrogen and carbon monoxide. Heat required to make this endothermic reaction proceed is provided by combustion of a portion of the coal. By-products of the reactions are carbon dioxide and pyrolysis products of coal.

In underground coal gasification (UCG) the reactions are carried out in the coal seam. In early applications mined channels were used for communication between the coal seam and the surface and within the coal seam. Technology now is based on channels created from the surface by directional drilling or by linking vertically drilled wells.

In the Canadian context, UCG is viewed as a method of recovering energy from coal resources which for economic or mining reasons lie outside the current limits of mining technology. In particular it should be applicable to very deep coal deposits or to deposits which include substantial amounts of non-combustible mineral matter and are not amenable to conventional mining.

The test described in the present paper dates back to a meeting held in the spring of 1975 at which the Alberta Research Council presented tentative plans for a UCG field test to representatives of interested companies. Response of the companies to the ARC proposal was favourable and over the following months more detailed plans for a field test were drawn up culminating in a meeting held in early February 1976 at which the companies agreed to proceed with the test and to provide part of the funds for it.

Following evaluation of a number of test sites, the Research Council decided upon a site located south of Forestburg, Alberta (about 120 miles southeast of Edmonton - see Figure 1) at the Vesta Mine of Manalta Coal Ltd. A detailed description of the test will be given in the following paragraphs. The test took place during the summer of 1976 with the following objectives:

(a) to better evaluate and understand current technological methods in underground coal gasification;

(b) to demonstrate the feasibility of those technological methods in a Canadian context;

(c) to demonstrate that gas with a low Btu content (a heating value of 100-200 Btu's/SCF) can be produced on a sustained basis; and

(d) to make a preliminary and basic assessment of the factors pertaining to the environment that may be affected by an underground coal gasification test.

Contribution No. 797 from the Alberta Research Council.

TEST SITE

1. Geological Description

The coal seam in which the test took place is in the Cretaceous, Horseshoe Canyon formation and located in the Battle River coal field. The coal underlies 60 feet of overburden and is immediately overlain by a bentonitic shale. The major fracture direction in the coal is 53° E of N while the minor fracture is at right angles to this at 143° E of N. Water pump tests indicated that the permeability of the coal was sufficiently great that preliminary fracturing would not be required.

Throughout the area of the test site, the coal is present as about 10 feet of coal in a 12 foot seam. There is a hard, continuous shale parting about two feet from the floor of the seam and a soft parting about two feet from the top of the seam. Two water pump tests were carried out to evaluate the directional permeabilities of the coal seam, one in October, 1975, and the other in April, 1976. In planning the test pattern, the major permeability direction used was 53° E of N.

The coal in the seam is subbituminous. Table 1 contains the proximate and ultimate analyses of the coal as well as its calorific value. The water level at the test site (i.e. piezometric height) prior to the test was approximately 8 feet above the top of the coal. Drilling indicated that the water source was located towards the lower portion of the coal seam.

TABLE 1

Coal Analysis *%

	Capacity Moisture Basis	Dry Ash Free Basis
Proximate		
Moisture	21.5	
Ash	23.9	
Volatile Matter	24.5	44.9
Fixed Carbon	30.1	55.1
Ultimate		
Moisture	21.5	
Ash	23.9	
Carbon	40.3	73.8
Hydrogen	2.7	5.0
Sulfur	0.4	0.8
Nitrogen	0.8	1.4
Oxygen	10.4	19.0
Calorific Value (Btu/lb.)	6820	12490

* Composite of samples from vertical water test well through coal seam.

2. Test Plan

The test planned for the Forestburg site was, as the objectives indicate, limited in scope. A rectangular well pattern was drilled to define an area 60 feet by 30 feet, the 60 foot side being in the direction of the major permeability. The test plan involved linking and gasifying the two shorter ends of the pattern in succession, then attempting a 'line drive' of one of the linked sections towards the other. In principle, this should create a long sweeping gasification front which should utilize most of the coal in the given area.

Linking of the wells was to be carried out by reverse combustion which was demonstrated successfully in UCG tests at Hanna, Wyoming. The line drive and gasification of the linked zones were to be carried out in the forward cambustion mode.

The effect of UCG on the groundwater was to be monitored by chemical analysis of samples taken prior to, during, and subsequent to the gasification test. Piezometric heights were also to be monitored for possible changes.

To detect movements of the ground at the test site which might be caused by subsidence in the reaction zone, monuments were placed inside and outside the test pattern as shown in Figure 2 and surveyed to provide base data for subsequent surveys during and after the test.

3. Physical Installation

(a) Flow System

The site plan is shown in Figure 2. The air was supplied from the blower and compressor bank or from a portable compressor. Surface piping was provided as shown in Figure 3 so that air could be fed to any well and product gas directed from any other well to the flare stack. The product gas passed through a knock-out drum upstream of the flare stack to remove tars and entrained water.

Gasification wells 1 through 4 were cased and grouted with high temperature grout. Figure 4 shows the method of completing and cementing the wells. Wells 2 and 4 were grouted to the lower part of the seam while wells 1 and 3 were grouted about midway into the coal seam. These wells were cased well into the coal seam to counteract gravity override during linking and gasification.

(b) Instrument System

In addition to the gasification wells, a series of instrumentation wells were drilled within the test pattern. These are shown in Figure 5 as series 1s through 9s and series 1o through 4o.

The 's' series of wells (sampling wells) contained a 1 inch steel pipe for gas sampling and as a support for thermocouples in and above the coal seam as shown in Figure 4. Within the coal seam the sample pipe was perforated. High temperature grout was used to seal and anchor the sampling line within the overburden.

The 'o' series of wells (overburden wells) contained thermocouples located from one to two feet above the top of the coal seam to monitor the penetration of heat into the overburden. These were also to assist in locating the gasification front during the line drive phase of the experiments.

Gas samples were taken from the production wells and gas sampling wells, passed through knock-out pots to remove tar and liquid water and then through lead lines for analysis in a gas chromatograph system located in the control trailer. Sample gas was passed through fibre filters immediately outside the trailer to remove the additional tar and water which condensed during cooling of the gas samples.

Thermocouples were connected to a scanner in the center of the test pattern which in turn was connected to the data logger and computer system for data storage and recording. The complete data collection and processing flow diagram is shown in Figure 6.

Sequencing of the recording of operating data was carried out by a PDP-8M computer having a dual DEC tape system. A teletype copy of the data was generated for the operator and the data stored on magnetic tape for future analysis. Some of the data were plotted by computer to provide a guide for operators during the test.

FIELD TEST OPERATION

Prior to gasification, it is necessary to dry out part of the coal seam and to establish communication within the seam so that air can be circulated. This was carried out in the Forestburg tests by flowing air through the seam between wells 3 and 4 for a number of days. Reverse combustion linking of the 3-4 segment was started August 19th with injection of air and insertion of an electric heater into well 3. The combustion was established in well 3 within three hours and air injection was then switched to carry out the reverse combustion linking stage. The link was completed between wells 3 and 4 by injecting air successively into wells 4s, 5s, 6s and 4. Following completion of the link, forward mode gasification proceeded until carbon dioxide and oxygen levels in the product gas from well 3 indicated that the gasification zone had reached the production well. At this stage the gasification test in the 3-4 zone was terminated and water injected to extinguish the fire prior to commencing operation in the 1-2 zone.

Comparative results from the gasification stage are shown in Figure 7. The volume of gas produced was less than twice the injected air while heating value of the gas produced ranged from 110 to 150 Btu's/SCF. During the gasification of the 3-4 zone, it is estimated that about 160 tons of coal were consumed.

Gasification of the section between wells 1 and 2 was started with ignition in well 1. Following ignition a similar procedure to that followed in the previous link was carried out: that is, the link was made to well 1 successively from wells 1s, 2s and 3s. During the linking stages up to well 3s it was noticed that the linking was more sensitive to variations in the injected pressure and flowrate than it had been in the 3-4 link, and it seemed that relatively small changes in flowrate would cause a change to forward gasification between the injection well and well 1.

When the link had been completed to 3s, it was not possible to get communication to well 2. Perforation of the lower 3 feet of well 2 was carried out to try to alleviate this problem and did in fact increase the air acceptance of well 2. The link was never, however, completed to the stage that sufficient air could be injected to satisfactorily carry out forward gasification of the 1-2 zone.

At this stage it was decided to abandon gasification in the 1-2 zone and to attempt to link directly to the gasified zone between wells 3 and 4. Accordingly, injection was continued into well 2 and also into well 1 with production from wells 3 and 4; that is, a forward

combustion link was attempted between zones 1-2 and 3-4. Communication was established quite rapidly with well 3 and there was indication from the thermocouples in well 7s that the reaction had passed by this area. At this stage in the test, however, lateral gas leakage became excessive and product gas was detected in wells beyond the test pattern. In an attempt to limit the loss of product gas to the formation, injection was switched to wells 3 and 4 with production from wells 1 and 2. Product gas continued to be detected outside the limits of the test pattern and the test was terminated.

POST BURN INVESTIGATION

One of the advantages of carrying out the Forestburg test in a shallow coal seam is that the post burn investigations of the gasified zone within the seam can be made more easily and at lower cost. While detailed plans for this post burn investigation are not finalized, several possibilities have been considered and a tentative decision made on the procedure to be followed.

One of the difficulties in evaluating the suitability of a particular coal deposit for underground gasification is the estimation of the utilization of coal within a given area. From previous work it is known that gravity has an influence on the coal utilization as the gasification zone tends to rise towards the top of the seam. For this reason production and injection holes for this test were drilled well into the coal seam. One of the more important and unique investigations in a past burn study of the gasified area would be to measure the degree of utilization of the coal for known conditions of air injection and gas production. Inspection of the boundary of the gasified zone would yield a better appreciation of the mechanism of the gasification process as shown by the separation of combustion and pyrolysis zones. Another factor of interest in post burn studies would be the subsidence of overlying formations into the gasified zone. Information of this kind is not available at present and cannot be deduced from subsidence studies of areas developed by underground coal mining since the overburden in that case, while dried out to some extent, is not subjected to temperatures as high as those encountered during gasification of coal.

Post burn inspection of the gasification area requires mining or excavation of the seam or insertion of remote sensing equipment into the gasified zone. Some of the possibilities are noted below.

The most promising method of post burn evaluation for a shallow site and the method for which detailed plans are now being developed for the Forestburg test site is excavation by strip mining techniques. This entails removal of overburden down to a few feet above the top of the coal seam followed by more careful mining of the gasified zone. Either dragline or scrapers could be used for the initial stripping although the dragline has some advantage if subsidence is anticipated.

Underground mining of the gasified zone has been considered but was ruled out because of safety considerations. Residual highly toxic gas from the gasification process would be an unwarranted hazard to personnel working underground.

Coring through the gasified zone was tried in the earlier Hanna tests. It is difficult, however, to drill into a gasified area without destroying the structure left by the gasification. Coring is useful for indicating the degree of heat penetration into the formations overlying and underlying the gasified zone provided that cores can be recovered.

An initially attractive method would be to suspend a remotely controllable movie camera, television camera or sonar device in the gasified zone. The zone can then be scanned by the remote device through a single borehole. The success of this method is dependent upon the presence of a well defined cavity. This is not likely to exist in this case.

SUMMARY

It is difficult to determine at the moment the differences between the gasification tests in zones 3-4 and 1-2. One obvious difference is that water availability was greater during the initial link and gasification in the 3-4 zone. Subsequent to gasification in the 3-4 zone, water levels throughout the pattern were lowered (up to 12 feet at the gasification wells). This decrease of water availability very likely had a marked influence on the lateral gas leakage noted during linking in the 1-2 zone.

The test did show that fuel gas having a heating value greater than 100 Btu/SCF can be produced from a shallow coal seam and that vertical containment is possible even at depths as shallow as 60 feet. More detailed evaluation of the test must await the analysis of all of the operating data and the results of the groundwater testing and site monitoring programs.

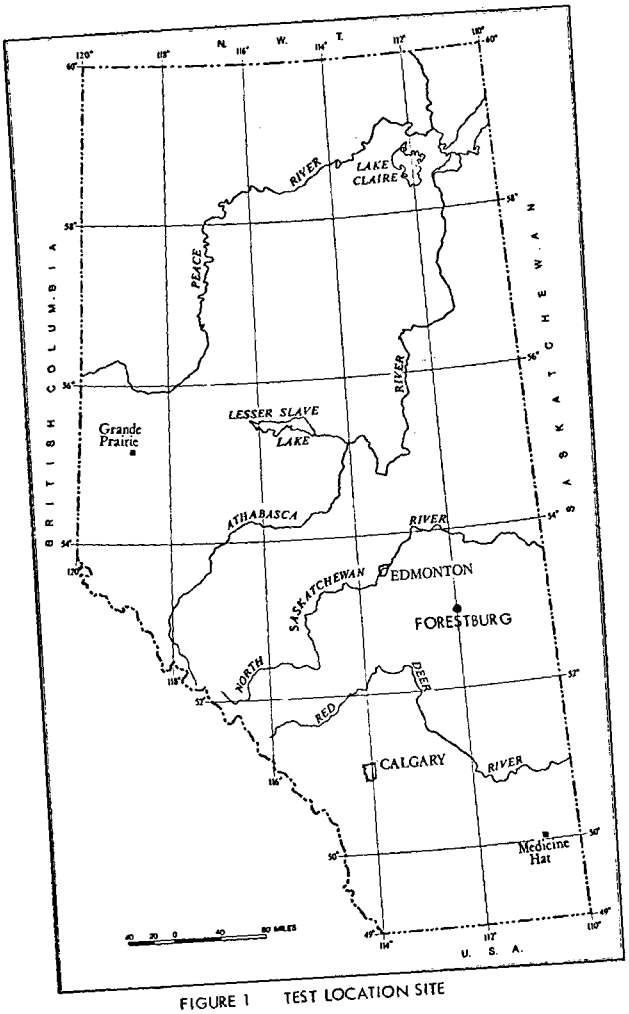

FIGURE 1 TEST LOCATION SITE

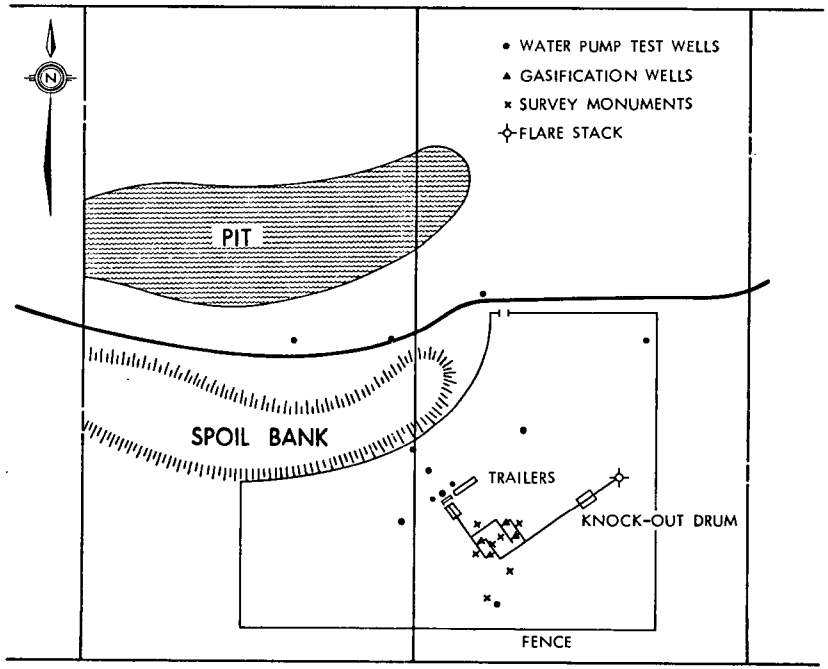

FIGURE 2 SITE PLAN

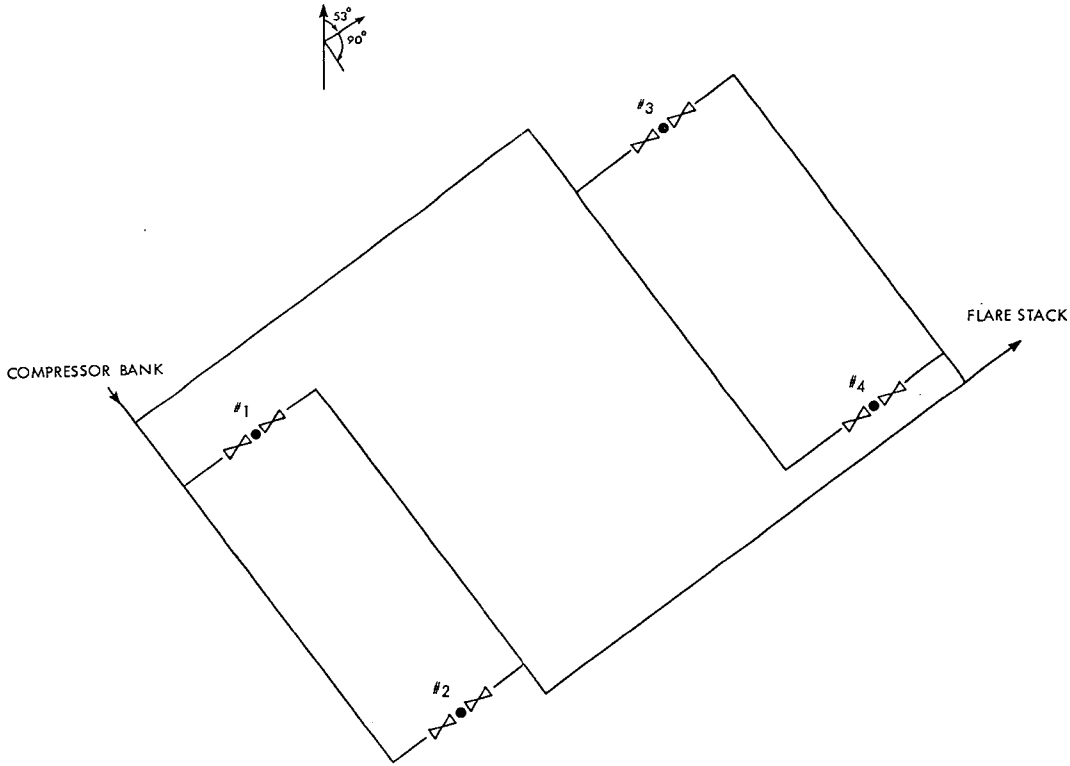

FIGURE 3 SURFACE PIPING PLAN

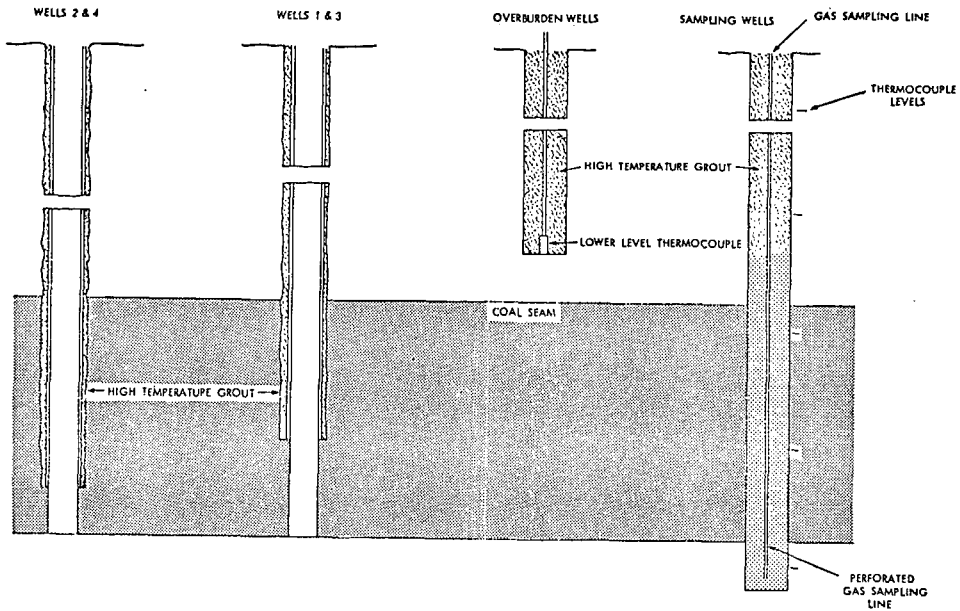

FIGURE 4 TYPES OF WELL COMPLETIONS

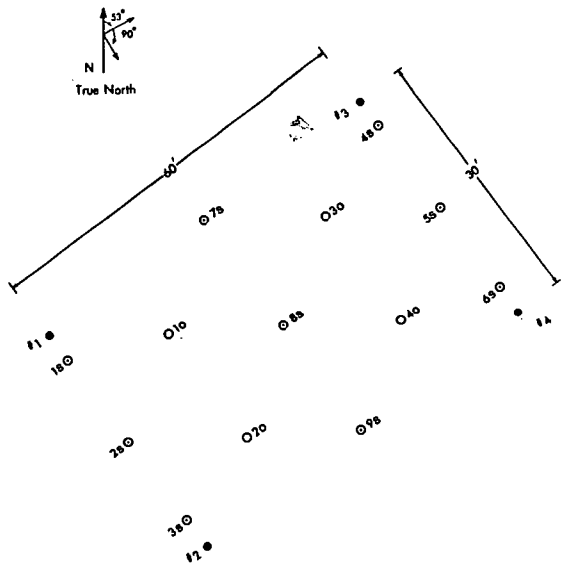

● GASIFICATION WELLS
⊙ SAMPLING WELLS
O OVERBURDEN WELLS

FIGURE 5 INSTRUMENTATION WELL PLAN

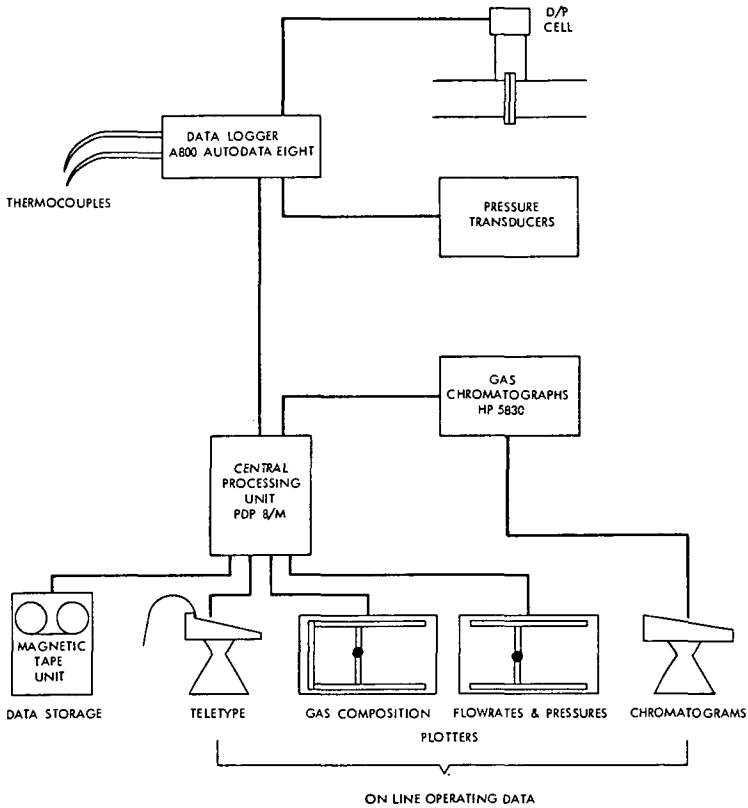

FIGURE 6 DATA PROCESSING NETWORK

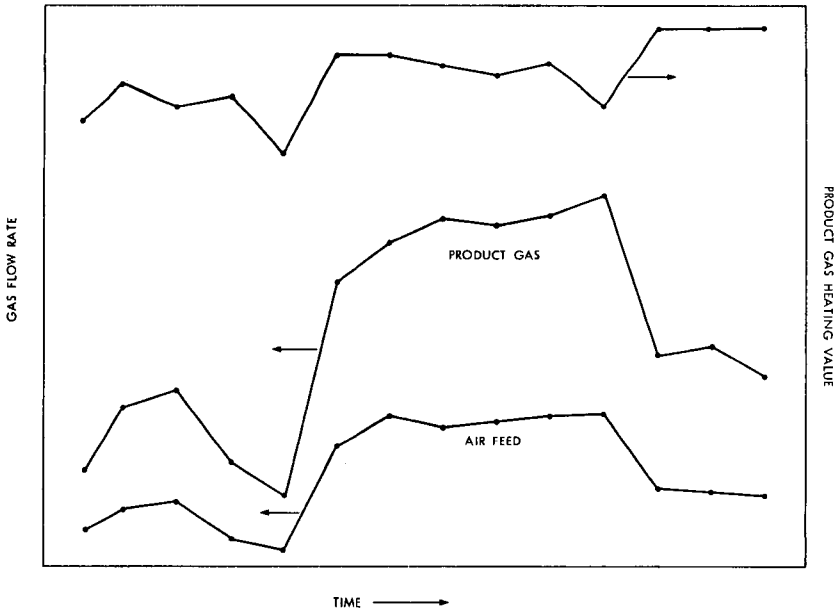

FIGURE 7 PRELIMINARY TEST RESULTS

POTENTIAL FOR UNDERGROUND COAL GASIFICATION IN THE SOUTHWEST

E. A. Walters and H. E. Nuttall

Departments of Chemistry and Nuclear and Chemical Engineering

University of New Mexico, Albuquerque, New Mexico 87131

INTRODUCTION

In occasional outcroppings and beneath the surface of the high plateaus and just west of the southern Rocky Mountains are large deposits of sub-bituminous coals. These coals were formed in the estuaries, swamps, and lagoons at the edges of the extensive epicontinental sea of the Late Cretaceous Period. Many millions of tons of this coal lie strippable depths (overburden is less than 250 feet), but perhaps 90% of the total deposits lie deeper. These deposits will probably only be tapped if underground gasification proves feasible. In this paper the question of the suitability of Southwestern coals for underground gasification is examined.

COAL RESERVES

The coal fields of the United States are shown on the map in Figure 1. Of the sub-bituminous basins in the Southwest the largest and most extensive is the San Juan Basin located in northwestern New Mexico. This study focuses attention solely on the San Juan Basin. The San Juan Basin is somewhat arbitrarily subdivided into 19 separate coal fields or coal areas, Figure 2. The general orientation of the fields is an exposure of coal seams on the western edges at elevations of 7,000 or more feet above sea level dipping gently but steadily to the east at an incline of 2 to 6 degrees. At the eastern extremities the lowest Cretaceous beds lie some 2,000 feet below sea level.

Stratigraphically the deposits are very complex. The coal beds are highly lenticular, a consequence of their formation from peats at the edges of Cretaceous swamps or estuaries. The lenses tend to be long and narrow and reflecting the irregular shape of Mesozoic costlines. Lengths vary from 1 to 30 miles and widths from 1/2 to 5 miles. At their thickest the lenses rarely exceed 12 feet, though isolated examples of seams as thick as 22 feet are known, and the most common thickness are between 3 and 6 feet. Lenses are stacked one above the next so that generally the thin portion of one overlies a thicker section of one beneath it. The deposit between seams is a wide variety of coastal sedimentary rocks, for example sandstones, shales, siltstones, and limestones. Seams themselves are frequently infiltrated with fine layers of clays or other sedimentary deposits. Interspersed between the major lenses are numerous thin seams of coal. Detailed stratigraphy varies drastically from site to site and is known well only for a few locations. The fundamental geologic structure is simple, however, and the basin is generally free from faults (1,2,3).

The coals of the San Juan Basin consistently fall into the range of sub-bituminous A or B in the deepest beds to high-volatile C or B bituminous nonagglomerating coals near the surface (2). In this respect and with regard to the low sulfur content (generally less than 1% of which half is typically organic sulfur) these coals are suitable for gasification.

The Southwest is a semi-arid region; annual precipitation in the coal basin is 4-6 inches. The only perennial stream in the entire San Juan Basin is the San Juan River itself which rises in southern Colorado and crosses the northwest tip of the coal basin before continuing westward to the Colorado River. In the coal bearing areas only normally-dry arroyos feed the San Juan River. The aridness carries

over to the coals which at strippable levels have moisture contents that average in the 12-15% range (3). There are no important aquifers at strip mining depths, the first aquifers lie about 1200 feet below ground surface. This water is of very low quality, but it is usable for livestock watering. There are persistent but largely unconfirmed reports of sporadic artesian activity in the basin. However, movement of ground water in the vicinity of most of the seams is restricted to a few feet per year.

There is coal at varying depths throughout the basin as pointed out above. The amount lying within 250 feet of the surface is estimated to be 5.97 billion tons (4). That lying between 250 feet and 3000 feet is estimated to be 122 billion tons while the amount still deeper is expected to be approximately double that amount (3,5). It is evident that in excess of 90% of the San Juan coal lies in deep seams.

The entire basin lies in a region of low population density and possess minimal agricultural value. The latter feature can be illustrated by the computation that the livestock carrying capacity of the western portions of the basin is about one adult sheep per 55 acres (3). The population density of the region is slightly more than seven people per square mile; this figure includes several sizable muncicipalities, so the population density of the vast open areas of the basin is very low indeed.

GASIFICATION PROPERTIES OF SAN JUAN COAL

Several properties of New Mexico's San Juan coal have been investigated and compared to Wyoming sub-bituminous coal in which successful in situ gasification tests have recent been performed by the Laramie Energy Research Center. In addition to chemical analysis, the properties compared are permeability, the extent of fracturing during pyrolysis and the apparent devolatilization rates.

As a first consideration in comparing New Mexico's San Juan and Wyoming's Hanna sub-bituminous coal, the chemical analysis and heating values of deep seam coals from both locations are very similar as shown in Table 1. San Juan coal, however, did exhibit a lower moisture content but this factor tends to vary widely depending upon sample handling.

Coal permeability is an important parameter for the in situ process. Western sub-bituminous coals typically display moderate permeability upon drying. The axial permeability of New Mexico's sub-bituminous coal was experimentally and the resulting values are presented in Table II. The measured permeabilities for dry samples compare favorably to values reported by Rozsa (6) for Wyoming Wyodak coal and to values published by Schrider, et. al., (7) for Hanna, Wyoming sub-bituminous coal. The nitrogen permeabilities were in the range of 1 to 5 darcies for coals from all these sources. This rather high natural permeability of sub-bituminous coals seems to result from cracks and fissures exposed during dehydration of the coals.

Devolatilization studies of San Juan coal have been performed recently and the results compared to Wyoming sub-bituminous coals. Coal devolatilization rates were determined by measuring the weight and product gas composition history of one inch diameter coal particles. The single particle reactor and system are shown in Figure 3. The reactor and its operation have been described elsewhere (8). Briefly, the sample is placed in a basket suspended from a load cell which is interfaced to a PDP-11 computer signal for data storage. Carrier gas is introduced at the desired temperature through a fluid heater. Thermocouples and pressure transducers located at various points are also interfaced with the computer so continuous temperature and pressure recorded is maintained. Product gases were sampled and collected and then analyzed either on a mass spectrometer or a gas chromatograph.

From these studies two factors relating to coal reactivity were observed. First from examining specially prepared and cross-sectioned samples of pyrolyzed particles, an extensive network of fissures and cracks was observed. Similar internal fissuring was also reported by Campbell (9) for Wyoming sub-bituminous coal. He found internal surface area increased from 4 to 200 m^2/g during pyrolysis of the coal. The observed immense increase in internal particle surface area accounts in part for the high reactivity of western sub-bituminous coals. Shrinking coals generally exhibit large surface area increases upon devolatilization.

The devolatilization rate of San Juan coal has also been measured by using weight data obtained from the single particle reactor mentioned previously (10). Comparison data but for smaller coal particles has also been taken using Wyoming coals. Both San Juan and Wyoming sub-bituminous coals exhibit similar devolatilization rates.

From these preliminary laboratory comparisons of San Juan and Wyoming coals, it appears that New Mexico's sub-bituminous coal behaves in a similar manner to the Wyoming coals which have recently been successfully gasified underground.

OTHER FACTORS INFLUENCING IMPLEMENTATION OF UNDERGROUND GASIFICATION IN THE SOUTHWEST

In addition to questions about coal reactivity, seam structure and stratigraphy, and quantities of reserves, several other factors are important in determining the likelihood of the actual implementation of underground gasification in the Southwest. First, there are environmental considerations. Sulfur content of these coals is low and approximately half of it is organic sulfur, so problems arising from this element will be minimal. Subsidence is very likely to occur but it should not be a problem because the land has little aesthetic value and currently has no agricultural value except for low density support of cattle or sheep. The impact on ground water is less clear. There are aquifers in the region, but most of these are deep and migration of water to them from gasification residue is unlikely. If gasification is conducted below the known aquifers then mechanisms exist for contamination of the water. Just how serious this might be is an unanswered question that must be addressed soon.

Secondly, gasification of coal with such a consistently low moisture content has not been well studied. Water plays a minimal role in the initial devolatilization but can be crucial in determining the nature of the product gas of the higher temperature gasification phase. In the Hanna tests there have always been rather large quantities of moisture in the reaction zone which can lead to a reductive reaction with coal. This will generally not be a possibility in the San Juan Basin.

Next, the southern and western portions of the country are those that are growing most rapidly, and ranking high among these are the areas around Phoenix and Tucson plus much of southern California. Southwestern coal is the closest sources of fossil energy available for the generation of electrical power demanded by these centers. Consequently, it is very likely the Southwestern coal will be consumed at ever increasing rates to meet an expanding regional demand for electrical power.

In the southwestern region a number of large power plants are presently operating on strip mined coal. As an example, the Four Corners Complex for electrical generation is fed by the Navajo mine which is the largest coal mine in terms of production in the United States. The current production rate is approximately 7 million tons per year. All of this coal is used to generate 2,100 megawatts of electrical power. The Four Corners Complex is a jointly owned enterprise in

which 48% of the power goes to Southern California Edison, 15% to Arizona Public Service Co., 13% to Public Service Company of New Mexico, 10% to Salt River Project and 7% each to Tucson Gas and Electric and El Paso Gas and Electric. Since the distribution of power generated in the San Juan Basin is established and the demand is increasing, this serves as an incentive for the development of the deep seam coal reserves through underground gasification.

Lastly, the potential market four southwestern coal is expanding not only because more people in the Southwest are requiring more electrical power, but also because the natural gas and oil supplied in the region are dwindling. Since an extensive pipeline network runs from this region. BTU gas and/or liquid fuels generated by underground methods could readily be shipped to distant consumers. Recognition of this fact has already been a major incentive for proposed sufrace gasification facilities and could well be a determining factor for the commercialization of underground gasification in the Southwest.

Summary

Laboratory studies of samples of San Juan (New Mexico) and Hanna (Wyoming) sub-bituminous coals reveal strong similarities in permeability, devolatilization reactivity, and fracturing when subjected to simulated underground gasification conditions. The results suggest that San Juan basin coal can be expected to gasify in a manner similar to Wyoming coal. The seam and bed structures are vastly different in the San Juan basin and the limitations imposed by thin, multiple seams that have low moisture content are not clear. On the other hand, underground gasification is a viable alternative from the point of view of environmental and economic considerations. More detailed reactivity studies of various coals of the basin and much more stratigraphic information followed by field tests are required before a definitive statement can be made about underground gasification in the Southwest. What can be said now is that indications are mixed, but tend to be positive.

REFERENCES

1. U.S. Energy Outlook - A Summary Report of the National Petroleum Council, National Petroleum Council, Washington, DC, 1972, pp. 135-171.

2. F. E. Kottlowski, J. W. Shomaker, and E. C. Beaumont, "New Mexico Coal Resources," in 1973 Keystone Coal Industry Manual, McGraw-Hill, Inc., 1973, pp. 503-510.

3. F. E. Kottlowski, "Report of the Coal Resources Committee," Governor's Energy Task Force Publication, NM Energy Resources Board, June, 1975.

4. E. C. Beaumont, "The Impact of Coal on Northwestern New Mexico," in Shomaker, et.al., Strippable Low Sulphur Coal Resources of the San Juan Basin of New Mexico and Colorado, NM Bureau of Mines and Mineral Resources, Memoir 25, 1971.

5. F. E. Kottlowski, "Annual Report for the Fiscal Year July 1, 1973 to June 30, 1974," NM Bureau of Mines and Mineral Resource, 1975.

6. Rozsa, R. B., "Overview of Laboratory Experiments in Support of the Lawrence Livermore Laboratory In-Situ Coal Gasification Program," Lawrence Livermore Laboratory, UCID-16845, July 15, 1975.

7. Schrider, Leo A., and J. Pasini III, Underground Gasification of Coal Pilot Test Hanna, Wyoming, American Gas Association Fifth Synthetic Pipeline gas Symposium, October, 1973.

8. H. E. Nuttall, W. G. Stoddart, and W. J. Chen, "Reactivity and Kinetics of Subbituminous New Mexico Coal". Department of Chemical and Nuclear Engr., University of New Mexico, Albuquerque, New Mexico.

9. Campbell, J. H., "Pyrolysis of Sub-bituminous Coal as it Related to In-Situ Gasification (Part 1: Gas Evolution)," Energy and Technology Review, 1 April, 1976).

10. Stoddart, Wendell, A Reactivity and Kinetic Comparison of Large Single San Juan and South African Sub-bituminous Coal Particles," M.S. Thesis, The University of New Mexico, 1977.

TABLE I

Analysis of San Juan and Wyoming Core Coals

	NM Core	Wyoming Core
Proximate Analysis		
% Moisture	3.22	7.82
% Ash	4.06	8.21
% Fixed Carbon	56.02	49.57
% Volatile Matter	39.92	42.22
Ultimate Analysis (Dry and ash-free basis)		
% Carbon	79.34	73.68
% Hydrogen	5.34	5.69
% Oxygen	12.60	18.22
% Nitrogen	1.72	1.82
% Sulfur	0.45	0.60
Calorific Value (Moisture free), Btu lb^{-1}	13,801	11,641

TABLE II

Permeability of San Juan Core Coal

Gas	B_o, darcys
air	3.45
N_2	3.66
Ne	11.09

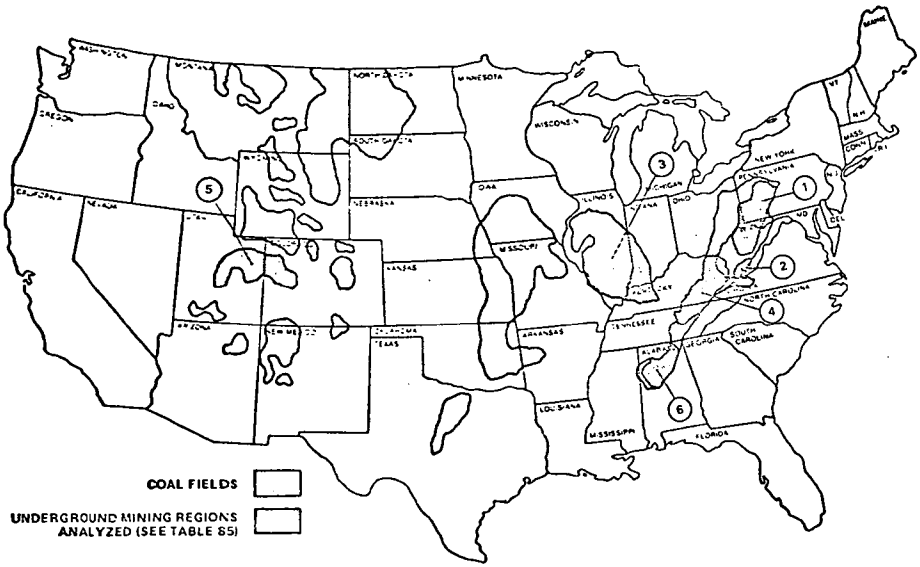
COAL FIELDS
UNDERGROUND MINING REGIONS ANALYZED (SEE TABLE 85)
1
2
3
4
5
6
NEW YORK
PENNSYLVANIA
NORTH CAROLINA
SOUTH CAROLINA
MISSISSIPPI
FLORIDA
LOUISIANA
ARKANSAS
TENNESSEE
MISSOURI
WISCONSIN
MINNESOTA
NEBRASKA
OHIO
MASS
CONN
R.I.
N.J.
MD
DEL
VT
N.H.
MAINE

Figure 1

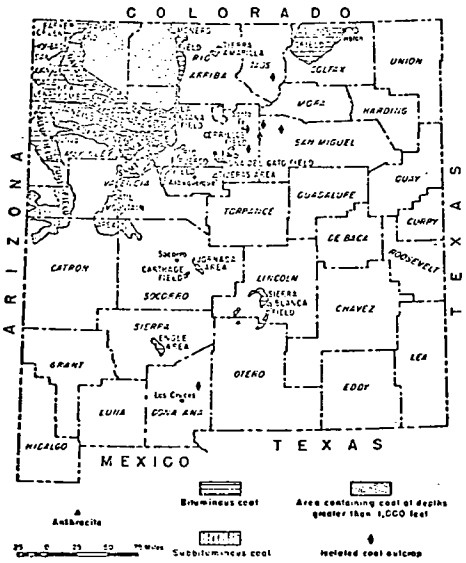
COLORADO
ARIZONA
TEXAS
MEXICO
TEXAS
UNION
COLFAX
MORA
HARDING
SAN MIGUEL
QUAY
GUADALUPE
TORRANCE
CURRY
DE BACA
ROOSEVELT
CATRON
SOCORRO
LINCOLN
CHAVEZ
SIERRA
GRANT
OTERO
LEA
EDDY
LUNA
DONA ANA
HIDALGO
Bituminous coal
Area containing coal at depths greater than 1,000 feet
Anthracite
Subbituminous coal
Isolated coal outcrop

Figure 2

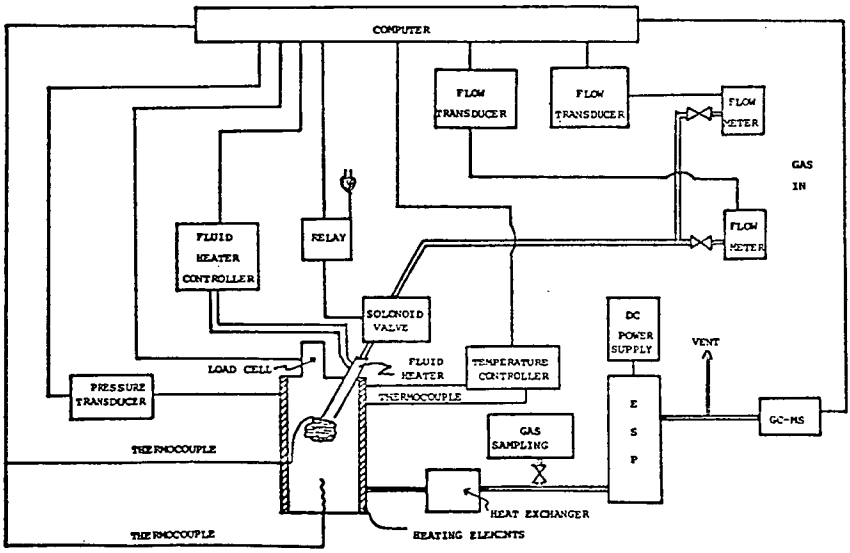

SCHEMATIC DIAGRAM OF COAL PARTICLE GASIFICATION REACTOR AND SUPPORTING EQUIPMENT.

Figure 3

AN INVESTIGATION OF AROMATIC FRACTIONS FROM COAL TAR PRODUCED BY AN UNDERGROUND COAL GASIFICATION TEST

S. B. King, F. D. Guffey, and G. W. Gardner

Energy Research and Development Administration
Laramie Energy Research Center
P. O. Box 3395, University Station
Laramie, Wyoming 82071

INTRODUCTION

As most people are well aware, the majority of fossil energy resources in the United States are in the form of coal. Current estimates place these resources at approximately 4 trillion short tons (1), yet only 10-25 percent of this resource is recoverable using present day technology.

The Energy Research and Development Administration is currently funding several projects to develop the technology of underground coal gasification. The objective of these projects is to increase the total recoverability of this vast resource. One of these projects is being conducted by the Laramie Energy Research Center and is referred to as the linked vertical well (LVW) process. This process is being developed at the Hanna, Wyoming, field site and has been under development since 1972.

The most recent test was completed in the summer of 1976. The results showed a total of 6700 tons of coal utilized and production rates up to 12 MM scf/day (2). The highest heating value obtained for a substantial period was approximately 175 Btu/scf. In addition to this low-Btu gas an organic condensate was produced. This organic condensate or coal tar comprised 1-1½ percent (by weight) of the gas stream. Its composition has been studied for various reasons, not the least of which is its value as a petrochemical feedstock or as a fuel. Another consideration is its possible environmental implications whether due to surface handling or effect on groundwater quality.

DESCRIPTION OF THE LINKED VERTICAL WELL PROCESS (LVW)

The coal seam at the Hanna site is a subbituminous coal, 30 feet thick and approximately 300 feet deep.

The LVW process is a two-step operation. The first step is to prepare the seam for gasification, since the virgin coal has a permeability too low to accept the high volumes of air necessary for gasification. This preparation is called "linking" and involves the drawing of a combustion front from the bottom of one well to an adjacent well using a reverse combustion technique. After this "linking" is complete,

the permeability between these two wells is sufficient to proceed with the second step or the gasification process. This involves injecting large volumes of air into one well and the gasification products being produced at the other well. It is during this step that the coal tars are produced and carried to the surface as a by-product of the overall gasification process.

EXPERIMENTAL

GLC analysis of the aromatic fractions were done on a HP-5712 chromatograph using a 10' x 0.093" 3% SP-400 on 80/100 Supelcoport column. With a flow rate of 30 ml/min, isothermal at 50° C for 2 minutes, then a 2° C/min increase to 300° C, a usable separation was obtained. Combined gas chromatography-mass spectroscopic studies were performed using a HP-5700A gas chromatograph coupled directly to an AEI MS-12 mass spectrometer. The GC separation was obtained using support coated open tabular columns.

Simulated distillations were performed with use of gas chromatography with residue defined as any material that does not boil below 1000° F.

The tar was separated into tar acids, tar bases and neutrals by acid-base extraction. The fractions were regenerated by pH adjustment and extraction with diethyl ether. Neutrals were also separated into aliphatic and aromatic fractions with the use of silica gel. Hexane was used to elute the aliphatics and methanol to remove the aromatics.

PHYSICAL PROPERTIES

Table I lists some of the physical properties of the sample to be discussed in detail. These are properties of the whole sample, not just the aromatic fraction.

Table I - Physical Properties

Specific gravity at 60° F	- 0.977
Viscosity at 100° F	- 13.16 centistokes
Heat of combustion	- 17,256 Btu/lb

Similar values have been measured for other samples collected during other tests. Their mobility (low viscosity) would make them easily handled in a surface facility and their heating value would qualify them as a possible fuel.

CHEMICAL PROPERTIES

The elemental analysis (Table II) is typical of the tars produced from the Hanna tests.

Table II - Elemental Analysis

C	- 86.33%
H	- 10.43
N	- 0.79
S_a	- 0.18
O	- 2.27

[a]Percentage determined by difference

The maximum values for nitrogen and sulfur that have been observed are 1 percent and 0.5 percent respectively.

Another technique used for analysis is simulated distillations. An interesting point is demonstrated by this technique, this being that none of the coal tar boils above 950° F. When compared with a coal tar produced by laboratory carbonization, the obvious difference is in the boiling point distribution. With the use of an internal standard, it was determined that the carbonized laboratory sample was 24 percent (by weight) residue versus 0 percent for the UCG sample (Table III).

Table III - Boiling Range Distribution

Sample	Amb-400°F	400-500	500-600	600-700	700-800	800-900	900-1000	Residue
Carbonized	0	11.3	16.3	13.1	15.2	12.4	7.5	24.2
UCG sample	6.2	16.9	25.6	28.2	16.0	5.3	1.8	0

This illustrates an important point about the UCG coal tar. It is a fractionated portion of the total coal tar produced underground in the seam. The passage through the production path, including the linkage path and well casing, acts as a preliminary separation step. The fate of the heavier components is questionable but there is certainly some cracking and perhaps eventual combustion of the remaining components.

These more volatile components that reach the surface provide a rather unique product for characterization when compared to "standard" coal tars produced in surface units.

The separation of numerous samples into tar bases, tar acids (strong and weak acids) and neutrals (aromatic and aliphatic) gave the following range of values (Table IV).

Table IV - Compositions wt % of Tar

Tar bases	2.5-8.0%
Tar acids	.1-1% - Strong acids 12-31% - Weak acids
Neutrals	55-77% - 70% Aromatic 30% Aliphatic

An interesting point was that after looking at many samples the relative amount of aliphatics versus aromatics was essentially constant (30:70). Previous investigations (3) of the tar bases indicate the composition to be primarily quinolines with some pyridines and anilines. The tar acids have been described (4) as alkylated phenols. The aliphatics (4) are mostly saturated with a C_9 to C_{31} normal series and a predominate C_{19} branched series.

AROMATICS

The aromatic fraction did not show any unusual components but did lack any alkylated benzenes, which were expected. The reason for this is believed to be the volatile nature of the methyl and polymethyl substituted alkylbenzenes and the technique that was used to collect the coal tar sample from the production stream. The collection procedure discriminated against the volatile components. The predominate type of alkylation found in the remaining aromatics was methylation. Table V lists the various compound types, or in some cases isomers, that were determined by GC-MS analysis.

Table V - Components of the Aromatics

Naphthalene
2 - Methyl Naphthalene
1 - Methyl Naphthalene
3 different Dimethyl Naphthalenes
Acenaphthalene or Biphenyl
A 1, 2, 3, 4 - Tetrahydronaphthalene w/ C_4H_8 substitutent
A Dipropyl Thiophene
4 different Trimethyl Naphthalenes
A Dimethyl - Ethyl Naphthalene
A Penta - Methyl Naphthalene
Anthracene and/or Phenanthrene
A Methyl Anthracene and/or Phenanthrene
An Ethyl Anthracene and/or Phenanthrene

The results presented in Table V show there is no evidence of PNA components and the majority of the alkylation is methyl.

COMPARISON OF AROMATIC FRACTIONS

As has been reported in a previous paper (4), the similarity of the separate fractions is remarkable. The same is true of the aromatic fractions. The three aromatic fractions that will be discussed are from three different tests. The first from December 10, 1973, during the Hanna I test, the second from June 25, 1975, during the Hanna II, Phase I test and the third from May 21, 1976, during the Hanna II, Phase II test.

Without doing a complete GC-MS analysis of all these samples and considering only the GC trace the striking similarity is obvious. The

assumption at present is that the aromatic fractions are similar in composition both qualitatively and quantitatively. This indicates a very constant liquid by-product from UCG.

CONCLUSIONS

Analysis of an aromatic fraction from a coal tar produced from an underground coal gasification test shows mostly methylated naphthalenes, anthracenes and phenanthrenes. The similarity between various aromatic fractions and the corresponding similarity of acid, base and aliphatic fractions suggests that the liquid product is very constant in composition with respect to time. This would in turn indicate that the LVW process approaches steady state conditions. The constancy of such a product would certainly be compatible and desirable with any facility that might utilize such a liquid for either a feedstock or as a fuel.

The lack of evidence for any PNA's in the aromatic fraction is certainly encouraging from an environmental standpoint and would probably be expected when considering the way in which the coal tar is produced.

As a by-product, the coal tar appears to be a desirable product which only enhances the outlook for underground coal gasification becoming a commercial process.

REFERENCES

1. P. Averitt, "Coal Resources of the United States, January 1, 1974," U.S.G.S. Bulletin 1412.

2. D. D. Fischer, C. F. Brandenburg, S. B. King, R. M. Boyd, and H. L. Hutchinson, "Status of the Linked Vertical Well Process in Underground Coal Gasification," presented at the Second Annual Symposium on Underground Coal Gasification, Morgantown, WV, August 1976.

3. S. B. King, C. F. Brandenburg, and W. J. Lanum, "Characterization of Nitrogen Compounds in Tar Produced from Underground Coal Gasification," presented at the Spring ACS meeting (Fuel Chemistry Division) in Philadelphia, PA, April 1975.

4. S. B. King, "Composition of Selected Fractions from Coal Tars Produced from an Underground Coal Gasification Test," presented at the Spring ACS meeting (Fuel Chemistry Division) in New Orleans, LA, March 1977.

NOTE: Any reference to specific brand names does not imply endorsement by the Energy Research and Development Administration.

MELTING BEHAVIOR OF COAL ASH MATERIALS FROM COAL ASH COMPOSITION

by

Karl S. Vorres
Institute of Gas Technology
Chicago, Illinois 60616

May 1977

INTRODUCTION

The melting behavior of coal ash materials is characterized by several temperatures relating to stages of deformation of cone-shaped ash samples on heating. Viscosity of coal ash melts through the molten temperature range is also useful for characterization. This information has been used primarily for design of steam generation equipment, but may be usefully extended to coal conversion processes such as gasification. Coal ash does not melt sharply like a pure compound, but rather softens over a temperature range as the temperature is increased. As it melts, the heated ash exhibits a plastic range between the solid and mobile liquid states. The temperature range corresponding to the plastic state, as well as viscosity and melting phemonena, depend on the composition of the ash and the gaseous environment. Studies of the melting and viscosity of ash melts over a range of temperatures and gaseous environments have demonstrated this dependence.[1,2,3]

The purpose of this paper is to provide some framework for understanding the observed behavior, and to suggest use of a concept that should be helpful in further studies of that behavior.

Acids and Bases

The melting and viscosity behavior has been described as a function of the composition of the coal ash in terms of acids and bases. The acids have been defined as oxides of Al, Si, and Ti, while the bases were oxides of Na, K, Ca, Mg, and Fe.

The structural inorganic chemical characteristics of the acids and bases will be of interest in establishing the reasons for labels such as acid or base, and in understanding the impact of the acid or base characteristics on the melting or viscosity properties of coal ash.

Inorganic cations may be characterized by ionic radii for their common valences. In general, the radii decrease with charge, and also with atomic weight for a given valence. The radii, according to Ahrens, for the inorganic cations indicated above are listed below in Angstrom units:

Si^{+4}	0.42	Fe^{+2}	0.74
Al^{+3}	0.51	Na^{+1}	0.94
Fe^{+3}	0.64	Ca^{+2}	0.99
Mg^{+2}	0.67	K^{+1}	1.33
Ti^{+4}	0.68		

The two values are given for iron because of the importance of both valence states.

In crystals, and in some cases for liquids, the cations are surrounded by a specific number of anions. This coordination number is determined by the ratio of the radii of the two oppositely charged species. A coordination number of four produces a tetrahedron and is expected between radius ratio limits of 0.225 and 0.414. A coordination number of six produces an octahedron and is expected between radius ratio limits of 0.414 and 0.732. The coordination number of eight is expected for somewhat larger radius ratios.

In coal ash the predominant anion is the oxide ion. Using a radius of 1.40 Å for the oxide and applying the radius ratio criteria, tetrahedral coordination is expected for cations with a radius smaller than 0.58 Å or specifically Si^{+4} and Al^{+3}. The octahedral configuration is expected for cations between 0.58 and 1.03 Å or Fe^{+3}, Mg^{+2}, Ti^{+4}, Fe^{+2}, Na^{+1}, and Ca^{+2}. The remaining K^{+} would be expected to have a cubic configuration with coordination number eight. Under proper conditions, these coordination numbers would be expected in melts.

Ionic Potential

Another useful concept is the ionic potential which is defined as the quotient of the valence and ionic radius for a given ion. This parameter indicates something about the ability of a cation to coordinate anions about it. A higher ionic potential indicates the ability of one cation type to compete effectively with other cations for available anions to form complex ions such as SiO_4^{-4} in a mixture like coal ash. The values for the ionic potentials of the species of interest are:

Si^{+4}	9.52	Fe^{+2}	2.70
Al^{+3}	5.88	Ca^{+2}	2.02
Ti^{+4}	5.88	Na^{+1}	1.06
Fe^{+3}	4.69	K^{+1}	0.752
Mg^{+2}	2.98		

The highest values belong to the acid group Si, Al, and Ti, while the lowest values belong to the bases.

It is suggested here that the ionic potential may be the physical characteristic which is useful in quantifying acid and base behavior, and would also be useful in future efforts to correlate melting behavior or viscosity with chemical composition.

The ionic potential is a measure of a cation's ability to compete for anions in order to form a complex ion of the form MO_x^{-n}. The ability is also dependent on the available oxide ions. The ability of Si to coordinate four oxide ions would be limited in the pure oxide SiO_2 if it were not for the possibility of sharing oxide ions between different Si. As a result, repeating SiO_2 groups in a V shape can form polymer type groupings. These groupings could be extremely long chains of linked tetrahedra. Other forms are also possible. If additional oxide ions became available, then they would provide the species needed to terminate the chains. As more oxide became available, the groupings would terminate more frequently and have a smaller agglomerate weight. A source for oxide ions would be oxides of cations with low ionic potential such as the alkalis or alkaline earths. These would be expected to dissociate into hard sphere ions, and the oxide ions would be coordinated by cations of the highest ionic potential.

It is suggested that the role of acids in coal ash melts is that of polymer formers with the greatest tendency to form polymers correlating with the greatest ionic potential. The role of bases is that of oxide ion donors. The oxide ions would be attracted to the ions of high potential to break up polymers and reduce viscosity.

In general, the available oxide ions from cations would tend to reduce the size of polymeric groups associated with cations of high ionic potential. Additions of compounds increasing the available oxide ion concentration would decrease the viscosity of a melt rich in Si and Al typical of eastern coal ash material. This effect has already been noted.

The Behavior of Iron

The two valence states of iron give significantly different values with the ferric ion being between the two groups. The special importance of iron can, in part at least, be correlated with the two valences it displays. This may be compared with the amphoteric behavior of certain other species. On the basis of the table of ionic potentials, the ferric ion may be thought of as a weak acid, and the ferrous ion as a base. In practice, the iron in coal ash in boilers will exist as a mixture of the two states. Only a minor part, frequently about 20%, is Fe_2O_3. The major part (about 80%) is FeO, with possibly some elemental iron. This indicates the appropriateness of classifying iron oxides (if they must be lumped into one type) with the bases, even though they are listed as Fe_2O_3.

The gaseous environment is important in determining properties of coal ash systems. Studies have shown a marked reduction of viscosity of melts in going from oxidizing to reducing conditions, which would significantly alter the proportion of ferric and ferrous ions. This change in properties would be consistent with a complex ion forming tendency for the ferric ion with its high ionic potential, and an oxide ion donor role for the ferrous ion with its lower ionic potential. Two factors would work to reduce the viscosity in a reducing environment: 1) reduction of concentration of polymer forming ferric ions, and 2) increase in oxide ion concentration available for cations with high ionic potential. The oxide ions would have been associated with the ferrous ions.

Conceptual Structural Considerations

Winegartner and Rhodes[3] indicated that the coefficients in front of the bases CaO, MgO, K_2O, and Na_2O should each be one when calculating the softening temperature using the base-to-acid ratio and expressing the ash composition for these materials in mole percentages rather than weight percentages. The implication of that observation in the context of this paper is that the bases are equally effective as oxide ion donors. Each formula contains one oxide unit. They further note that Fe_2O_3 should really be expressed as FeO. This is also consistent with characterizing FeO as a base and indicating the role of oxide ion donor for FeO.

The melting process may be pictured as application of energy to disrupt the crystal lattice of a solid. The lattice of the solid may be modified by the impurities to permit easier melting through introduction of additional large oxide ions in the acid oxide structure. Insertion of base cations would probably occur in the available interstices appropriate for the base coordination number. The resultant lattice strain would yield a lower thermal requirement for melting or a lower melting point. The further implication of Winegartner and Rhodes work is that the number of oxide ions is most significant, and that the nature of the base cations is not significant in affecting the softening temperature.

SUMMARY

The ionic potential (valence divided by ionic radius) may be used as a measure of acids and bases in predicting coal ash melting and viscosity from the chemical composition. The role of an acid is that of a complex ion former with anions provided by bases which in coal ash systems are oxide ion donors. In systems containing acids and limited oxide ion concentrations, polymers tend to form in the melts. Addition of bases reduces polymer size and would decrease viscosity. The gaseous environment may alter the relative concentration of ferric and ferrous ions, interconverting acid and base ions. In general, bases are reported to be equally effective oxide ion donors. The effects of base addition are proportional to the amount of oxide ion provided to the system.

REFERENCES CITED

1. Sage, W. L. and McIlroy, J. B., J. Engineering for Power, 82, 145 (1960).

2. Rees, O. W., Ill. State Geological Survey, Circular 365 (1964).

3. Winegartner, E. C. and Rhodes, J. Engineering for Power, 97, 395 (1975).

CHARACTERISTICS OF ASH AGGLOMERATES FROM AN ASH-AGGLOMERATING GASIFIER

David M. Mason

Institute of Gas Technology
3424 S. State Street
Chicago, Illinois 60616

INTRODUCTION

An ash-agglomerating fluidized-bed gasifier has been under investigation at the Institute of Gas Technology (IGT). In such a process, carbon utilization can be substantially improved over that obtained when ash is removed by continually discharging a nonselective portion of the fluidized bed containing both ash and carbon.

The pilot plant gasifier has a diameter of 4 feet and operates at near atmospheric pressure. The schematic diagram of Figure 1 shows that agglomerated ash leaves the gasifier through a centrally located venturi tube through which part of the gaseous feed (steam plus air or oxygen) is introduced to the reactor. Details of the gasifier and its operation have been described by Sandstrom, Rehmat, and Bair in a recent paper (8). In the present paper, we describe the agglomerated ash obtained during gasification of coke breeze and FMC char, and we discuss the probable mechanisms of their formation.

EXPERIMENTAL

Petrographic samples were mounted, sectioned, and polished mostly according to methods employed in coal petrography (1). Our apparatus for microscopical observations and determination of reflectance has been described (4).

Iron oxides and sulfides can usually be recognized by appearance, especially when more than one oxide or sulfide is present. Ferrous sulfide is brilliant, though not as brilliant as pyrite, and has a yellowish cast. Ferrous oxide is dead white, while magnetite is darker and gray in color. In initial observations and if doubt is aroused, measurement of reflectance is useful. Reflectance in air is used in ore petrography. Our own approximate measurements with oil immersion, arranged in order of increasing reflectance, are shown below, together with literature values for reflectance in air. Values for some of the compounds can vary with orientation and composition.

Mineral or Compound	Formula	Reflectance % In Air (3)	Reflectance % In Oil (Approx)
Iron Spinel	$FeO \cdot Al_2O_3$	--	0.9-1.2
Magnetite	Fe_3O_4	21.1	7-8
Ferrous Oxide	$Fe_{1-x}O$	--	18-24
Ferrous Sulfide	$Fe_{1-x}S$	42	18-24
Pyrite	FeS_2	54.5	33-44
Iron Metal	Fe	--	40-50

Scanning electron microscopy was carried out under the direction of Dr. Oom Johari at IIT Research Institute.

Ash samples were analyzed by the lithium borate fusion method of Boar and Ingram (2), with aluminum, calcium, iron, silicon, and titanium finished by atomic absorption and with sodium and potassium by flame emission. Sulfate was determined by the Eschka method. Acid-soluble iron was extracted by boiling with 3N hydrochloric acid and was determined by atomic absorption.

Agglomerated Ash From Coke Breeze

The ash product consisted predominantly of well-rounded particles (beads) ranging from about 1/16 to 1/4 inch in diameter, sometimes accompanied by some angular coke particles (Figure 2a).

Beads from an early run (No. 17) were subjected to detailed examination. The air-to-steam ratio in this test was about 4:1 by weight; temperature in the fluidized bed ranged from about 1880° to 1930°F.

For microscopic observation the beads were mounted in epoxy resin, sectioned, and polished. A composite photomicrograph of a whole 1-inch briquet, taken with vertical illumination, is shown in Figure 3. Residual coke appears as light areas here, both as the main constituent of the angular particles and as the very small constituent particles of the rounded beads. These small particles are situated mostly on the periphery of the beads, although a few are buried in the interior.

The many rounded black areas in the bead are empty vesicles. Others, connected by passageways to the exterior, were filled with the epoxy resin during mounting. (The system is evacuated before covering the sample with the resin, and the liquid resin is forced into some of the vesicles by the readmitted atmospheric pressure.)

A composite photomicrograph of the same briquet taken with oblique illumination is shown in Figure 4. With this illumination, the continuous phase of glassy, melted ash in the rounded beads can be distinguished from many of the embedded, unmelted particles.

We did not attempt to identify all of the unmelted ash particles; however, we think that some with high reflectance are probably particles of high-alumina refractory from the walls of the unit. When the reflectances of some of these high-reflectance particles were measured, they agreed with that of the similarly mounted refractory. Very small vesicles in the melted ash appear as pinpoints of reflected light. Some of the large, empty vesicles are partly illuminated on one side.

The distribution of the residual carbon indicated by microscopic observation was substantiated by further investigation: A sample of the residue was separated by hand into beads and angular particles; analyses for carbon then showed only 1.9 weight percent in the beads and 70.4 weight percent in the angular particles. That most of the residual carbon in the beads is not embedded and is available for reaction was shown by igniting a sample of the beads for 1/2 hour at about 1550°F, followed by an analysis for unburned carbon. Only 0.36 weight percent remained.

The surface energy of a melt (or solid) of this kind is high compared with that of carbonaceous solids, and thus melted ash does not wet or spread on the low-energy surface of the coke (7). This is confirmed by the observation (under the microscope) that coke particles appear to float on the surface of the glassy phase, as shown in the photomicrograph of Figure 5. The observed apparent contact angle between coke and the glassy phase varied from about 90 degrees to much more than that. This explains why so little coke is entrapped inside the melted ash.

We investigated the composition of the continuous or melt phase of the beads. Microscopic observations of polished sections (at higher magnification than shown in Figures 3 and 4) show the presence of crystals. The view in the photomicrograph of Figure 6 is typical, but occasional areas are found where the crystals are larger and comprise a larger fraction of the crystal-in-glass composite. Occasional particles of ferrous oxide and metallic iron have also been found and identified by measuring their reflectance. X-ray emission spectra of the crystals, obtained with a scanning electron microscope, indicated presence of iron and aluminum. Iron, aluminum, and silica were similarly identified as the major components of the matrix or continuous phase; titanium, potassium, and calcium were also detected in it.

It is well known that the fusibility of ash containing substantial amounts of iron (from pyrite in the original coal) depends on the oxidation-reduction potential of the atmosphere. The presence of occasional particles of metallic iron in the beads indicates that the atmosphere in at least some zones of the bed was reducing enough for reduction of ferrous oxide, although the product gas generally had too low a carbon monoxide-carbon dioxide ratio to expect such reduction. The phase diagram for the FeO-Al_2O_3-SiO_2 system in equilibrium with metallic iron is thus of interest for an understanding of the ash behavior.

The phase diagram of Osborn and Muan (6) for the FeO-Al_2O_3-SiO_2 system under this condition is shown in Figure 7. Note the narrow quadrilateral field for crystallization of iron cordierite, $2FeO \cdot 2Al_2O_3 \cdot 5SiO_2$. The minimum liquidus temperature in the presence of hercynite ($FeO \cdot Al_2O_3$) and fayalite ($2FeO \cdot SiO_2$), at the lower left corner of the field, is 1990 ± 9^0F. However, iron cordierite tends not to crystallize in the absence of seed crystals, and instead a metastable eutectic of fayalite, hercynite, and tridymite may form at 1963 ± 9^0F (5). In the presence of impurities, still lower liquidus temperatures may occur. Thus, Snow and McCaughy, working with mixtures prepared from clays containing impurities, found a liquidus temperature of 1778^0F for this eutectic (9). However, no crystals typical of a eutectic were seen either by optical or scanning electron microscopy, nor was any fayalite detected by X-ray diffraction. Instead, it appears that a glass is formed when the melted ash cools.

Agglomerated Ash from FMC Char

The FMC char was much more reactive than the coke breeze, resulting in a lower bed temperature with comparable gas feed. On the other hand, more severe operating conditions (higher temperature or higher ash content of the bed) were required to obtain agglomerates large enough to be discharged automatically and in sufficient quantity to maintain the ash content of the bed in a steady state without periodic dumping. Steam had to be eliminated from the gas feed to obtain the required temperatures.

Agglomerated particles from two runs operating with FMC char as feed (Nos. 57 and 60) were examined. The feed for the first of these runs had been prepared from Illinois coal and that for the latter from Western Kentucky coal.

The agglomerated ash particles differed considerably from those produced from the coke breeze, being smaller and subangular instead of well-rounded. Particles from Run 60 are shown in Figure 2b with small beads from coke for comparison. In polished sections under the optical microscope, the clay of the coal ash appeared to be well-sintered, but no ferrous aluminum silicate was detected by X-ray emission in the scanning electron microscope. Instead, the iron appeared mostly in the form of ferrous sulfide and magnetite. In both feed chars, the iron appeared as ferrous sulfide; in the agglomerated ash from an early period of Run 57, some magnetite had appeared, but most of it was ferrous sulfide, much of it as separate particles. Some was occluded in the agglomerated

clay as dispered, 1 to 10-μm particles, and some had spread over the surface of the clay particles as shown in Figure 8. In the agglomerates from a later period of the run, much of the exposed iron, but not the occluded particles, had been converted to magnetite. In the agglomerated ash from a late period of Run 60, a portion of the magnetite on the outer zone of the particles had been reduced to wüstite (FeO). Rings of ferrous sulfide, similar in shape to those found on separate particles, were observed in the interior of the agglomerates. Formation and automatic discharge of these agglomerates occurred in Run 60 with a bed temperature of about 1950°F and an ash content of about 50% in the fluidized bed.

DISCUSSION

Differences in elemental composition among the three feed materials (Table 1) are probably not very significant in interpretation of the agglomeration process; however, analysis for acid-soluble iron indicated that a large part of the iron in the coke had already reacted with the clay minerals to form the acid-insoluble, low-melting ferrous aluminosilicate. (Pyrite also is insoluble in hydrochloric acid but is decomposed or oxidized in the preparation of the coke and char. Soluble iron compounds occluded in sintered clay also do not dissolve.)

Table 1. PROPERTIES OF ASH IN COKE AND CHAR FEEDS

		FMC Char	
Elemental Composition, wt %	Coke	From Ill. Coal	From Ky. Coal
SiO_2	47.1	35.7	39.9
Al_2O_3	20.8	17.5	23.4
Fe_2O_3	18.9	24.1	24.1
TiO_2	0.81	0.88	0.51
CaO	3.25	3.50	0.43
MgO	1.01	0.85	0.74
Na_2O	0.54	4.03	0.60
K_2O	1.72	2.48	0.65
SO_3	2.26	5.15	1.95
Total	96.4	93.4	92.3
Acid-Soluble Iron, % of total iron	47	98	97
Ash Fusibility, °F			
Reducing Atmosphere			
IT	2085	1780	2005
ST	2155	1950	2050
HT	2230	1980	2080
FT	2440	2160	2340
Oxidizing Atmosphere			
IT	2510	2215	2475
ST	2630	2300	2520
HT	--	2360	2540
FT	--	2500	2560

Thus, two different modes of ash agglomeration are indicated, namely, iron oxide fluxing (formation of molten ferrous aluminum silicate), and, under more severe conditions, clay sintering. Possibly the presence of relatively low-melting (and thus prone to sintering) ferrous sulfide (mp 2180°F) on the exterior of clay particles may have aided in their agglomeration.

Prediction of the performance that will be obtained with other types of feed is uncertain. The form of the iron in the feed is obviously important; iron in hydrogasification residue, for example, is likely to have been converted to ferrous oxide and would thus be in a much readier form to react with and flux the clay than it is in char. This may also be the case even with raw coal as the feed, because a gasification atmosphere has a higher oxidation potential than a pyrolysis atmosphere does.

ACKNOWLEDGMENTS

This work was conducted as part of the HYGAS® coal gasification program jointly sponsored by the United States Energy Research and Development Administration (ERDA) and the American Gas Association. This program is under the technical direction of Dr. C. Lowell Miller and Mr. Stephen C. Verikios of ERDA and Dr. Ab Flowers of the American Gas Association.

REFERENCES

1. ASTM 1975 Annual Book of ASTM Standards, Part 26 — Gaseous Fuels; Coal and Coke; Atmospheric Analysis, D 2797, "Preparing Coal Samples for Microscopical Analysis by Reflected Light." Philadelphia: American Society for Testing and Materials, 1975.

2. Boar, P. L. and Ingram, L. K., "Comprehensive Analysis of Coal Ash and Silicate Rocks by Atomic-Absorption Spectrophotometry by a Fusion Technique," Analyst (London) 95 (1127), 124-30 (1970).

3. Cameron, E. N., Ore Microscopy. New York: John Wiley, 1961.

4. Mason, D. M. and Schora, F. C., Jr., "Coal and Char Transformation in Hydrogasification," Adv. Chem. Ser. No. 69, 18-30 (1967).

5. Muan, A., "Phase Equilibrium Relationships at Liquidus Temperatures in the System $FeO-Fe_2O_3-Al_2O_3-SiO_2$," J. Amer. Ceram. Soc. 40, 420-31 (1957).

6. Osborn, E. F. and Muan, A., in Levin, E. M., Robbins, C. R. and McMurdie, H. F., Eds., Phase Diagrams for Ceramists, 241. Columbus: The American Ceramic Society, 1964.

7. Raask, E., "Slag-Coal Interface Phenomena," J. Eng. Power 88 (No. 1), 40-44 (1966).

8. Sandstrom, W. A., Rehmat, A. G. and Bair, W. G., "The Gasification of Coal Chars in a Fluidized-Bed Ash-Agglomeration Gasifier." Paper presented at the A. I. Ch. E. 69th Annual Meeting, Chicago, November 28-December 2, 1976.

9. Snow, R. B. and McCaughy, W. J., "Equilibrium Studies in the System $FeO-Al_2O_3-SiO_2$," J. Amer. Ceram. Soc. 25, 151-60 (1942).

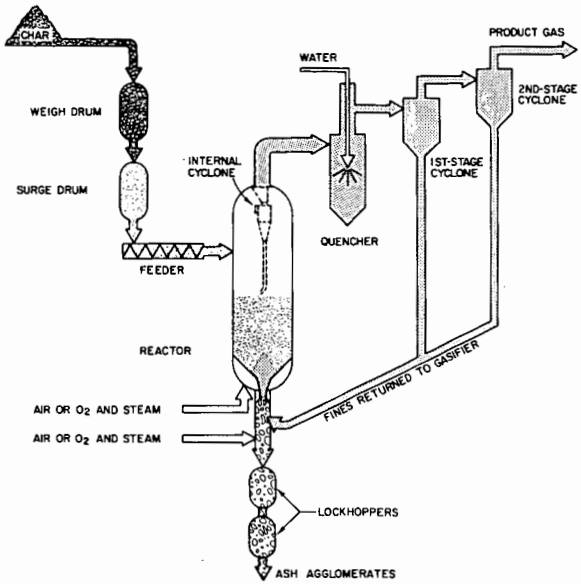

Figure 1. SCHEMATIC DIAGRAM OF ASH-AGGLOMERATING GASIFIER

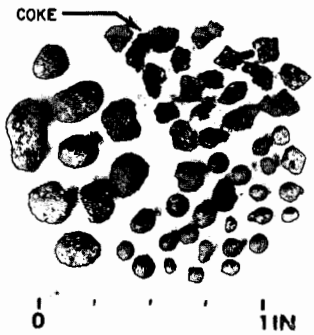

Figure 2a.
ASH AGGLOMERATES FROM COKE, WITH COKE PARTICLES

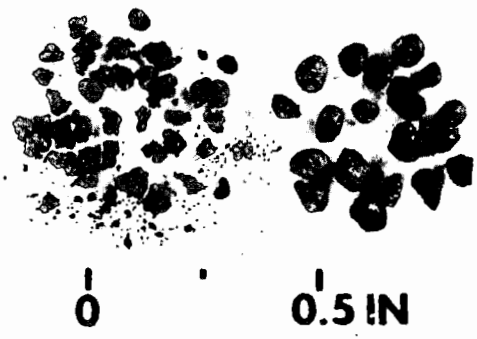

Figure 2b. ASH AGGLOMERATES FROM FMC CHAR (Left), AND COKE (Right)

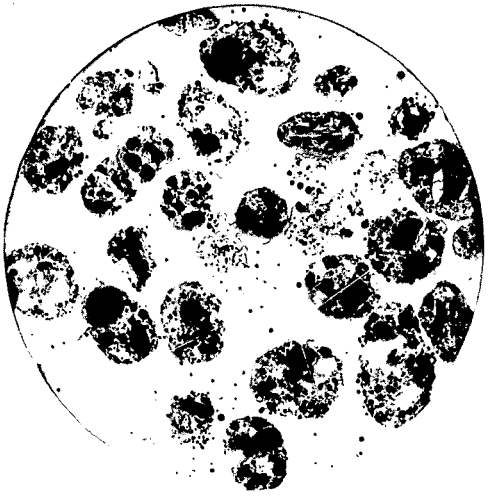

Figure 3. AGGLOMERATED ASH BEADS FROM COKE – VERTICAL ILLUMINATION

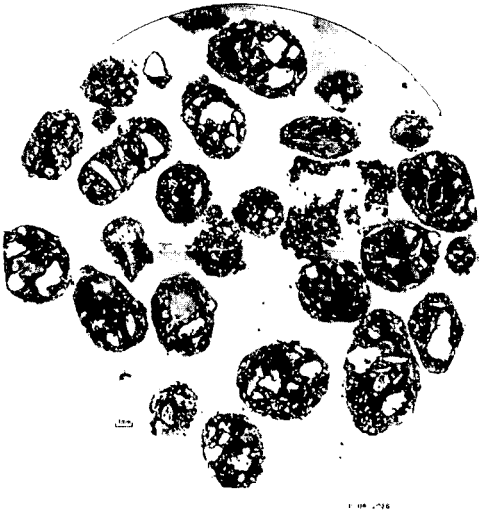

Figure 4. AGGLOMERATED ASH BEADS FROM COKE – OBLIQUE ILLUMINATION

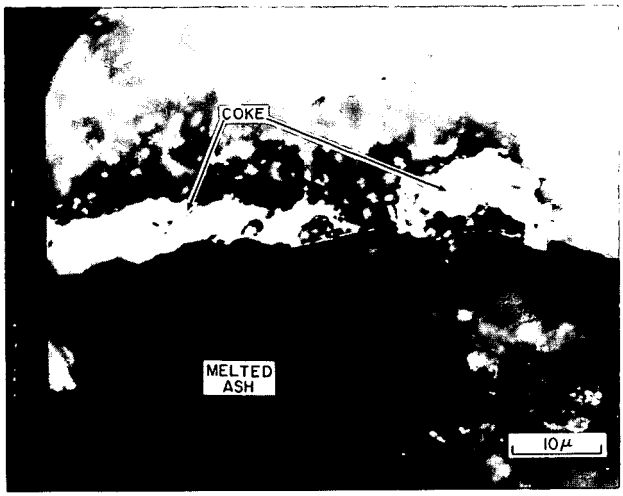

Figure 5. COKE PARTICLES ON SURFACE OF MELTED AND RESOLIDIFIED ASH OBSERVED BY OPTICAL MICROSCOPE WITH OIL IMMERSION

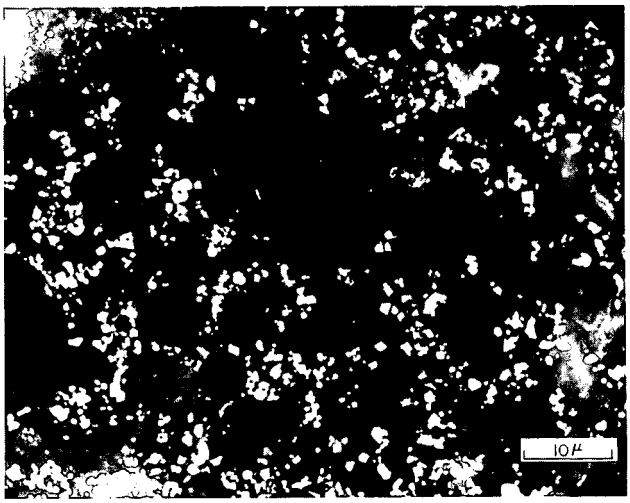

Figure 6. CRYSTALS OF HERCYNITE ($FeO \cdot Al_2O_3$) IN MELTED AND RESOLIDIFIED ASH OBSERVED BY OPTICAL MICROSCOPE WITH OIL IMMERSION

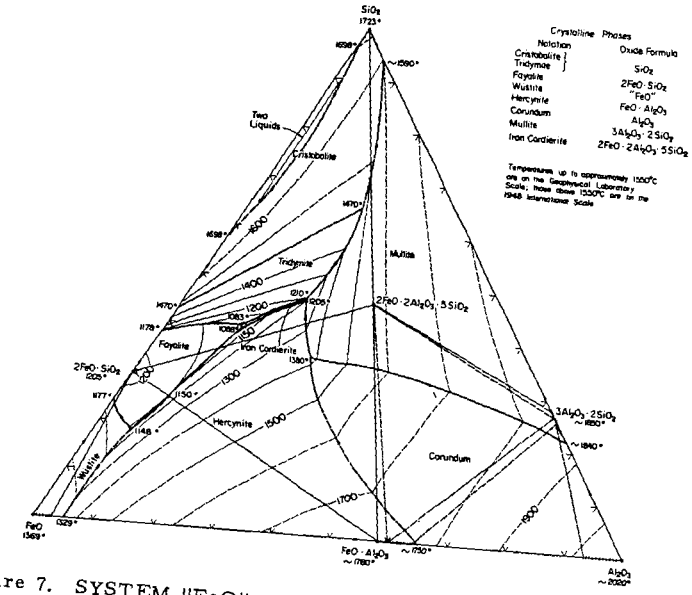

Figure 7. SYSTEM "FeO"–Al_2O_3–SiO_2; COMPOSITE, BY WEIGHT (Oxide Phases in Equilibrium With Metallic Iron)(6)

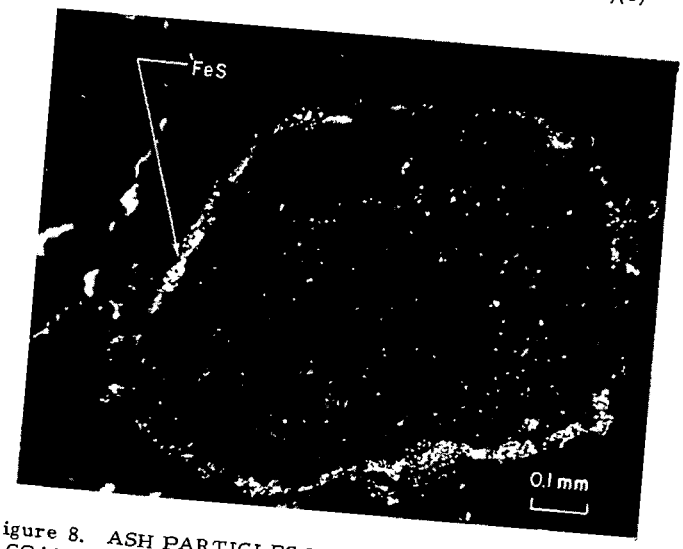

Figure 8. ASH PARTICLES FROM FMC CHAR SHOWING A COATING OF FERROUS SULFIDE ON SINTERED CLAY

Petrochemistry of Coal Ash Slags. 1. Formation of Melilite and a High Temperature Glass from a Calcium-Rich, Silica-Deficient Slag.

H. H. Schobert,[1/] D. L. Barbie,[2/] O. D. Christensen,[3/] and F. R. Karner[4/]

Grand Forks Energy Research Center
Box 8213, University Station
Grand Forks, ND 58202
and
Department of Geology
University of North Dakota
Grand Forks, ND 58202

The Grand Forks Energy Research Center (GFERC) of the Energy Research and Development Administration is conducting pilot plant studies of a fixed-bed slagging coal gasification process. The pilot plant was originally operated from 1958-1965 by the Bureau of Mines. The design and operation of the gasifier and the Bureau of Mines test results have been documented (1,2). Recent papers (3,4) have described the program objectives for the reactivated plant and have presented some preliminary results.

A schematic diagram of the gasifier is shown in Figure 1. Lignite or subbituminous coal is reacted with steam and oxygen at pressures to 27 atmospheres psig and at hearth zone temperatures exceeding 1650° C. A gas mixture is produced of which 90% is carbon monoxide and hydrogen at 2:1 ratio and the balance is composed of methane, carbon dioxide, and nitrogen. The hearth zone temperatures are maintained sufficiently high to cause melting of the ash. The molten slag drains into a water quench bath through a taphole in the hearth. Maintaining a steady flow of slag is crucial to the successful operation of the gasifier, since a build-up of slag on the hearth or a plug forming in the taphole will result in a premature shutdown of the test.

The petrochemistry of the slag is of considerable importance as a factor in hearth section design. Refractory selection will depend in part upon the chemical relationship between slag constituents and the refractories. If a phase transformation in the slag should produce a liquid having a composition well outside the design specifications, a rapid chemical degradation of the refractory structures could occur. The temperature dependence of slag viscosity is a function of slag composition. Since design of slag discharge orifices will be influenced in part by the expected viscosity range, viscosity changes caused by corresponding composition changes could alter slag flow characteristics.

Additional interest in slag petrochemistry arises from a similarity of slag compositions to naturally-occurring silicate melts. Thus the slagging operations in the gasifier can provide opportunities for studies of igneous rock petrology.

During operation, the slag is removed from the gasifier by periodically discharging the slag lock. The discharged slag is recovered as black, glassy granules (Fig. 2). In some tests the slag has been found to contain structures of

1/ Research Chemist, Grand Forks Energy Research Center.
2/ Physical Science Aide, Grand Forks Energy Research Center.
3/ Assistant Professor of Geology, University of North Dakota.
4/ Professor of Geology, University of North Dakota.

unusual or atypical appearance. Samples of these are retained for detailed chemical and petrographic analysis. It is of particular concern to identify the phases formed, to determine or suggest the mechanism of the phase separation, and to predict the effect on such parameters as refractory attack, slag viscosity, and heat transfer.

The current series of tests in the GFERC gasifier uses lignite from the Indianhead mine of the North American Coal Company near Zap, North Dakota. Slag analyses are done using x-ray fluorescence. The analysis of the bulk slag varies slightly from run to run. Table 1 shows the slag analysis for a recent test and the range of observed values.

TABLE 1. Product Slag Analysis, Indianhead Lignite.

Oxides	Wt.,%	Range, %
SiO_2	39.5	31.1 - 39.7
Al_2O_3	13.6	11.8 - 13.6
Fe_2O_3	11.0	4.4 - 11.4
TiO_2	0.7	0.4 - 0.7
P_2O_5	0.3	0.3 - 0.6
CaO	17.9	17.9 - 33.7
MgO	5.3	5.3 - 7.4
Na_2O	6.6	0.1 - 10.5
K_2O	1.0	0.6 - 1.0
SO_3	4.1	1.9 - 4.1
TOTAL	100.0	

The composition is similar to that of a calcium-rich pyroxene.

Figure 3 shows a specimen of two-layered nodules recovered from the product slag of an early test (No. RA-4) in the current program. Table 2 shows the results of analysis of the inner and outer layers of the nodules, as well as the analysis of a bulk sample of the slag.

TABLE 2. Analyses of Regions of Indianhead Slag Nodules, Test RA-4

	Weight Percent		
	Inner Layer	Outer Layer	Bulk Sample
SiO_2	65.0	36.6	38.2
Al_2O_3	19.3	13.6	12.7
Fe_2O_3	5.8	13.0	8.0
TiO_2	0.9	0.7	0.6
P_2O_5	0.1	0.4	0.5
CaO	1.7	20.6	24.3
MgO	2.6	5.6	6.4
Na_2O	1.4	5.8	3.5
K_2O	2.9	0.8	0.9
SO_3	0.2	3.0	3.0
TOTAL	99.9	100.1	98.1

A thin section of one of these nodules is shown in Figure 4. Optical and x-ray diffraction study shows that the inner material is a vesicular glass with a small amount of disseminated quartz grains or fragments. The vesicles vary in size across the thin-sectioned chips, typically occurring in zones of smaller (0.01 mm) and larger (0.04 mm) approximate average diameter. In addition to the vesicles, numerous similar, spherical structures with pale tan color are present. These often contain or partly contain quartz grains. The outer layer of the nodules is very similar to the original slag.

Figure 5 shows a portion of a SiO_2-CaO-MgO ternary slice through the SiO_2-CaO-MgO-Al_2O_3 quarternary system, at 15 pct Al_2O_3. (Points are plotted on the basis of SiO_2 + CaO + MgO + Al_2O_3 = 100 pct). The composition of the inner layer lies in the cristobalite field, while both the outer layer and bulk slag compositions lie in the pyroxene field. The fact that crystallization of the inner layer was not more pronounced is very likely due to undercooling, since reported (5) slag discharge temperatures of 2300° F (1260° C) are less than 100° C above the fluid temperature of Indianhead slag.

The three-layered nodules were recovered from the slag in a more recent test (RA-7). The analysis of each layer is given in Table 3, along with an analysis of the bulk slag.

TABLE 3. Analyses of Regions of Indianhead Slag Nodules, Test RA-7

	Inner Layer	Middle Layer	Outer Layer	Bulk Sample
SiO_2	36.6	37.8	39.2	33.1
Al_2O_3	10.2	8.9	12.5	13.1
TiO_2	0.3	0.3	0.5	0.5
P_2O_5	0.5	0.5	0.5	0.6
CaO	40.5	38.7	31.1	22.6
MgO	7.9	9.5	6.8	5.4
Na_2O	0.3	0.5	1.2	6.1
K_2O	0.3	0.3	0.6	0.8
SO_3	3.1	2.5	1.4	2.4
Fe_2O_3	0.2	1.0	6.1	11.4
TOTAL	99.9	100.0	99.9	96.0

Thin section photographs of a three-layered nodule are shown in Figures 6 and 7. Optical and x-ray diffraction data show that the inner layers contain abundant melilite while the outer core is a glass. Melilite occurs as two types of clusters of radiating, zoned crystals. One type has zoning produced by dark, reddish cores, probably resulting from abundant iron-rich inclusions and exhibits a well developed dendritic intergrowth texture, probably from quenching. The second type of melilite has zoning shown by birefringence characteristics, probably from oscillatory or reverse chemical zoning and subhedral to euhedral crystal form.

In both cases these phase transformations can be related to temperature fluctuations in the gasifier hearth. Hearth zone temperatures are measured by a thermocouple mounted on the bottom of the hearth plate, and another in the gasifier wall approximately 5-1/2 feet above the hearth. Figures 8 and 9 show the two temperatures as a function of time for tests RA-4 and RA-7, as well as test RA-8, in which no slag phase separation was observed. Temperature data from RA-4 and RA-7 show sharp fluctuations, whereas the data from RA-8 show relatively stable temperatures.

The slag-refractory chemistry was found not to be significantly affected by either phase transformation described here. The slags have been characterized by calculating the base to acid ratio:

$$B/A = \frac{CaO + MgO + Na_2O + K_2O + Fe_2O_3}{SiO_2 + Al_2O_3 + TiO_2}$$

In the case of glass formation, the bulk slag has a basicity/acidity ratio of 0.84, while the liquid phase which would remain after formation of the glass nodules has a value of 0.90 (calculated from the analysis of the outer layer of the nodules). The corresponding values for the melilite formation are, respectively, 0.99 and 0.88. Neither situation represents a drastic change in slag basicity. Accelerated chemical degradation of hearth zone refractories is therefore an unlikely consequence of these phase transformations.

Changes in slag viscosity were estimated by calculating viscosities from a modified form of the Watt-Fereday equation (7),

$$\log \eta = 10^7 M/(T-150)^2 + C$$

where M and C are empirical constants which are functions of slag composition, the viscosity in poise, and the temperature in degrees Centigrade. Preliminary results from current GFERC research on adapting the Watt-Fereday equation to lignite slags were used to estimate order-of-magnitude viscosity changes. Viscosities were calculated from the bulk slag analysis and from the analysis of the outer layer of the nodules. Massive formation of melilite from Indianhead slag would leave a residual liquid having a calculated viscosity of 125 poise at 1350° C, while the calculated viscosity of the bulk slag is only 8 poise.

The change in slag viscosity will also affect hearth zone heat transfer relationships. For example, the calculation of the heat transfer coefficient between the slag and hearth plate is dependent upon the Grashof and Prandtl numbers for the flowing slag, both of which are functions of viscosity (8).

The results of this study show that the characteristics of the coal ash slag can be affected by temperature fluctuations in the gasifier hearth. Chemical, flow, and heat transfer behavior are all susceptible to change as a result.

REFERENCES

1. G.H. Gronhovd, A.E. Harak, W.R. Kube, and W.H. Oppelt. "Design and Initial Operation of a Slagging, Fixed-Bed, Pressure Gasification Pilot Plant." U.S. Bureau of Mines RI 6084 (1962).

2. G.H. Gronhovd, A.E. Harak, M.M. Fegley, and D.E. Severson. "Slagging Fixed-Bed Gasification of North Dakota Lignite at Pressures to 400 psig." U.S. Bureau of Mines RI 7408 (1970).

3. R.C. Ellman and B.C. Johnson. "Slagging Fixed-Bed Gasification at the Grand Forks Energy Research Center." Presented at the Eighth Synthetic Pipeline Gas Symposium, Chicago, IL, October 1976.

4. R.C. Ellman and H.H. Schobert. "Pilot Plant Operation of a Fixed-Bed Slagging Gasifier." Presented at the National Meeting of the American Chemical Society, New Orleans, LA, March 1977.

5. G.H. Gronhovd. "Quarterly Technical Progress Report, April-June, 1976." ERDA Report GFERC/QTR-76/4 (1976).

6. B. Mason. "Principles of Geochemistry." Second Ed., John Wiley and Sons, Inc, New York, NY 1958.

7. J.D. Watt and F. Fereday. "The Flow Properties of Slags Formed From the Ashes of British Coals: Part 1: Viscosity of Homogeneous Liquid Slags in Relation to Slag Composition." J. Inst. Fuel, 42, 99 (1969).

8. C.O. Bennett and J.E. Myers. "Momentum, Heat, and Mass Transfer." Second Ed., McGraw-Hill Book Co., New York, NY 1974.

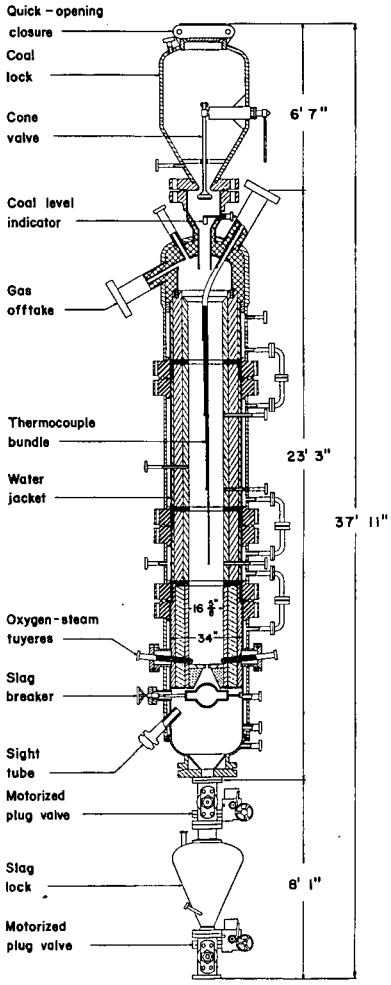

Figure 1. GFERC Gasifier

Figure 2. Typical Discharged Slag

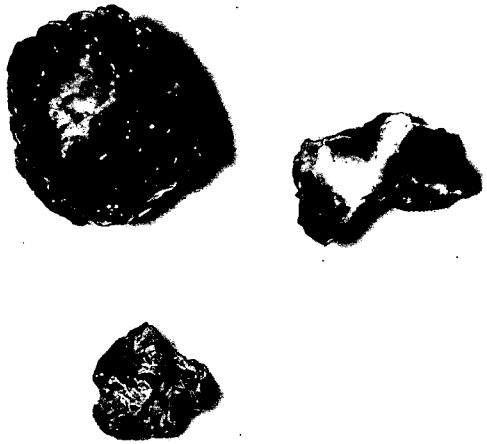

Figure 3. Two-layered Slag Nodules

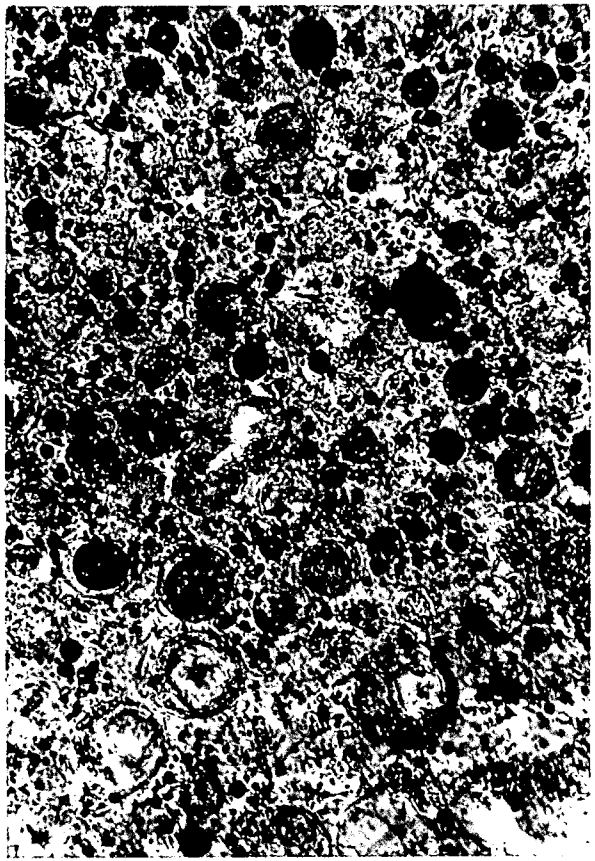

Figure 4. Thin section photograph of glassy part of two-layered nodule, showing two types of spherical structures. Photo taken using partly crossed polars; field of view, 0.7 mm.

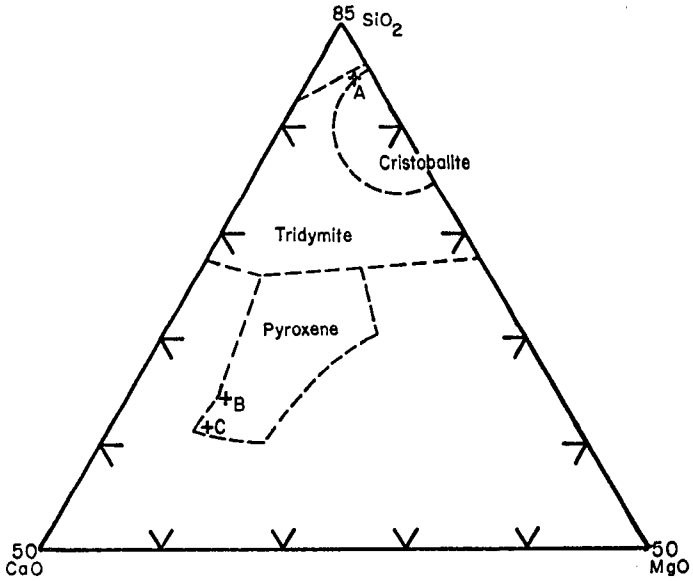

Figure 5. SiO_2-CaO-MgO Ternary at 15% Al_2O_3

A=Glass, B=Outer Layer of Nodule, C= Bulk Slag Composition

Figure 5. SiO_2-CaO-MgO Ternary slice of SiO_2-CaO-MgO-Al_2O_3 system. (15% Al_2O_5).

Figure 6. Melilite in three-layered nodules. Intergrowth of dendritic crystals with iron-rich cores. Photo taken in plane polarized light. Field of view, 3 mm.

Figure 7. Melilite in three-layered nodules. Crystal with chemical zoning shown by birefringence characteristics. Photo taken with crossed polars. Field of view, 1.2 mm.

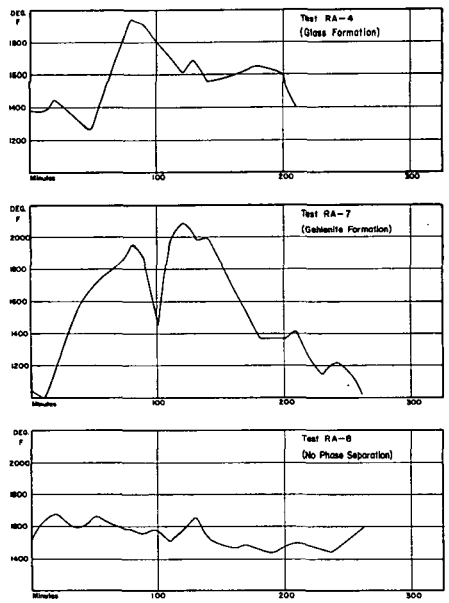

Figure 8. Hearth Plate Temperature Vs. Slagging Time.

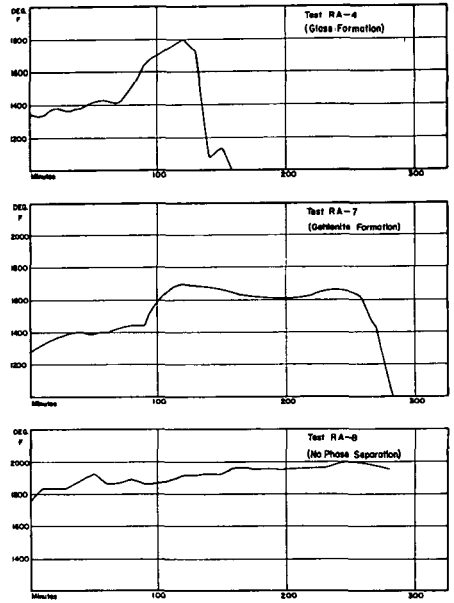

Figure 9. Gasifier Wall Temperature (Hearth Section) Vs. Slagging Time.

Petrochemistry of Coal Ash Slags. 2. Correlation of Viscosity with Composition and Petrographic Class

Harold H. Schobert

Grand Forks Energy Research Center
Box 8213, University Station
Grand Forks, ND 58202

The Grand Forks Energy Research Center (GFERC) of the Energy Research and Development Administration has reactivated a fixed-bed slagging coal gasification pilot plant which was formerly operated by the Bureau of Mines. Design of the gasifier, the Bureau of Mines test results, and preliminary results from the ERDA program have been documented (1-4).

A detailed study of the slagging operation is one aspect of the current GFERC pilot plant program. The objective of this study is to develop accurate knowledge of the flow and heat transfer behavior of the slag, both to improve operation of the GFERC plant and to suggest design approaches for future generation gasifiers. One of the important parameters in this work is the slag viscosity.

The experimental determination of slag viscosity as a function of temperature is a difficult procedure. Consequently, many efforts have been made to develop an approach to calculate this relationship. The equations generally proposed incorporate one or more terms which are calculated from the slag composition.

The equation

$$\log_{10}\eta = \frac{10^7 M}{(T-150)^2} + C \qquad [1]$$

has been suggested in several publications (5-7) for calculating viscosity as a function of temperature. In this equation, T is expressed in degrees Centigrade, and η in poises. M and C are terms calculated from the slag composition, being functions of SiO_2, Al_2O_3, Fe_2O_3, and CaO content. Various equations have been proposed for calculating C and M. These equations differ slightly in the values of the coefficients of the composition terms. The work done by Watt and Fereday (6) is based on British coals, while that reported by the Institute of Gas Technology (7) is based on synthetic melts.

Attempts were made to use equation [1] for the calculation of viscosities of some lignite ash slags for which experimental viscosity data was available at GFERC. Both the Watt-Fereday method (5,6) and the modified equations suggested by Bomkamp (7) were used. A test temperature was selected from the center of the temperature range over which viscosity data was available at GFERC (8). Some of the results are given in Table 1.

TABLE 1. Calculated Values of Lignite Slag Viscosities.[A/]

Lignite Slag	Temperature	Method 1[B/]	Method 2[C/]	Expt'l Value
Baukol-Noonan	1175°	197	11,600	42
Indianhead	1260°	21	2,276	60
Velva	1385°	<1	1	350

A/ Sources and compositions of the coal ash slags are given in the appendix.

B/ Watt-Fereday Method. C/ Modified Watt-Fereday Method.

Since the results shown in Table 1 are clearly unsatisfactory, the development of additional modifications to equation [1] was undertaken. Since the GFERC gasification program will test a variety of Western lignite and subbituminous coals, it was desired to develop an equation applicable to the widest possible range of slag compositions. Viscosity-temperature data were available for slags having the range of compositions shown below.

TABLE 2. Range of Slag Compositions Used in GFERC Study

Component	Range, Pct	Component	Range, Pct
SiO_2	15-49	MgO	1-10
Al_2O_3	9-27	Na_2O	.3-12
Fe_2O_3	7-23	K_2O	.1-4
CaO	3-43		

Equation [1] was rewritten as

$$Y = MX + C$$

where $X = 10^7/(T-150)^2$ and $Y = \log_{10}\eta$. The experimental data were then used to compute values of M and C for each slag, using a standard linear regression computer program. The results are given in Table 3.

TABLE 3. Values of C and M Computed by Linear Regression

Slag[A/]	C	M
Baukol-Noonan	-1.2180	.3069
Bentinck	- .8604	.5851
Cronton-19[B/]	-1.2194	.5288
Cronton-27[C/]	- .9997	.5849
Dickinson	-4.1015	.5945
Disco	- .5266	.4240
Disco-Flux[D/]	- .8429	.2948
Indianhead	-4.0781	.7264
Thoresby	- .7840	.4892
Velva	-7.2934	1.4996

A/ Source and composition data is given in the appendix.
B/ 19 pct ash coal. C/ 27 pct ash coal.
D/ 3 lb. blast furnace slag added per lb. of ash.

The computed values of C and M were used as input data for a multiple linear regression analysis for the development of equations relating C and M to slag composition. Repeated computer trials failed to produce a satisfactory fit of the data. As a result, attention was then focused on performing regression analyses for slags only of a single petrographic class. (In this paper petrographic classifications and terminology refer to igneous rock petrography, rather than to coal petrography.)

The test slags were divided into two groups on the basis of similarity of composition: Baukol-Noonan, Disco-Flux, and Indianhead in the first group; and Bentinck, Cronton-19, Cronton-27, Disco, and Thoresby in the second. Detailed petrographic analyses were done for Indianhead and Thoresby slags, the compositions of which are given in the appendix. The petrographic classification was done by the C.I.P.W. method (9), following the procedure outlined by Johannsen (10). This procedure is a taxonomic method for comparing chemical analyses from a petrological aspect. The analytical data is recalculated in terms of a set of standard mineral molecules. Indianhead slag was found to be pyroxene normative and Thoresby to be feldspar normative.

Correlation coefficients were calculated between each of the major slag components and the values of C and M, for both classes of slag. The calculations were done using a standard linear correlation computer program. This work was done so that the results would serve as a guide to which slag components might best be used in a multiple regression analysis for developing equations to calculate C and M. The computed values of the correlation coefficients are given in Table 4.

TABLE 4. Linear Correlation Coefficients Between Slag Composition and Computed Values of C and M.

	Pyroxene-normative Slags		Feldspar-normative Slags	
Component	C	M	C	M
SiO_2	-.369	.444	.681	.094
Al_2O_3	.554	-.485	-.573	.570
Fe_2O_3	-.996	.999	-.019	-.512
CaO	.360	-.283	.168	.255
MgO	.209	-.129	-.495	.200
Na_2O	-.140	.059	.030	.140
K_2O	-.589	.521	-.760	.940

Multiple linear regression analysis of the feldspar normative group developed the following equations:

$$C = -4.5413 - .2158\ (K_2O) + .0883\ (SiO_2) + .0091\ (Al_2O_3) \qquad [3]$$

$$M = 0.3676 + .0783\ (K_2O) - .0043\ (Al_2O_3) \qquad [4]$$

In these equations the concentration terms use the actual weight percent values determined from the chemical analysis.

The viscosity-temperature relationship for Cronton-19 slag was calculated by substituting equations [3] and [4] into equation [1]. The appropriate analytical data for this slag are 3.5 pct K_2O, 43.6 pct SiO_2, and 24.6 pct Al_2O_3. Figure 1 shows the experimental (11) and calculated viscosity curves.

Although only limited data are available for the pyroxene normative slags, a regression analysis was done to fit C and M values to Fe_2O_3 content because of the high correlation between these parameters. Equations [5] and [6] resulted.

$$C = 0.8143\ (Fe_2O_3) - 4.8749 \qquad [5]$$

$$M = 0.1135\ (Fe_2O_3) - .5219 \qquad [6]$$

The viscosity-temperature curve for Indianhead slag (Fe_2O_3 = 11.0 pct) calculated from equations [5], [6], and [1], is given in Figure 2.

These results demonstrate that this approach produces improved results for the specific slags studied thus far. It is suggested that classification of slags by a petrographic procedure may be more useful than other methods for the production of viscosity effects.

REFERENCES

1. G.H. Gronhovd, A.E. Harak, W.R. Kube, and W.H. Oppelt. "Design and Initial Operation of a Slagging, Fixed-Bed, Pressure Gasification Pilot Plant." U.S. Bureau of Mines RI 6084 (1962).

2. G.H. Gronhovd, A.E. Harak, M.M. Fegley, and D.E. Severson. "Slagging Fixed-Bed Gasification of North Dakota Lignite at Pressures to 400 Psig." U.S. Bureau of Mines RI 7408 (1970).

3. R.C. Ellman and B.C. Johnson. "Slagging Fixed-Bed Gasification at the Grand Forks Energy Research Center." Presented at the Eighth Synthetic Pipeline Gas Symposium, Chicago, IL, October 1976.

4. R.C. Ellman and H.H. Schobert. "Pilot Plant Operation of a Fixed-Bed Slagging Gasifier." Presented at the National Meeting of the American Chemical Society, New Orleans, LA, March 1977.

5. British Coal Utilization Research Association, Annual Report (1963).

6. J.D. Watt and F. Fereday. "The Flow Properties of Slags Formed from the Ashes of British Coals: Part 1: Viscosity of Homogeneous Liquid Slags in Relation to Slag Composition." J. Inst. Fuel, 42, 99 (1969).

7. Institute of Gas Technology. "Preparation of a Coal Conversion Systems Technical Data Book." Energy Research and Development Administration Report FE-1730-21 (1976).

8. G.H. Gronhovd. Private communication.

9. H.S. Washington. "Chemical Analyses of Igneous Rocks." U.S. Geological Survey Professional Paper 99 (1917).

10. A. Johansen. "A Descriptive Petrography of Igneous Rocks." The University of Chicago Press, Chicago, IL (1939).

11. H.R. Hoy, A.G. Roberts, and D.M. Wilkins. "Some Investigations with a Small Cyclone Combustor." J. Inst. Fuel, 31, 441 (1958).

APPENDIX

Composition and Source Data for Slags Used in this Study

Slag:	Baukol-Noonan	Bentinck	Cronton-19	Cronton-27	Dickinson	Disco	Disco & Flux	Indian-head	Thorseby	Velva
Source:	North Dakota	British	British	British	North Dakota	Pennsyl-vania	A/	North Dakota	British	North Dakota
Rank:	Lignite	Bituminous	Bituminous	Bituminous	Lignite	Bituminous		Lignite	Bituminous	Lignite
Slag Analysis, wt. %	B/	C/	C/	C/	B/	B/	B/	B/	C/	B/
SiO_2	33.0	48.9	43.6	47.7	21.8	48.0	39.8	39.5	46.7	14.7
Al_2O_3	13.5	23.2	24.6	27.1	9.1	23.0	15.6	13.6	23.4	11.1
Fe_2O_3	7.3	6.6	17.4	11.8	23.1	18.5	7.2	11.0	6.9	6.7
CaO	14.5	10.5	3.5	2.7	18.4	3.3	27.2	17.9	8.4	43.3
MgO	4.4	1.6	2.3	1.9	7.2	1.0	6.6	5.3	2.9	10.1
Na_2O	12.1	1.7	0.8	0.5	0.6	0.3	0.4	6.6	2.4	4.4
K_2O	1.0	3.5	3.4	4.2	0.1	1.9	0.5	1.0	3.0	0.3

A/ Disco ash fluxed with 3 lb. blast furnace slag per lb. of ash.
B/ GFERC data.
C/ Data of Hoy, Roberts & Wilkins (11).

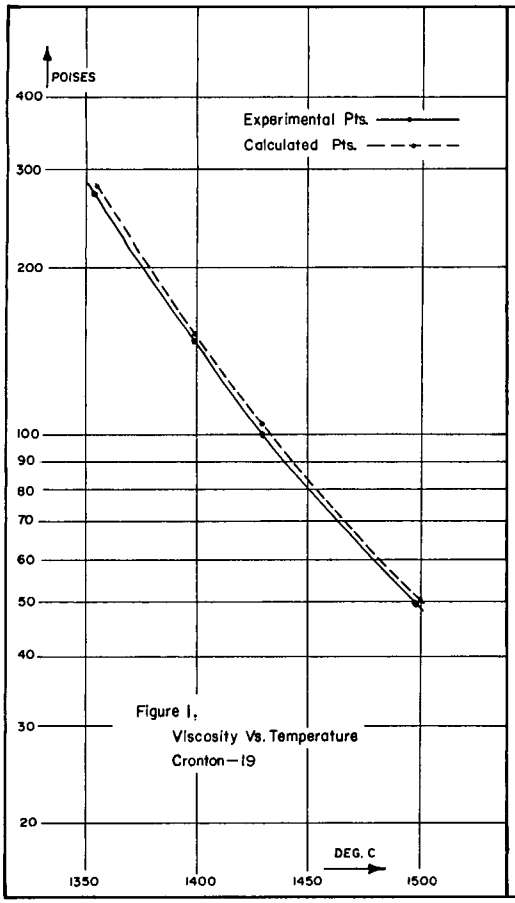

Figure 1.
Viscosity Vs. Temperature
Cronton—19

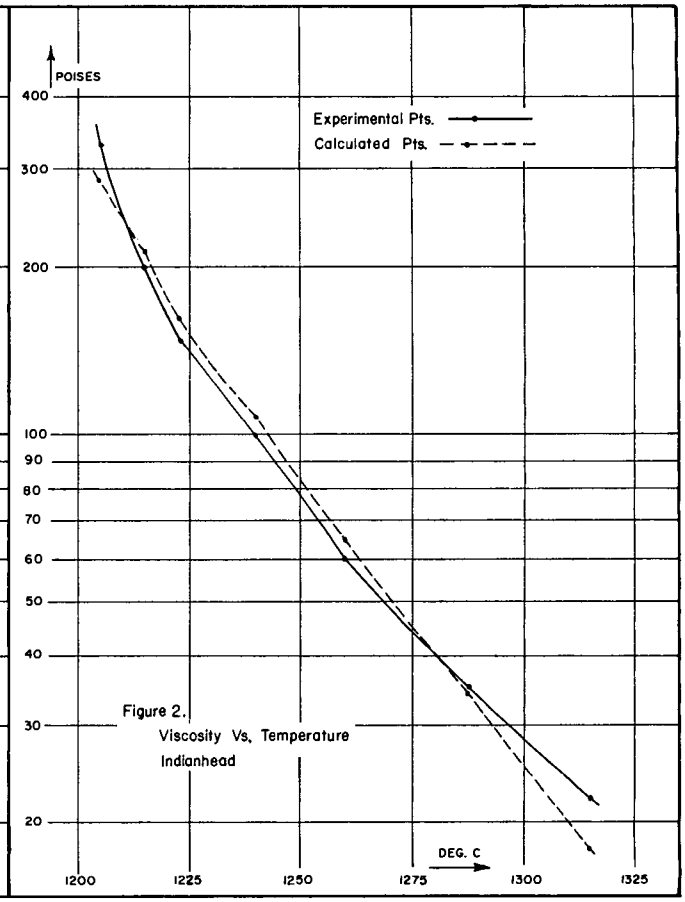

Figure 2.
Viscosity Vs. Temperature
Indianhead

SIZE-DEPENDENCE OF THE PHYSICAL AND CHEMICAL PROPERTIES OF COAL FLY ASH*

G. L. Fisher,[1] B. A. Prentice,[1] D. Silberman,[1] J. M. Ondov,[2]
R. C. Ragaini,[2] A. H. Bierman,[2] A. R. McFarland,[3] and J. B. Pawley.[4]

[1]Radiobiology Laboratory, University of California, Davis, CA 95616
[2]Lawrence Livermore Laboratory, Livermore, CA 94550
[3]Civil Engineering Department, Texas A & M University, College Station, TX 77843
[4]Donner Laboratory, University of California, Berkeley, CA 94720

In order to aid in the assessment of the potential biomedical and environmental consequences of coal combustion for electric power generation, we have performed detailed collaborative studies of the physical and chemical properties of size-fractionated coal fly ash. In this report, we demonstrate that many of the physical and chemical properties of aerodynamically size-classified fly ash depend on the relative size distributions of each fraction.

Aerodynamically size-classified fly ash was collected downstream from the electrostatic precipitator (ESP) in the stack breeching of a large southwestern U. S. power plant burning low sulfur (0.5%), high ash (23%) coal. The specially designed collection system (1) which consists of two cyclones and a centripeter separator is capable of size-classifying *in situ* kilogram quantities of stack fly ash. When used for 12 days to collect fly ash from stack gas, the apparatus yielded a total of 8.08 kg of fly ash in fractions with volume median diameters (VMD) of 20 μm (fraction 1), 6.3 μm (fraction 2), 3.2 μm (fraction 3) and 2.2 μm (fraction 4) all with geometric standard deviations of approximately 1.8. The size distribution data determined by optical sizing, centrifugal sedimentation and Coulter analyses are presented in Table 1.

Physical Studies

Based on light microscopic study of the four fly ash fractions, we have developed a particle morphogenesis scheme (Fig. 1). The physical characteristics of opacity, shape and type of inclusion utilized in the morphogenesis scheme appear to be related to degree and extent of exposure of the fly ash to combustion zone temperatures.

Eleven particle types and their probable matrix composition are classified (Fig. 1): 1) amorphous, non-opaque, 2) amorphous, opaque, 3) amorphous, mixed opaque and non-opaque, 4) rounded, vesicular, non-opaque, 5) rounded, vesicular, mixed opaque and non-opaque, 6) angular, lacy, opaque, 7) non-opaque, cenosphere (hollow sphere), 8) non-opaque, plerosphere (sphere packed with other spheres), 9) non-opaque, solid sphere, 10) opaque sphere and 11) non-opaque spheres with either surface or internal crystals. We have quantified the relative abundances of each of the 11 morphologic particle types in the four fractions (Table 2). The relative abundance of all particle types except non-opaque, solid spheres appears to increase with the increasing particle size of the fly ash fractions. The relative abundance of non-opaque, solid spheres is inversely dependent on particle size. Chi-square analyses of the relative distribution data of the morphologic particle types in the four fly ash fractions indicated highly significant ($p < 0.001$) differences for all six possible comparisons.

The apparent densities of the four fractions (Table 2) can be negatively correlated ($r = -0.978$; $p < 0.05$) with the VMD's. Furthermore, linear regression analyses of the fractional distribution data with the densities of the individual size fractions indicate significant ($p < 0.05$) positive correlations for the following particle types: 1) amorphous, non-opaque, 4) rounded, vesicular, non-opaque, 7) non-opaque cenospheres and 10) opaque sphere. Significant negative correlation was found only for solid, non-opaque spheres ($p < 0.01$).

*This work was supported by the US Energy Research and Development Administration.

Chemical Studies

The fly ash fractions were analyzed for 35 elements by instrumental neutron activation analysis (INAA) at the Lawrence Livermore Laboratory and for 18 elements by atomic absorption spectroscopy (AAS) at the Radiobiology Laboratory. The analytical techniques have been previously described (2). Before analyses of the fly ash fractions were undertaken both laboratories performed analyses of the National Bureau of Standards (NBS) Standard Reference Material, Trace Elements in Coal Fly Ash (SRM 1633). Agreement of all analytical results from both laboratories with previously published (3) or NBS certified values was excellent. The interlaboratory comparison has been reported by Ondov *et al.* (2).

Summary tables of the analytical results are presented for those elements displaying concentrations independent of particle size (Table 3) and dependent on particle size (Table 4). For elements analyzed by both INAA and AAS, the data reported are the results of the analytical technique with the smaller coefficient of variation. Data from atomic absorption analyses are the average of two independent determinations; the INAA data are the weighted averages of three independent determinations. Concentration dependence with particle size was determined qualitatively with the criteria that consistent concentration trends beyond experimental uncertainty were observed for each fraction, although significantly higher concentrations of the element may have been observed in the finest fraction relative to the coarsest fraction.

With the exception of silicon, which appears to decrease with decreasing particle size, the major element composition of the fractionated fly ash is relatively independent of particle size. Greater than 92% of the mass of the fractionated fly ash can be accounted for by oxides of Si, Al, Fe and Ca. An enhancement factor was defined as the ratio of the element concentration in cut 4 (finest) to its concentration in cut 1 (coarsest). The more volatile elements (or their oxides), Cd, Zn, Se, As, Sb, Mo, Ga, Pb and V display clear-cut increases in concentration with decreasing particle size, in agreement with the vapor-condensation mechanism of Natusch and Wallace (4). It is important to note, however, that refractory elements also display concentration trends inversely dependent on particle size. Therefore, processes other than vapor condensation are involved in the concentration-size relationship. The elements U and Cr are associated with the organic fraction of coal (5) and may be released in the combustion process as fine particles which may agglomerate with other particles. The elements Fe, Mn, Ba, and Sr (5) may in part be present as carbonate minerals which decompose to form fine particles during coal combustion and again agglomerate with other particles. Copper is probably present in part as the sulfide and Be as the aluminosilicate in the coal (5). Thus, mineral decomposition and elemental distribution may in part explain the elemental trends of the high boiling chemical species.

In summary, many physical and chemical properties of coal fly ash are dependent on particle size. Apparent density varies inversely with particle size and may be explained by the higher relative abundance of vesicular particles and lower relative abundance of solid, non-opaque spheres in larger size fractions. The elements Al, Fe, Ca, Na, K, Ti, Mg, Sr, Ce, La, Rb, Nd, Th, Ni, Sc, Hf, Co, Sm, Dy, Yb, Cs, Ta, Eu and Tb do not display clear-cut concentration trends with particle size. Silicon was the only element analyzed with clear-cut direct concentration dependence with particle size. Inverse concentration dependence with particle size was observed for Cd, Zn, Se, As, Sb, W, Mo, Ga, Pb, V, U, Cr, Ba, Cu, Be and Mn. Although a vapor-condensation mechanism may explain the concentration trends for the volatile elements, mineral decomposition and elemental distribution within the coal are probably important processes contributing to the inverse concentration dependence observed for the higher boiling chemical species.

References

1. McFarland, A. R., Fisher, G. L., Prentice, B. A., Bertch, R. W. Submitted to Environ. Sci. Technol.

2. Ondov, J. M., Ragaini, R. C., Heft, R. E., Fisher, G. L., Silberman, D., Prentice, B. A. Proc. NBS 8th Materials Research Symposium, Gaithersburg, MD. September, 1976, in press.

3. Ondov, J. M., Zoller, W. H., Omez, I., Aras, N. K., Gordon, G. E., Rancitelli, L. A., Abel, K. H., Filby, R. H., Shah, K. R., Ragaini, R. C. Anal. Chem. 47, 1102 (1975).

4. Natusch, D. F. S., Wallace, J. R. Science 186, 695 (1974).

5. Murchison, D., Westoll, T. S. "Coal and coal-bearing strata", 418 pp, American Elsevier, N. Y., 1968.

Table 1. Size Parameters for the Fly Ash Fractions

Fraction	CMD[1]		MMD[2]		VMD[3]	
	μm	σg[4]	μm	σg	μm	σg
1	2.73	2.20	18.5	2.8	20.0	1.8
2	2.58	1.86	6.0	2.0	6.3	1.8
3	1.14	1.73	3.7	1.7	3.2	1.8
4	0.92	1.52	2.4	1.8	2.2	1.9

[1]Count median diameter determined from scanning electron micrographs.
[2]Mass median diameter determined from Stokes differential settling in aqueous dispersion.
[3]Volume median diameter determined by Coulter analysis.
[4]Geometric standard deviation.

Table 2. Relative Abundance (%) of Morphologic Particle Types in the Four Fly Ash Fractions[1]

	Particle Type	Fraction 1	2	3	4
1.	Amorphous, non-opaque	7.25	2.13	0.79	0.33
2.	Amorphous, opaque	0.42	0.18	--	--
3.	Amorphous, mixed opaque and non-opaque	0.77	0.09	--	--
4.	Rounded, vesicular, non-opaque	12.39	6.67	2.91	2.99
5.	Rounded, vesicular, mixed opaque and non-opaque	2.27	0.24	--	0.03
6.	Angular, lacy, opaque	1.34	0.57	0.27	0.33
7.	Non-opaque, cenosphere	41.11	26.22	13.20	7.91
8.	Non-opaque, plerosphere	0.51	0.21	--	--
9.	Non-opaque, solid sphere	25.58	56.01	79.16	86.99
10.	Opaque sphere	1.56	0.90	0.33	0.24
11.	Non-opaque sphere with crystals	6.80	6.79	3.18	0.95
12.	Combined[2] particle types 2 and 6	--	--	0.15	0.24
	VMD (μm)	20	6.3	3.2	2.2
	Density[3] (g/cm^3)	1.85	2.19	2.36	2.45

[1]A total of approximately 3000 particles for each size fraction were classified from random fields using three microscope slides per fraction.
[2]Combined due to inability to distinguish between these classes for the finer particles.
[3]Apparent density determined by gravimetric displacement of 1-propanol.

Table 3. Elemental Concentrations Independent[1] of Particle Size

Element	Technique	Fraction 1 (VMD = 20 μm)	Fraction 2 (VMD = 6.3 μm)	Fraction 3 (VMD = 3.2 μm)	Fraction 4 (VMD = 2.2 μm)
		Concentration in %			
Al	AAS[2]	13.8(0.1)	14.4(0.1)	14.2(0.8)	14.1(0.3)
Fe	INAA[3]	2.5(0.1)	2.9(0.2)	3.0(0.1)	3.2(0.1)
Ca	AAS	2.12(0.14)	2.23((0.08)	2.30(0.14)	2.38(0.09)
Na	AAS	1.19(0.13)	1.75(0.05)	1.83(0.06)	1.85(0.03)
K	AAS	0.74(0.01)	0.80(0.07)	0.82(0.08)	0.81(0.03)
Ti	AAS	0.62(0.05)	0.76(0.05)	0.77(0.11)	0.78(0.06)
Mg	AAS	0.47(0.01)	0.56(0.01)	0.60(0.02)	0.63(0.01)
		Concentration in μg/g			
Sr	INAA	410(60)	540(140)	590(140)	700(210)
Ce	INAA	113(4)	122(5)	123(6)	120(5)
La	INAA	62(3)	68(4)	67(11)	69(3)
Rb	INAA	51(3)	56(4)	57(3)	57(8)
Nd	INAA	45(4)	47(4)	49(7)	52(6)
Th	INAA	25.8(0.6)	28.3(0.6)	29(1)	30(2)
Ni	AAS	25(3)	37(1)	43(4)	40(2)
Sc	INAA	12.6(0.5)	15.3(0.6)	15.8(0.6)	16.0(0.2)
Hf	INAA	9.7(0.4)	10.3(0.3)	10.5(0.3)	10.3(0.5)
Co	INAA	8.9(0.2)	16.3(0.8)	19(1)	21(1)
Sm	INAA	8.2(0.3)	9.1(0.4)	9.2(0.4)	9.7(0.4)
Dy	INAA	6.9(0.3)	8.5(0.9)	8.1(0.3)	8.5(0.8)
Yb	INAA	3.4(0.4)	4.1(0.4)	4.0(0.2)	4.2(0.3)
Cs	INAA	3.2(0.1)	3.7(0.2)	3.7(0.2)	3.7(0.2)
Ta	INAA	2.1(0.1)	2.3(0.2)	2.5(0.3)	2.7(0.1)
Eu	INAA	1.0(0.1)	1.2(0.2)	1.2(0.2)	1.3(0.4)
Tb	INAA	0.90(0.05)	1.06(0.06)	1.10(0.07)	1.13(0.06)

[1]Concentration dependence with particle size was determined qualitatively with the criteria that consistent concentration trends beyond experimental uncertainty were observed for each fraction.

[2]AAS values are the averages of two independent determinations; the ranges are given in parentheses.

[3]INAA values are the weighted averages of three independent determinations; uncertainties (in parentheses) are the largest of twice the weighted standard deviation, the range, or an estimate of the accuracy.

Table 4. Elemental Concentrations Dependent[1] on Particle Size

Element	Technique	Fraction 1 (VMD = 20 μm)	Fraction 2 (VMD = 6.3 μm)	Fraction 3 (VMD = 3.2 μm)	Fraction 4 (VMD = 2.2 μm)	Enhancement Factor[2]
		Concentration in μg/g (unless indicated)				
Cd	AAS[3]	0.4(0.2)	1.6(0.3)	2.8(0.4)	4.6(0.2)	11.5
Zn	AAS	68(1)	189(4)	301(10)	746(218)	11.
Se	INAA[4]	19(2)	59(2)	78(2)	198(20)	10.4
As	INAA	13.7(1.3)	56(14)	87(9)	132(22)	9.6
Sb	INAA	2.6(0.1)	8.3(0.4)	13.0(0.7)	20.6(0.7)	7.9
W	INAA	3.4(0.2)	8.6(1.6)	16(2)	24(2)	7.1
Mo	INAA	9.1(2.5)	28(1.4)	40(5)	50(9)	5.5
Ga	INAA	43(12)	116(52)	140(23)	178(90)	4.1
Pb	AAS	73(3)	169(2)	226(4)	278(3)	3.8
V	INAA	86(44)	178(17)	244(18)	327(40)	3.8
U	INAA	8.8(1.9)	16(3)	22(4)	29(4)	3.3
Cr	AAS	28(3)	54(3)	66(3)	71(4)	2.5
Ba(%)	AAS	0.168(0.001)	0.245(0.002)	0.320(0.013)	0.409(0.018)	2.4
Cu	AAS	56(1)	89(1)	107(4)	137(1)	2.4
Be	AAS	6.3(0.2)	8.5(0.2)	9.5(0.3)	10.3(0.5)	1.6
Mn	AAS	209(7)	231(5)	273(7)	309(3)	1.5
Si(%)	AAS	29.6(0.7)	28.0(0.1)	27.5(0.3)	26.8(0.1)	0.90

[1]Concentration dependence with particle size was determined qualitatively with the criteria that consistent concentration trends beyond experimental uncertainty were observed for each fraction.
[2]Ratio of concentration in Fraction 4 to that in Fraction 1.
[3]AAS values are the averages of two independent determinations; the ranges are given in parentheses.
[4]INAA values are the weighted averages of three independent determinations; uncertainties (in parentheses) are the largest of twice the weighted standard deviation, the range, or an estimate of the accuracy.

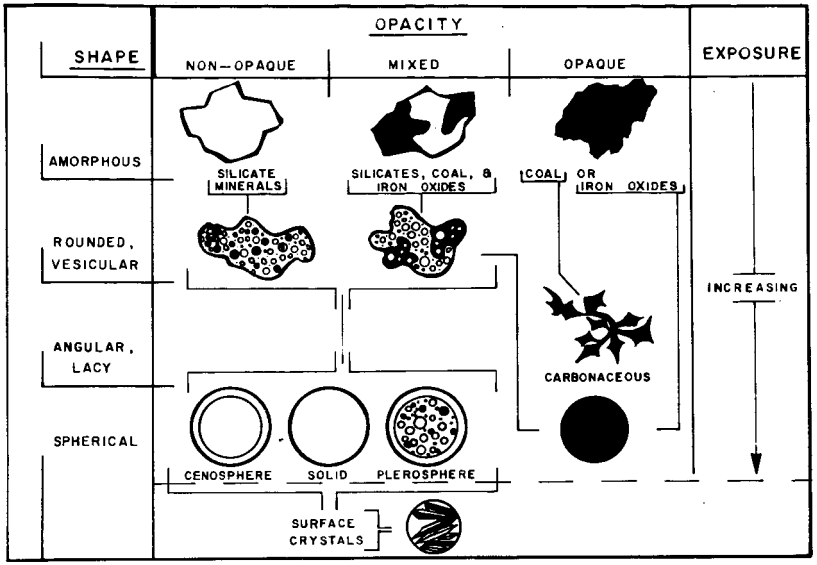

Fig. 1. Fly ash morphogenesis scheme illustrating probable relationship of opacity and shape to particle composition and exposure in the combustion chamber.

NOT FOR PUBLICATION
For Presentation Before the Division of Fuel Chemistry
American Chemical Society
Montreal, Quebec, Canada, May 1977

THE BEHAVIOR OF THE NATURAL RADIONUCLIDES IN WESTERN COAL-FIRED POWER PLANTS

David G. Coles, Richard C. Ragaini, and John M. Ondov

Division of Environmental Research, Lawrence Livermore
Laboratory, University of California, Livermore, CA 94550

The projected dependence of the nation on coal-produced electrical energy necessitates a thorough study of the associated environmental risks. One potential hazard worthy of further investigation is the release of natural radionuclides upon coal combustion. Radioactive effluents from both fossil-fuel and nuclear power plants have been compared.[1,2] However, oversimplifications and lack of good emission data for radionuclides from the fossil-fuel plants lead to differing conclusions. Hull[3] has compared the inorganic-effluent releases of the fossil-fuel plants to the radionuclide releases from nuclear plants in terms of accepted environmental standards for each type of effluent. Moore et al.[4] have calculated that anthropogenic sources contribute 6.5% of the total ^{210}Po atmospheric flux for the continental U.S. Fossil-fuel burning makes up 14% of these anthropogenic sources or 1% of the total ^{210}Po input. One can determine a maximum concentration indirectly from the ^{210}Pb content in the coal, since ^{210}Pb is the grandparent of ^{210}Po in the ^{238}U-decay series. None of the fossil-fuel-plant studies have concentrated on the radionuclide-combustion chemistry, which is necessary to make valid comparisons between fossil-fuel and nuclear plants. It is the purpose this work to study the chemical fractionation of the natural radionuclides in coal during combustion.

Experimental

Coal, bottom-ash, and electrostatic precipitator (ESP) fly-ash samples were obtained from two western coal-fired power plants. Plant A burns low-sulfur (0.52%), low-ash (9.2%) coal and Plant B burns low-sulfur (0.46%), high-ash (23.2%) coal. We also obtained from Plant B kilogram quantities of particle-sized stack fly ash. This stack fly ash was collected by a large cyclone separator mounted at the outlet of one of the ESP units.[5] Two separate sets of the four sized fractions were obtained. For each fraction as determined by centrifugal sedimentation, the mass median diameters (mmd) were 17, 6, 3.8, and 2.5 μm, Geometric standard deviations of the fractions were approximately 2.3, 2.1, 1.7, and 1.8 μm, respectively.

All samples were ground to 200 mesh when necessary, homogenized, packaged, and then counted for natural gamma radiation on an ultra-low background, Compton-suppression, gamma-ray spectrometer.

The ^{238}U natural radioactive-decay-chain series was found to be in secular equilbrium in the coal samples but not in the ash samples. During the combustion process a potential exists for decay-chain disequilibrium to occur, since many of the daughter radionuclides have quite different chemical and physical characteristics. Secondary post-fractionation radionuclides are those whose half-lives are long enough to produce gamma rays or gamma-ray-emitting daughters after secular equilibrium has been disrupted by the combustion process. The actual measured gamma ray may originate from a daughter further along the decay chain but prior to the next long-lived species.

The half-lives of these intermediary radionuclides are short enough so that secular equilibration can be assumed to have been reestablished for that section of the decay chain. The packaged samples were allowed to sit for 6 months. This provided the longest-lived intermediary radionuclide ^{234}Th (24.1 day) the opportunity to come to within 1% of secular equilibration with its parent ^{238}U.

Discussion

Enrichment factors relative to the input coal were calculated for the radionuclide contents observed. The enrichment factor (EF) is defined as the ratio of the concentration of a radionuclide (X) and ^{40}K in the sample, divided by the corresponding ration in the input coal.

$$EF = \frac{[X]\ \text{sample}/[^{40}K]\ \text{sample}}{[X]\ \text{coal}/[^{40}K]\ \text{coal}}$$

This effectively normalizes the apparent enrichment resulting from loss of carbon during the combustion process. Potassium-40 is used in this normalization calculation because its concentration remains constant in all samples; hence it was assumed to be a tracer for the alumino-silicate-dominated ash matrix.

Table 1 presents the EF value for the different samples from both plants. The ESP fly ash and bottom ash from both plants show no enrichment of the ^{232}Th-decay-chain daughters. This is expected since thorium and radium are essentially refractory elements and should remain with the ^{40}K in the ash matrix. Uranium behaves in quite

Table 1. Enrichment factor relative to input coal and normalized to ^{40}K[a]

Decay-chain origin	^{232}Th		^{238}U			^{235}U
Source after fractionation	^{228}Th	^{228}Ra	^{210}Pb	^{226}Ra	^{238}U	^{235}U
Plant A[b]						
ESP fly ash	0.89	0.90	0.48	1.02	0.71	0.70
Bottom ash	0.96	0.97	0.24	0.99	0.70	0.64
Plant B[c]						
ESP fly ash	0.96	0.98	0.74	1.02	0.94	0.85
Bottom ash	0.91	0.89	0.29	0.90	0.76	0.73
Scrubber ash	1.01	1.03	0.95	1.08	0.97	0.88

[a] ±10 to 20% propagated 1σ error from the mean.

[b] Samples from Plant A; input coal contains 11.3% H_2O, 9.2% ash, and 0.52% sulfur.

[c] Samples from Plant B; input coal contains 6.8% H_2O, 23.2% ash, and 0.46% sulfur.

a different manner. Both ^{235}U and ^{238}U show significant depletion in the fly ash from Plant A (low-ash coal) and the bottom ash from both Plants. The fly ash is not nearly as depleted in these uranium isotopes from Plant B (high-ash coal).

Lead-210 appears to be the most volatile radionuclide measured. It is quite depleted in the bottom ash from both plants and is less depleted in the fly ash from Plant B (high-ash coal). All EF values for the scrubber ash are close to unity. The wet scrubber is more efficient than the ESP for fly-ash removal (99.2% vs 97.%) and, therefore, retains more ash by weight than the ESP unit although it releases higher numbers of submicron particles to the atmosphere.[6] Since the wet scrubber is more efficient, its EF value might be expected to be near unity, and consequently any chemical enrichment in the submicron particulates would be obscured.

The ^{210}Pb depletion in the ESP bottom ash probably occurs as volatilization and later condensation onto the fly-ash matrix. Since heterogeneous condensation is a surface-area phenomenon, the lead would be expected to be enriched on the finer fly-ash particles. In Fig. 1, the stack (post ESP) sized fly ash shows a very strong increase in EF with decreasing particle size. This effect is consistent with the depletion of lead on the larger-sized ESP fly ash. Davison et al.[7] discuss this condensation mechanism more fully.

Assuming that secular equilibration exists between ^{210}Pb and ^{210}Po in the coal samples, the specific activity for both nuclides will be identical and therefore the total inventory of ^{210}Po for the coal combustion system can be estimated. Its post-combustion behavior was not studied in this work; but since polonium is more volatile than lead, it will probably condense onto the extremely small fly-ash particles after combustion. A study of the combustion chemistry and deposition properties of this important radionuclide is in progress.

Uranium's definite association with small particles has been previously observed.[8,9] It is slightly depleted in the bottom ash of both plants. Plant B (high-ash coal) has a fly-ash EF close to unity. However, this plant's sized stack fly ash shows a very definite EF increase with decreasing particle size (see Fig. 1). We propose a bimodal mechanism to explain this behavior. The coal contains uranium in two different phases, which affects its volatility upon combustion. Klein et al.[9] observed that uranium behaves in a manner intermediate between those elements remaining with the slag and those elements concentrating on the fly ash.

Breger[10] suggests that uranium enters the coal bed from ground water as the soluble uranyl dicarbonate $Na_2[UO_2(CO_3)_2]$ or sodium uranyl tricarbonate $Na_4[UO_2(CO_3)_3]$ complex. The slightly acidic environment of the coal decomposes this complex and the uranium quickly becomes absorbed by the coal with subsequent reduction to uraninite UO_2. If sufficient silica is present in solution, the mineral coffinite $U(SiO_4)_{1-x}(OH)_{4x}$ can form instead of uraninite. Since the uranium is in solution, it can migrate from cracks and joints into the coal matrix for some distance and can, therefore, be expected to reside in the coal in a very highly dispersed state. Uranium is enriched over thorium in these samples (Th/U = 2.0) compared to the average crustal ratio (Th/U = 4.0),[11] thus indicating the high mobility of uranium as compared to thorium during ground and surface water transport.

The characteristics of uranium during the combustion process depend upon the conditions of the furnace as well as its chemical and physical form in the input coal. Coal-fired power plants operate their burners with about a 10% stoichiometric excess of oxygen.[12] This should result in an oxidizing combustion environment with a temperature range of 1500 to 1600°C. Under these conditions, the volatile species UO_3 could be expected to form.[13,14] The possibility also exists for uranium to become incorporated into a silica melt during combustion if it were originally associated with a silicate (i.e., coffinite).

The existence of uranium bimodally in the coal can therefore give rise to both a volatile and nonvolatile species simultaneously, since both uraninite and coffinite can coexist in the pulverized and semihomogenized coal. The data in Table 1 support this relationship. The Plant B (high-ash coal) fly ash shows less uranium depletion than the Plant A (low-ash coal) fly ash. A higher percentage of the uranium is probably associated with the alumino-silicate minerals and is consequently available for incorporation into the silica-rich fly-ash matrix.

Thorium-228 could be slightly enriched in the stack fly ash when compared to INAA (Instrumental Neutron Activation Analysis) data for cerium, a nonenriched element

(see Fig. 1). Thorium (and to some extent uranium) is normally associated with the very chemically resistant mineral zircon $ZrSiO_4$,[15] which is a ubiquitous accessory mineral in many common rocks. Zircon does not weather easily and is commonly found in sedimentary environments. It is conceivable that the thorium observed in the coal system was deposited contemporaneously with the coal along with the other silicate-based minerals. These minerals make up the ash after the coal is burned. The small resistant mineral grains could be carried with the gases after combustion and follow the course of the fly ash. The thorium behavior in the sized fly ash could be explained if thorium existed in the coal as submicron particles.

The enrichment of ^{228}Ra and ^{226}Ra (see Fig. 1) is difficult to explain. Klein et al.[9] observes that barium (and hence probably radium) and thorium become incorporated into the fly-ash matrix. However, barium is known to form a volatile species $Ba(OH)_2$ in the presence of steam, and radium may also form a corresponding species. Figure 1 shows ^{226}Ra with a greater EF than ^{228}Ra. A portion of the ^{226}Ra will reside with the uraninite fraction of its ^{238}U parent as described earlier. This probably allows ^{226}Ra to form a more mobile species than the silicate bound ^{228}Ra (from the ^{232}Th chain) in a manner similar to the bimodally located uranium.

The behavior of the natural radioactive decay series throughout the coal deposition, combustion, and emission system can be described by the following:

- Associated with the accumulation of orgainic matter is a significant fraction of clay minerals, sand, and other inorganic sedimentary material. These materials contain the alumino-silicate minerals that will later comprise the coal fly ash and bottom ash. Herein is found the source of the ^{232}Th, ^{40}K, and a part of the silicate associated uranium.

- The organic accumulation environment ceases and a deposition environment prevails, which buries the organic matter. Coal metamorphism occurs.

- Ground and surface waters penetrate down through the overburden, invading the coal. These waters contain uranium as soluble uranyl carbonate salts and varying amounts of soluble silica.

- Uranium is absorbed by the coal and reduced to uraninite or coffinite, depending on the silica content of the water.

- Coal is mined, pulverized, and fed into the furnace for power production. Much of the alumino-silica minerals (mostly clay) form a melt and drop out as slag. Most of the thorium and radium isotopes follow. Lead-210 remains volatile and continues along with the gases and fly ash to the emission control system. Much of the uranium that is associated with the clays, or that which was mineralized as coffinite, also remain with the bottom ash. The uranium that is dispersed in the coal as uraninite becomes volatile as the UO_3 species and continues along with the gases, lead, and the fly ash.

- Somewhere down the flue line, first uranium and then lead preferentially condense out on the finer fly-ash particles because they have a high surface to mass ratio.

- The ESP collects most of the particulate mass. Those finer particles that bypass the ESP continue up the stack with the gases. They are very enriched in ^{210}Pb relative to the coal, and moderately enriched in ^{235}U and ^{238}U. Some slight enrichment is observed for ^{226}Ra (probably that associated with uraninite), ^{228}Ra, and ^{228}Th. The thorium is probably associated with fine zircon grains.

The degree to which each of the many possible mechanisms affect the final radionuclide concentrations cannot be ascertained from these data. The actual situation may be one mechanism, or more probably a combination of mechanisms. The mineralogical or chemical form in which the radionuclides or trace elements exist in the coal does have an important effect on their subsequent combustion chemistry and emission characteristics.

References

1. Eisenbud, Merril and Henry G. Petrow, Science 144, 228 (1964).
2. Martin, J.E., Harward, E.D., Oakley, D.T., Smith, J.M., and Bedrosian, P.H., in IAEA Symposium on Environmental Aspects of Nuclear Power Stations, New York, IAEA Conf. 700810-24 (1969) paper - IAEA-Sm-146/19, 325-337.
3. Hull, A.P., Nuclear News, 51-55, (April, 1974).
4. Moore, H.E., Martell, E.A., and Poet, S.E., Environ. Sci. Technol. 10, 586, (1976).
5. McFarland, A.R., Fisher, G.L., Prentice, B.A., and Bertch, R.W., Submitted for publication in Environ. Sci. Technol. (1976).
6. Ondov, J.M., Ragaini, R.C., and Biermann, A.H., presented at Amer. Chem. Soc. Meeting, Div. of Environ. Chem., Preprint UCRL-78050, 1976.
7. Davison, R.L., Natusch, D.F.S., and Wallace, J.R., Environ. Sci. Technol. 8, 1107 (1974).
8. Ragaini, R.C., Ondov, J.M., Proc. Int. Conf. Modern Trends in Activation Analysis, Munich, 1976, I, 654; Lawrence Livermore Laboratory, Preprint UCRL-77669.
9. Klein, D.H., Andren, A.W., Carter, J.A., Emery, J.F., Feldman, C., Fulkerson, W., Lyon, W.S., Ogle, J.C., Talmi, Y., Van Hook, R.I., and Bolton, N., Environ. Sci. Technol. 9, 973 (1975).
10. Breger, I.A., in IAEA Symposium on the Formation of Uranium Ore Deposits, Athens, IAEA-SM-183/29 (1974) pp. 99-124.
11. Mason, B., Principles of Geochemistry, 3rd. Ed., John Wiley & Sons (1966).
12. Babcock and Wilcox, Steam, Its Generation and Use, 38th Ed., Babcock and Wilcox, New York, 1972.
13. Rand, M.H., and Kubaschewski, O., The Thermochemical Properties of Uranium Compounds, Interscience (Wiley), New York, 1963.
14. Ackermann, R.J., Thorn, R.J., Alexander, C., and Tetenbaum, M., J. Phys. Chem. 64, 350 (1960).
15. Kirby, H.U., Mound Laboratory, Rept. MLM-2111 (1974).

NOTICE

"This report was prepared as an account of work sponsored by the United States Government. Neither the United States nor the United States Energy Research & Development Administration, nor any of their employees, nor any of their contractors, subcontractors, or their employees, makes any warranty, express or implied, or assumes any legal liability or responsibility for the accuracy, completeness or usefulness of any information, apparatus, product or process disclosed, or represents that its use would not infringe privately-owned rights."

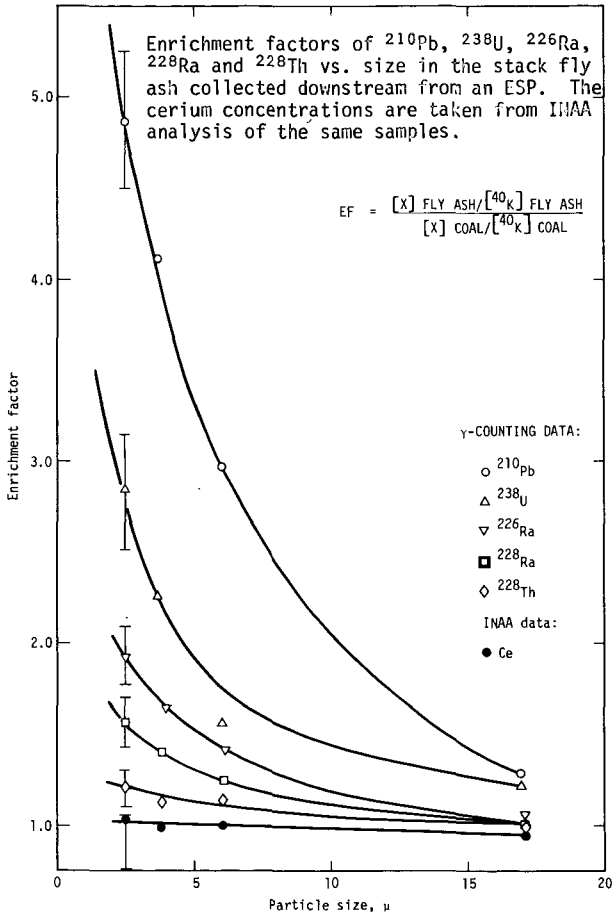
Enrichment factors of ^{210}Pb, ^{238}U, ^{226}Ra, ^{228}Ra and ^{228}Th vs. size in the stack fly ash collected downstream from an ESP. The cerium concentrations are taken from INAA analysis of the same samples.
$EF = \frac{[X]\ FLY\ ASH/[^{40}K]\ FLY\ ASH}{[X]\ COAL/[^{40}K]\ COAL}$
γ-COUNTING DATA:
^{210}Pb
^{238}U
^{226}Ra
^{228}Ra
^{228}Th
INAA data:
Ce
Enrichment factor
5.0
4.0
3.0
2.0
1.0
0
5
10
15
20
Particle size, μ